2012

Land Use Effects On Energy And Water Balance-developing A Land Use Adapted Drought Index

Chi Han Cheng
University of Central Florida

LAND USE EFFECTS ON ENERGY AND WATER BALANCE-DEVELOPING A REGIONAL LAND USE ADAPTED DROUGHT INDEX

By

CHI-HAN CHENG

B.S. Chung Yuan Christian University, 2002
M.S. National Central University, 2004

A dissertation submitted in partial fulfillment of the requirements
for the degree of Doctor of Philosophy
in the Department of Civil, Environmental and Construction Engineering
in the College of Engineering and Computer Science
at the University of Central Florida
Orlando, Florida

Spring Term
2012

Major Professor: Fidelia N. Nnadi

ABSTRACT

Climate change is expected to increase the frequency, intensity and duration of droughts in all parts of the United States (US). Snow packs are disappearing earlier in the spring and summer, with reduced stream-flow. Lower reservoir levels, higher temperatures, and greater precipitation variability have been observed. Drought events in the US have threatened drinking water supplies for communities in Maryland and Chesapeake Bay as observed in 2001 through September 2002; Lake Mead in Las Vegas in 2000 through 2004; Peace River and Lake Okeechobee in South Florida in 2006; and Lake Lanier in Atlanta, Georgia in 2007.

ENSO influences the climate of Florida; where El Niño years tend to be cooler and wetter, while La Niña years tend to be warmer and drier than normal in the fall through the spring, with the strongest effect in the winter. Both prolonged heavy rainfall and drought potentially have impacts on land uses and many aspects of Florida's economy and quality of life. Drought indices could integrate various hydrological and meteorological parameters and quantify climate anomalies in terms of intensity, duration, and spatial extent, thus making it easier to communicate information to diverse users. Hence, understanding local ENSO patterns on regional scales and developing a new land use drought index in Florida are critical in agriculture and water resources planning and managements.

Current drought indices have limitations and drawbacks such as calculation using climate data from meteorological stations, which are point measurements. In addition, weather stations are scarce in remote areas and are not uniformly distributed. Currently used drought indices like the

PDSI and the Standardized Precipitation Index (SPI) could not fully demonstrate the land use effects. Other limitations include no single index that addresses universal drought impact. Hence, there is a renewed interest to develop a new "Regional Land Use Drought Index (RLDI) that could be applied for various land use areas and serve for short term water resources planning.

In this study, the first and second research topics investigated water and energy budgets on the specific and important land use areas (urban, forest, agriculture and lake) in the State of Florida by using the North American Regional Reanalysis (NARR) reanalysis data. NARR data were used to understand how drought events, EI Niño, La Niña, and seasonal and inter-annual variations in climatic variables affect the hydrologic and energy cycle over different land use areas. The results showed that the NARR data could provide valuable, independent analysis of the water and energy budgets for various land uses in Florida. Finally, the high resolution land use (32km×32km) adapted drought indices were developed based on the NARR data from 1979 to 2002. The new regional land use drought indices were developed from normalized Bowen ratio and the results showed that they could reflect not only the level of severity in drought events resulting from land use effects, but also La Niña driven drought impacts.

ACKNOWLEDGMENTS

I am very thankful to my professor Dr. Ola Nnadi for her guidance, support and patience. I want to express my gratitude to her for being a very good advisor and most importantly a great person. Special thanks go to my dissertation committee members—Drs. Dingbao Wang, Manoj Chopra and David M Sumner—for encouraging and devoting time in my Ph.D. study.

The love of family and friends provided my inspiration and was my driving force. It has been a long journey and completing this work is definitely a high point in my academic career. I could not have come this far without the assistance of many individuals and I want to express my deepest appreciation to them.

Thanks would go to my beloved parent for their loving considerations and great confidence in me all through these years. I also owe my sincere gratitude to Yu-Wen, Wang. Thank for your encouragement and consideration.

TABLE OF CONTENTS

LIST OF FIGURES

LIST OF TABLES

CHAPTER 1:

INTRODUCTION

1.1 Introduction

Water is one of Earth's most critical resources. Essential to every ecosystem, water sustains all life, and helps maintain the environmental balance of our planet too. Water is essential in human development from personal water needs to the demands of agriculture and industry.

However, climate change resulting from increasing atmospheric concentrations of greenhouse gases could have significant effect on water resources. Climate change is consistently associated with changes in a number of components of hydrological cycle and systems such as: changing precipitation patterns, intensity and extremes; widespread melting of snow and ice; increasing atmospheric water vapor; and change in soil moisture and runoff (IPCC, 2007). For example, increasing frequency or magnitude of extreme rainfall events occurred in the winter or spring when the ground is frozen or soil moisture levels are high, thus producing more rapid runoff and greater flooding.

Moreover, climate change is expected to increase the frequency, intensity and duration of droughts in all parts of the US. Already, reduced snow packs disappear earlier in the spring and summer, and reduced stream-flow, lower reservoir levels, higher temperatures, and precipitation variability have been observed (IPCC, 2007). For example, recent drought events in the US have threatened drinking water supplies for communities in Maryland and Chesapeake Bay in 2001 through September 2002, Lake Mead in Las Vegas in 2000 through 2004, the Peace River and

Lake Okeechobee in South Florida in 2006, and Lake Lanier in Atlanta, Georgia 2007 (Chang, 2008). In 1995, the Federal Emergency Management Agency (FEMA) estimated annual losses from drought to be $6-8 billion, which is higher than any other natural weather related disaster, including hurricane and flood (FEMA, 1995).

Drought is the most complex of all natural hazards. The lack of progress in drought preparedness planning and development of national drought policies is a reflection of this complexity. Although climate (particularly precipitation) is a primary contributor to hydrological drought, other factors such as land use also affect water and carbon cycles and thus regional climate. For example, as soil water supply or plant stomatal closure limit atmospheric moisture and water vapor flux, the near surface atmospheric humidity deficit and temperature are increased. In turn, this leads to increased thickness of atmospheric boundary layer, enhanced entrainment of warm and dry air, and an overall positive feedback for continued surface drying (Entekhabi et al., 1999). Therefore, developing improved drought monitoring and early warning system in support of drought preparedness planning and policy is an urgent need for all drought-prone countries (Wilhite et al., 2008).

1.2 Background

Within the hydrologic cycle, evapotranspiration (ET) or latent heat (LE) is driven primarily by the evaporative power of the net radiation and establishes a fundamental linkage between energy and water balances. The partitioning of net radiation between sensible and latent heat flux is markedly dependent on the amount of available water on the surface. During wet conditions, ET

is principally limited by the atmospheric demand of water vapor, and driven by solar energy. Hence, because of the importance of solar energy, ET varies with latitude, season of year, time of day, and cloud clover. In contrast, during dry conditions, changes in evaporation and transpiration depend on the availability of moisture at the onset of drought and the severity and duration of a drought. Hence, the availability of soil moisture becomes the primary control of ET and differences in capacity of plants to access water, often dictated by the rooting depth, can result in contrasting evaporative losses across vegetation types. Decrease in ET during droughts is generally greater in agriculture areas because crop die or their foliage (and, therefore, their ability to transpire water) is severely stunted during prolonged droughts. Hence, the drought's duration and intensity would be different on various land use types. Drought indices have been used to reflect the level of severity in drought events in relation to land use effects.

1.2.1 Surface Radiation

The Earth exchanges energy with its spatial environmental through radiation (gain from solar energy and loss by infrared emission). In fact, shortwave radiation from the sun penetrates through spaces to the outer edge of atmosphere unimpeded by the vacuum of outer space. A portion of shortwave is reflected to space and the remainder is absorbed by the earth and atmosphere. As a result solar heat is redistributed from the equator to the poles. The fraction of the incident sunlight that is reflected is called albedo. An ideal white body has 100% albedo,

while an ideal black body has 0%. The typical amounts of solar radiation reflected from various objects are shown in table 1.1.

Table 1.1: Reflectivity Values of various Surfaces (Oke, 1998; Ahrens, 2001)

Surface	Details	Albedo
Soil	Dark& wet versus	0.05-
	Light &dry	0.4
Sand		0.15-0.45
Grass	Long &versus	0.16-
	Short	0.26
Agricultural crops		0.18-0.25
Tundra		0.18-0.25
Forests	Deciduous	0.15-0.20
	Coniferous	0.05-0.15
Water	Small zenith angle versus	0.03-0.1
	Large zenith angle	0.1-1
Snow	Old	0.4-
	Fresh	0.95
Ice	Sea	0.3-0.45
	Glacier	0.20-0.40
Clouds	Thick	0.60-0.90
	Thin	0.30-0.50

1.2.1.1 Downward Longwave Radiation

To balance the incoming shortwave energy, the surface atmosphere system ultimately emits radiation to space in the radiation or longwave domain (4-10mm). The amount of energy emitted is primarily dependent on the temperature of the earth's surface. The hotter the surface the more radiant energy it will emit. Greenhouse gases such as water vapor, carbon dioxide, ozone and methane, which slow its escape from the atmosphere, absorb the heat caused by infrared radiation. This absorbed radiation is emitted in all directions with the downward direction portion being downward longwave radiation.

The accurate estimate of downward longwave radiation is necessary for calculating the net radiation, which in turn modulates the magnitude of the surface energy budgets, including latent heat (Crawford et al., 1999). However, the longwave radiation is difficult and more expensive to measure than shortwave radiation because it is not a conventional measurement and thus its measurement is rarely included in the meteorological stations (Kruk et al., 2009). Moreover, due to poor vertical resolution of water vapor data and the difficulties associated in the atmospheric emissivity and temperature, many reasonably successful techniques have been developed in recent decades that estimate downward longwave radiation (LW_d) based on the screen-level humidity and air temperature measurements. Ångström (1918) first observed an empirical relationship between downward longwave clear-sky irradiance and vapor pressure. Following his pioneering works, several parameterizations have been developed for LW_d radiation using

synoptic observations (Sherwood, 1969; Maykut and Church, 1973; Jacobs, 1978; Aubinet, 1994; Dilley and Brien, 1998; Duarte et al., 2006; Lhomme et al.,. 2007).

1.2.1.2 Cloud Effects

Cloud cover plays an important role to prevent radiation deficit. Thick clouds primarily reflect solar radiation and cool the surface of the earth. High and thin clouds mainly transmit incoming solar radiation; at the same time, they trap some of the outgoing infrared radiation emitted by the earth and radiate it back downward, thereby warming the surface of earth. Several researchers have proposed locally adjusted equations for downward longwave radiation (LW_d) fluxes in cloudy condition, LW_d radiation in clear-sky condition, LW_{dc} (Wm^{-2}), such as Jacobs (1978) for Baffin Island, Canada, Maykut and Church (1973) for Alaska, United States, Sugita and Brutsaert (1993) for Kansas, United States, Konzelmann, van de Wal et al. (1994) for Greenland, and Crawford, et al. (1999) for Oklahoma, United States.

1.2.1.3 Net Radiation

Radiation balance of the earth system is an accounting of incoming and outgoing components of radiation. These components are balanced over long time period and over the earth as whole. A simple schematic of the radiation budget is given in Figure 1.1, where the components of longwave radiation are given by Stefan's law.

The radiation balance equation is:

$$R_n = SW_{in}(1 - A) + \varepsilon_a \varepsilon_s \sigma T_a^4 - \varepsilon_s \sigma T_s^4 = SW_{in}(1 - A) + \varepsilon_s LW_d - LW_u \quad (1.1)$$

where SW_{in} (or SW_d) is incoming (or downward) shortwave (SW) radiation, SW_u is upward shortwave radiation, A is surface albedo, ε_a is air (atmospheric) emissivity, ε_s is surface emissivity, σ is the Stefan-Boltzman constant (5.67*10-8 W/m^2K^4), T_a (K) is air .temperature, T_s (K) is surface temperature, LW_d is downward longwave (LW) radiation, and LW_u is upward longwave radiation. All radiation terms are in Wm^{-2}.

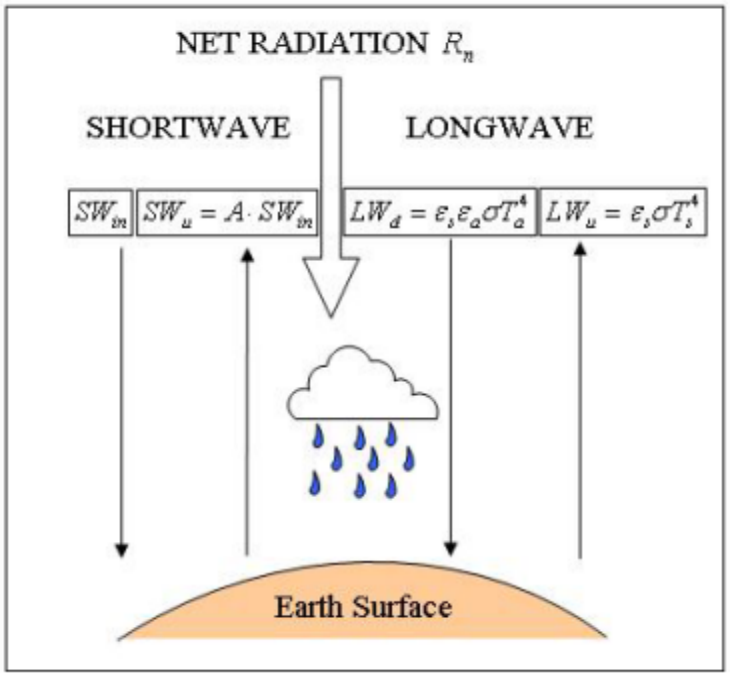

Figure 1.1: Schematic of radiation budget (Rizou and Nnadi, 2008)

Sellers et al. (1990) suggested that estimating the four components of R_n could cause error accumulation, especially when estimating the net longwave flux, because both downward and upward longwave radiation are large components, so the difference would be small and liable to large uncertainty. Consequently, a high priority should be given to the accurate prediction of the radiation fluxes, especially the downward longwave radiation. Therefore, an improvement of the existing downward longwave radiation models is necessary for increasing accuracy of net radiation.

Moreover, net radiation (R_n) is also the main energy flux driver of evapotranspiration (ET), which exhibits the significant temporal and spatial variability. Penman (1948, 1956) used net radiation and other meteorological factors to estimate evaporation rates. If estimates of radiation are to be used for estimating evaporation rates then the net radiation estimates must be of acceptable accuracy (McCuen and Asmussen, 1976). The principal use of net radiation is in the phase change of water (latent heat, LE), air temperature (sensible heat, H), and subsurface (ground heat, G). The simple equation is as following:

$$R_n=H+LE+G \tag{1.2}$$

1.2.2 Evapotranspiration

Within hydrologic cycle, evapotranspiration (ET) or latent heat (LE) is driven primarily by evaporative power of net radiation. The partitioning of net radiation between sensible and latent

heat flux is markedly dependent on the amount of available water on the earth surface. ET (or LE) is an important part of water and energy balance at the global surface. Figure 1.2 shows the ET account for the large portion of water and energy resources. In the hydrologic budget of Florida, ET is the second important component after precipitation (Jones et al., 1984). Therefore, accurate estimation of ET is necessary in evaluating parameterization schemes used in hydrologic and climatic models, qualifying agricultural application (such as crop yield and water use), assessing the environmental aspects of natural ecosystems, and improving water management techniques (Rizou and Nnadi, 2008).

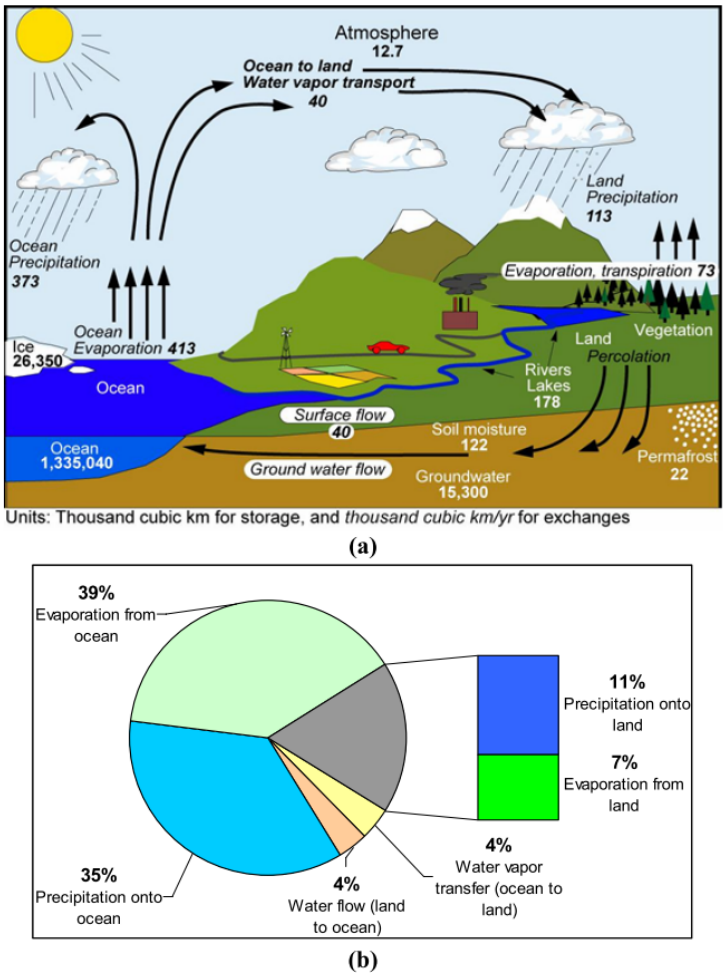

Figure 1.2: (a) Mean global water cycle showing storage (regular font) and exchanges (italic font); (b) long-term budget of water flows (Trenberth et al., 2007

1.2.2.1 ET method

Large scale ET estimation is a great concern in numerous studies from regional water resources management to local irrigation scheduling (Bastiaanssen et al., 1998a; 1998b; Kite and Droogers,

2000; Schuurmans et al., 2003). Basically, point measurement of ET can be made through: (a) crop coefficient and climatic parameters and (b) soil moisture monitoring, and vapor flux measurement or energy balance using eddy covariance method. These methods including the Priestley-Taylor method, the Penman-Monteith method, and reference ET method are introduced as below, while Table 1.2 summarizes the input data requirements of each method.

Table 1.2: Input required in ET method (Chang, 2008)

Parameter	PET Method		REF ET Method
	PT	PM	PMFAO
a. Solar Radiation	X	X	X
b. Incoming Longwave Radiation	X	X	
c. Outgoing Longwave Radiation	X	X	
d. Albedo, Emissivity	X	X	
e. Ground Heat flux	X	X	
f. Tempature	X	X	X
g. vapor Pressure/Relative Humidity		X	X
h. Wind speed		X	X
i. Aerodynamic Resistance		X	
j. Bulk Surface Resistance		X	
k. Vegetation index			

X:calculation is required

The Priestley-Taylor: The Priestley-Taylor method uses the concept of theoretical lower limit of evaporation from a wet surface as the "equilibrium" evaporation to estimate potential ET. The equation is:

$$\lambda\rho_w ET_0 = \alpha\frac{\Delta}{\Delta+\gamma}(R_n - G) \quad (1.3)$$

where ET_o is potential ET (mm day^{-1}); λ is latent heat of vaporization (Jg^{-1}); ρ_w is density of water (gm^{-3}); α=1; Δ is slope of the saturation vapor pressure temperature curve; γ is psychometric constant; R_n is net radiation (Wm^{-2}), and G is soil heat flux (Wm^{-2}).

Equilibrium conditions reflect evaporation from a wet surface under conditions of minimum advection that result in the actual vapor pressure of the air approaching the saturation vapor pressure. Priestly and Taylor (1972) showed that for conditions of minimum advection with no edge effects, α=1.26. In this case, the aerodynamic term of the combination equation is effectively assigned a constant percent of the radiation term.

The Penman Monteith model: The Penman Monteith model is extension of the Penman equations that allows the equation to be applied to a range of surface vegetation through the introduction of plant -specific resistance factors and is given as:

$$\lambda\rho_w ET_0 = \frac{\Delta(R_n-G)+\rho_a c_p(e_s-e_d)/r_a}{\Delta+\gamma(1+\frac{\gamma_s}{\gamma_a})} \quad (1.4)$$

where $e_s - e_d$ is vapor pressure deficit of the air (mb); e_s is saturation vapor pressure of the air (mb); e_d is actual vapor pressure of the air (mb); ρ_a is mean air density at constant pressure; c_p is specific heat of air, γ_s is bulk surface resistance, and γ_a is aerodynamic resistances.

The aerodynamic resistance is estimated using Monin-Obukhov similarity and assuming neutral conditions by

$$\Upsilon_a = \frac{\ln[(z-d)/z_0]\ln[(z-d]/Z_{ov}}{k^2 u} \quad (1.5)$$

where z is the height at which the wind speed u was measured, d is displacement height estimated to be 0.67 Z_{veg}, Z_{veg} is vegetation height, Z_0 is roughness height for momentum was approximated as 0.1 Z_{veg}, Z_{ov} is roughness height for water vapor and was approximated as 0.1 Z_0 and k is the Von Karmen's constant (0.4).

Reference Evapotranspiration: Reference Evapotranspiration using Penman-Monteith Method was developed by the Food Agriculture Organization of the United Nation (FAO) (Walter et al., 1998; Allen et al., 2005b). The ASCE Evapotranspiration in Irrigation and Hydrology Committee (ASCE-ET) also recommends, for the intended purpose of establishing uniform ET estimates and transferable crop coefficients, two standardized reference ET surfaces: 1) a short crop (similar to grass) and 2) a tall crop (similar to alfalfa). ASCE-ET also recommends one standardized reference ET equation based on the Penman-Monteith equation (Allen et al., 1998; Walters et al., 2000). As a part of the standardization, the "full" form of the Penman-Monteith equation and associated equations for calculating aerodynamic and bulk

surface resistance were combined and reduced to a single equation having two constants. The constant vary as a function of the reference surface and time step (hourly or daily). The ASCE PM-2000 method standardizes values for short and tall reference crops on a daily and hourly basis.

The FAO56-PM method (Allen et al., 1998) is an hourly or daily grass reference ET equation derived from the ASCE PM-90 by assigning certain parameter values based on a specific reference surface. The surface has an assumed height of 0.12m, a fixed surface resistance, γ_s of 70 sm^{-1} and an albedo of 0.23. The zero plane displacement height and roughness lengths are estimated as a function of the assumed crop height, so that γ_a become a function of only the measured wind speed. The height for the temperature, humidity, and wind measurements is assumed to be 2 m. The latent heat of vaporization (LE) is assigned a constant value of 2.45 MJ kg^{-1}. For a grass reference on daily basis, the ASCE 2000 method is identical to FAO 1998 Pennman-Monteith equation.

1.2.3 Land use effects

At land scale, human activities affect regional climate by changing land use characteristics, which impact distributions of ecosystem, energy (latent and sensible heat), and mass fluxes (e.g. water vapor, trace gases and particulates). These contrasting land use patterns induce convection and circulation that affect cloud formation and precipitation. For example, when large areas of forests are cleared, reduced transpiration result in less cloud formation, less rainfall, and increase

drying of surface (Dale, 1997). Therefore, understanding the consequences of changing vegetation cover for surface energy and water budget is important for better understanding of the role that vegetation feedbacks have on larger scale process such as cumulus cloud formation and rate of precipitation (Eltahir and Bras, 1996).

1.2.3.1 Interaction between atmosphere, land and vegetation

Vegetation strongly influences exchanges of energy and moisture between land and atmosphere through 1) vegetation's response to incoming radiation and its emission of longwave radiation; 2) vegetation's physical presence; and 3) plant's transpiration. These process affect diurnal temperature range, processes in atmospheric boundary layer, cloud cover, rainfall, differential heating, and atmospheric circulations (McPherson, 2007). The fraction of solar radiation that is reflected by the land surface (its albedo) can strongly influence the temperature by affecting how much energy the land absorbs. For example, high albedo of snow tends to result in localized cooling because it reflects so much radiation. Conversely, forests are usually darker and absorb more radiation than non-forested land. Hence, energy that is absorbed by the land surface can either cause direct heating or drive the evaporation of water creating a cooling effect. The balance between the two processes controls changes in the surface temperature.

The presence of vegetation can further increase the evaporative (cooling) flux component in at least two ways 1) using their roots, plants can extract additional water from the soil that would otherwise not evaporate easily because it resides at some depth; and 2) vegetation, particularly

forest, makes the surface rougher than bare land and this increases wind turbulence near the surface, thus enhancing evaporation (Meir et al., 2006). This is why tropical rain forests tend to lower maximum temperature relative to grassland or savannah.

To facilitate discussions of the physical process of land use change, a general schematic is provide in Figure 1.3 as an example of the conversion from forest to grassland. When forestlands converted to grass lands, the consequence is that the decreased root depth would reduce the ability for water saturation in the soil. This conversion also decreases roughness length, hence decreases in turbulent mixing length in the boundary layer and therefore decreased evapotranspiration. Furthermore, increasing non-water stressed bulk stomatal resistance would effectively reduce the ability for water to pass from the plant to the atmosphere, which will result in less evapotranspiration. Hence, these direct hydrological effects suggest a net decrease in evapotranspiration, and more energy becomes available for sensible heat flux and surface temperature (T_{surf}) increase.

The decrease in latent heat flux and increases in sensible heat flux and surface temperature would decrease the low cloud cover because of the increase of buoyancy and decrease of moisture content in the near surface atmospheric. Moreover, increased surface temperature is accompanied by an increase in the amount of longwave (LW) radiation leaving the earth's surface (LW_u) and, because of the reduced low cloud cover, less of this radiation is returned to surface (LWd). These two effects yield a decrease in net longwave radiation at the surface. The decreased low cloud cover also allows more incoming shortwave radiation to reach the surface (SWin).The increase in downward shortwave radiation at the surface, however, is opposed by a

decrease in absorbed shortwave radiation resulting from the changes to surface albedo. Finally, if the net surface radiation balance is negative, both latent and sensible heat fluxes may decrease, and surface temperature may also decrease. Hence, we can clearly understand how land use changes affect the physical processes.

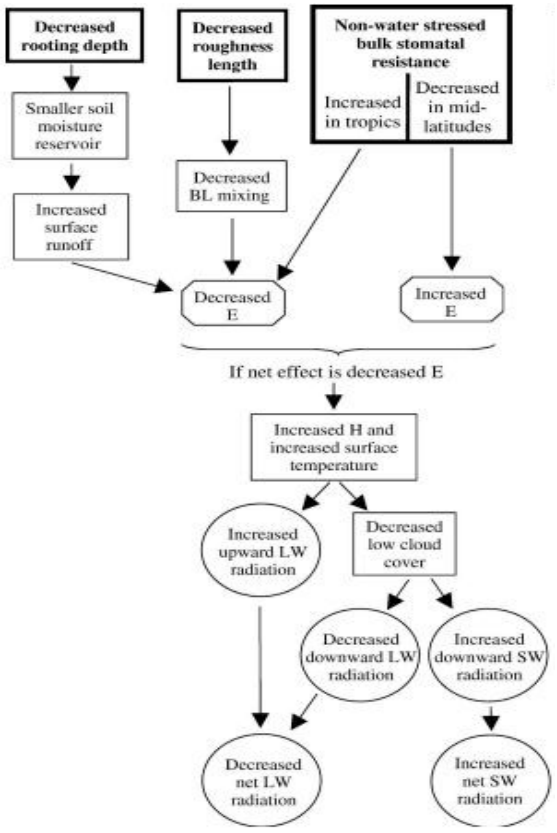

Figure 1.3: Idealized schematic of physical processes influenced by the conversion of forests to grasslands. [Model prescribed physical parameters are in bold; BL: boundary layer, E: evapotranspiration, H: sensible heat flux, LW: longwave, and SW: shortwave. All radiative fluxes (in circules) are surface fluxes (positive toward the surface)] (Revised from Findell et al., 2007)

1.2.4 Drought index

Drought is difficult to describe and to measure by an index because of the wide variety of disciplines affected by drought, its diverse geographical and temporal distribution, and the varying scales in drought events (Chang, 2008). Traditional, drought has been classified according to the hydrologic compartment in which there is a water deficiency. Meteorological drought results from a shortage of precipitation, while hydrological drought describes a deficiency in the volume of water supply, which includes stream-flow, reservoir storage, and/or groundwater depths (Wilhite, 2000). Agricultural drought relates to a shortage of available water for plant growth and is assessed as insufficient soil moisture to replace evapotranspirative losses [World Meteorological Organization (WMO), 1975]. Hence, many qualitative indices of drought have been developed based on climatic and meteorological observations, and are useful for describing the varying of drought.

A drought index can be used for (1) examining the spatial and temporal characteristics of drought, the severity of drought and making comparisons between different regions (Alley, 1984, 1985; Soule, 1992; Kumar and Panu, 1997; Dai et al., 1998; Nkemdirim and Weber, 1999), (2) providing information for decision-makers in business, government and to the public stakeholders, (3) calculating the probability of drought termination (Karl et al., 1987), (4) determining drought assistance (Wilhite et al., 1986) and assessing forest fire hazard and dust storm frequency (Wilhite et al., 1986), and (5) predicting crop yield(Sakamoto, 1978; Kumar and Panu, 1997). More commonly used schemes include the Palmer Drought Severity Index (PDSI) and the Moisture Anomaly Index (Z-index) (Palmer, 1965), the Rainfall Anomaly

Index (RAI) (van Rooy, 1965), the Crop Moisture Index (CMI) (Palmer, 1968), the Bhalme–Mooley Index (BMDI) (Bhalme and Mooley, 1980), the NOAA Drought Index (NDI) (Strommen et al., 1980; Titlow, 1987), the Standardized Anomaly Index (Katz and Glantz, 1986), the Standardized Precipitation Index (SPI) (McKee et al., 1993, 1995), Percent Normal, Deciles (Gibbs and Maher, 1967), and the Normalized Difference Vegetation Index-based Vegetation Condition Index (Kogan, 1995).

Among all, the Palmer Drought Severity Index (PDSI), the Standardized Precipitation Index (SPI), and the Crop Moisture Index (CMI), are the main drought indices used by United Stated now. The Palmer Drought Severity Index (PDSI) is calculated based on all the terms of the hydrological equation including precipitation, temperature, and available water content (AWC) of the soil. It uses a 0 as normal, and drought is shown in terms of minus number; for example, minus 2 is moderate drought, minus 3 is severe drought, and minus 4 is extreme drought. The advantage of the Palmer index is that it is the first comprehensive drought index and standardized to local climate, so it can be applied to any part of the country to demonstrate the relative drought or rainfall condition. The disadvantage is that it may lag emerging drought by several months, and less well-studied for mountainous land or areas of frequent climatic extremes. Hence, it only works best of Continental Divide (Karl, 1983; Heddinghaus et al., 1991; Heim, 2000)

The Standardized Precipitation Index (SPI) is an index calculating the probability distribution of the month and seasonal observed precipitation totals, and the probabilities are normalized using the inverse normal (Gaussian) function. The index is negative for dry, and positive for wet

conditions. As a drought event occurs any time, the SPI is continuously negative and reaches the intensity where the SPI is -1.0 or less. The event ends when the SPI becomes positive. The SPI is computed by the National Climatic Data Center (NCDC) for several time scales, ranging from one month to 24 months, to capture the various scales of both short-term and long term drought (Guttman et al., 1992; Guttman, 1998).

The Palmer Crop Moisture Index (CMI) also uses a meteorological approach to monitor week crop conditions and quantifies drought impacts on agriculture during the growing season. This index was designed to evaluate short-term moisture conditions across major crop producing regions. It is based on the mean temperature and total precipitation for each week within a Climate Division without considering the localized conditions such as soil type, crop type, rooting depth, or stages of crop development (Hayes, 2003). Table 1.3 is the summary of the main drought indices

Table 1.3: The summary of main drought indices (Tsakiris, 2007)

Index	Description and Use	Strengths	Weaknesses
Meteorological Drought Indices			
Percent of Normal Precipitation and Accumulated Precipitation of Departure	Simple calculation used by general audiences	Effective for comparing a single region or season	Precipitation does not have a normal distribution values depend on location

Index	Description and Use	Strengths	Weaknesses
Meteorological Drought Indices			
			and season
Deciles Gibbs and Maher(1967)	Simple calculation grouping precipitation into deciles used by the Australian Drought Watch System	Accurate statistical measurement simple calculation provides uniformity in drought classifications	Accurate calculations require a long climatic data record
Standardized Precipitation index (SPI) Mckee et al. (1993)	Based on the probability of precipitation for any time scale. Used by many droght planners	Computed for different time scales, provides early warning of drought and help assess drought severity	Values based on preliminary data may change Precipitation is the only parameter used
Palmer Drought Severity Index (PDSI) Palmer (1965) Alley (1984)	Soil moisture algorithm calibrated for relatively homogeneous regions Used in the USA to trigger drought relief programs and contingency plans	The first comprehensive drought index, used widely Very effective for agricultural drought since include soil moisture	PDSI may lag emerging droughts. Less well suited for mountainous areas of frequent climatic extremes complex. Categories not necessarily consistent, in terms of probability of occurrence, spatially

Index	Description and Use	Strengths	Weaknesses
Meteorological Drought Indices			
			or temporally
Crop Moisture Index (CMI) Palmer (1968)	Derivative of the PDSI Reflects moisture supply in the short term	Identifies potential agricultural droughts	It is not a good long-term drought monitoring tool
Recoinnaissance Drought Index (RDI) Tsakiris (2004)	similar to SPI Basic variable P/PET	Drought is based on both precipitation and potential evapotranspiration. Appropriate for climate change scenarios	Data needed for calculation of PET
Hydrological Drought Indices			
Palmer Hydrological Drought (PHDI) Palmer(1965)	Same as PDSI but more exigent to consider a Drought end. The drought terminates only when the ratio of Pe (moisture received to moisture required) is 1	Same as PDSI	Same as PDSI
Surface water Supply index (SWSI) Shefer and Dezman (1992)	Developed form the Palmer index to take into account the	Represents surface water supply conditions and includes water	Management dependent and unique to each basin, which

Index	Description and Use	Strengths	Weaknesses
Meteorological Drought Indices			
	mountain snowpack	management. Simple calculation combines hydrological and climatic features. Considers reservoir storage	limits inter-basin comparisons. Does not represent well extreme events

1.3 Problem Statement

Evapotranspiration varies with vegetation as a result of plant effects on water demand and supply. Under wet conditions, ET is principally limited by the atmospheric demand of water vapor, driven by advection and radiation. For example, the high aerodynamic roughness of forests allows exchanges of heat and water vapor between canopy surface and air to occur at rates up to 10 times higher than those possible for shorter vegetation, creating contrasting ET patterns under wet conditions (Kelliher et al., 1993; Calder, 1998). While, under drier conditions, the availability of soil moisture becomes the primary control of ET, and differences in capacity of plants access water, often dictated by rooting depth, can result in contrasting evaporative losses across vegetation types (Calder, 1998). Tree tend to have deeper roots than herbaceous

plants (Canadell et al., 1996; Schenk and Jackson, 2002), and hence can maintain higher ET than grasslands when the supply declines (Calder et al., 1997; Sapanov, 2000).

In reality, parameters like land use/cover and soil properties vary widely and are sparsely measured by ground-based measurements. As human activities affect land use characteristics, which impact the distribution of ecosystem, energy (latent and sensible heat), and mass fluxes (e.g. water vapor, trace gases and particulates), contrasting land use patterns induce convection and circulation that affect cloud formation and precipitation. Therefore, the drought's duration and intensity would be different on various land use and drought index should be able to reflect the level of severity in drought events resulting from land use effects.

However, current drought indices could not fully demonstrate land use effects. Table 1.4 shows characteristics of current drought indices. The simplistic approaches based on some measures of rainfall deficiency, such as, Declies, SPI, RI, RAI, and BMDI, would underestimate the severity of drought (Tsakiris and Vangelis, 2005). More complex drought indices, which are based on water balance model, PDSI and CMI, assumed that parameters such as land use/land cover, and soil properties are uniform over the entire climatic zone (7000–100,000 km^2) (Narasimhan and Srinivasan, 2005). The SWSI does not directly consider other elements of the hydrological cycles that are critical for drought monitoring, such as evaporation, soil moisture and land use characteristic (Keyantash, 2004). Hence, developing a land use adapted drought index is urgent for better understanding of land use effects on the drought events.

To develop a new drought index, investigating energy and water balances for various land use areas is very important and necessary. The existing energy at soil-canopy interface can be

partitioned into evapotranspiration, which establishes a fundamental linkage between energy and water balances (Kustas and Normanm, 1996). The balance of energy flux at terrestrial surface is critical for appropriate interpretation of water balance, carbon dioxide fluxes, and local microclimate and should be justified in a wide variety ecosystem. Figure 1.4 showed the energy, water and carbon cycles in forest ecosystem as tightly coupled through the evapotranspiration (ET) processes. Therefore, quantifying the water and energy balance on ecosystem could provide insights to how management affects the microclimate of ecosystem and the feedbacks of land use change to climate change at a regional scale (Gholz and Clark, 2002; Powell et al., 2005; Restrepo and Arain, 2005; Jackson et al., 2005; Pielke et al., 2007; Liu et al., 2008)

Table 1.4: Characteristics of current drought indices (Byun and Wilhite, 1999)

Name	Factor used	Timescale	Main concept	Source, year created
PDSI	r, t, et, sm, rf	m (2w)	Based on moisture input, output, and storage. Simplified soil moisture budget	Palmer (1965)
RAI	r	m,yr	Compared r to arbitrary values of +3 and -3, which are assigned to the mean of 10 extreme + and - anomalies of r	Rooy (1965)
Deciles	r	m	Dividing the distribution of the occurrences over a long-term record into sections, each represents 10%	Gibbs and Maher (1967)

CMI	r, t	w	Like the PDSI, except considering available moisture in top 5 ft of soil profile	Palmer (1968)
BMDI	r	m,yr	Percent departure of r from the long-term mean	Bhalme and Mooley (1980)
SWSI	P,sn	m	Weighted average of standardized anomalies of the main elements of water budget	Shafter and Dezman (1982)
SMDI	Sm	yr	Summation of daily sm for a year	Hollinger et al. (1993)
CSDI	Ev	s	Summation of the calculated et divided into possible et during the growth of specific crops	Meyer et al.(1993)
SPI	r	3m,6m,12m, 24m, 48m	Standardized anomaly for multiple time scales after mapping probability of exceedance from a skewed distribution	Mckee et al. (1993)
RI	r	yr,c	Pattern and abnormalities of r on a continental scale	Gommes and Petrassi (1994)
RDI	r,t,sn,st, rs	M	supply element-demand element	Weghorst (1996)

Abbreviations: P- factors used in PDSI, r- precipitation, et- evapotranspiration, ev: evaporation, t-temperature, sm-soil moisture, rf-runoff, sn-snowpack, st-streamflow, rs-reservoir storage, w-week, m-month, s-season, yr-year, c-century, and 3m-3 months.

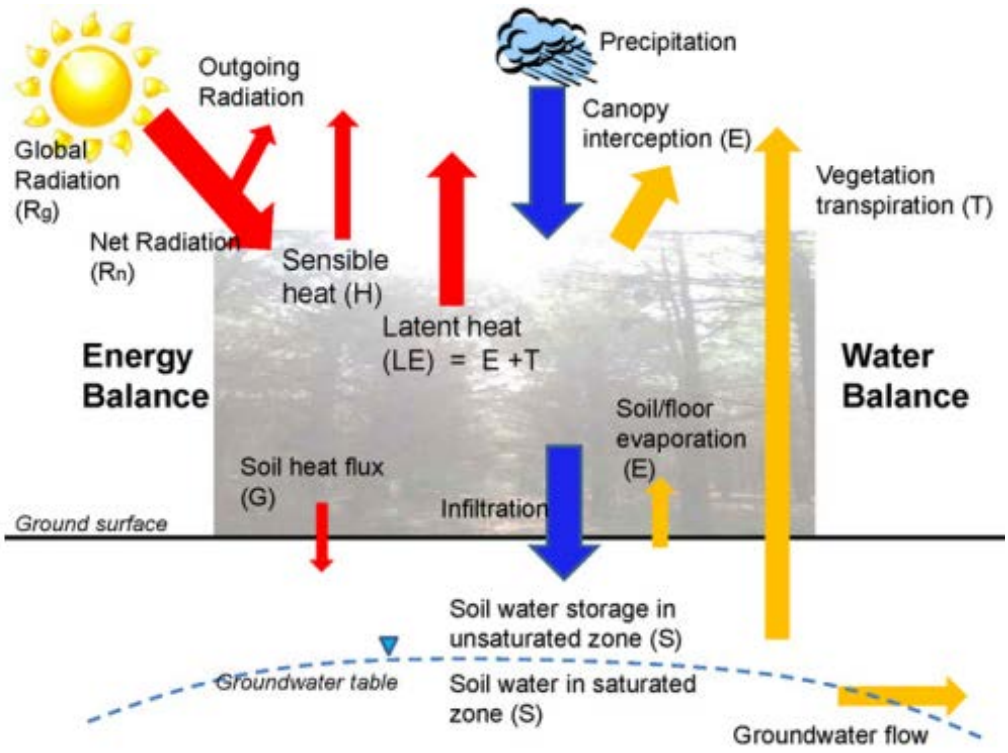

Figure 1.4: A sketch showing the coupling of energy and water cycle in a drained loblolly pine forest (Sun et al., 2010)

However, the conventional technologies for quantifying water and energy budgets, including in-situ and spatially-remote measurements, have the limitations in data sources. For example, characterization of the surface hydrologic cycle requires adequate long-term records of not only precipitation but also runoff and evaporation, however such records are lacking in observational data (Ming et al., 2006).

Modeling studies have advantages in extending scopes and overcoming limitations of traditional field experiments, which is particularly true when addressing regional and global issues including land use and climate change impacts. However, a drawback of a model-only approach for water and energy budget estimations is that models are not perfectly parameterized and calibrated as errors and biases exist and propagate through time (Ming et al., 2006). Therefore, developing a new method of quantifying water and energy budgets for various land use areas is necessary and critical.

To accurately calculate the net radiation, which in turn controls all the surface energy budget components, including latent heat flux, improved longwave radiation estimates are important (Crawford and Duchon, 1999; Duarte, 2006). Many reasonably successful techniques have been developed in recent decades that estimate downward longwave radiation (LW_d) based on the surface observations alone (Crawford and Duchon, 1999). Those equations are empirical and specific for the atmospheric conditions and have to be redefined or calibrated for each location (Bilbao et al., 2007).

Air temperature and water vapor pressure, which are more commonly used as inputs in existing models for estimating LW_d, would be affected by heterogeneous land use patterns and temporal changes in atmospheric circulation patterns. Hence, Rizou and Nnadi (2007) developed a land use adapted model, which superpositioned nonlinear temperature effects and water vapor in one equation, to account for the net impact on clear sky emissivity. Their land use adapted clear sky LW_d model was robust and adaptable for different land use areas, and had the smaller values of normalized Mean Bias Errors (MBE) and Root Mean Square than those of other existing models.

In their study, three months data in spring 2004 at current study area were analyzed but the seasonal variation and cloud effect were not considered on the various land use effects. Hence, improvements of the land use adapted model by considering the seasonal variation and cloud effects is indispensable and significant.

1.4. Dissertation Objectives and Organization

This dissertation addresses three main objectives: (1) propose a new land use adapted model that considering the seasonal and cloud effects; (2) quantify the differences in both energy and water balance on various land use areas and understanding climatic variables that affect the energy and water exchange between terrestrial ecosystem and the atmosphere; (3) develop a new regional land use adapted drought index using results of objectives 1 and 2. More specifically, this work, which consists of four independent studies, sought to:

1. Propose a new land use adapted model that considers seasonal and cloud effects (Chapter 2).
    - Analyze a yearly in-situ downward longwave data. The seasonal variation of LW_d radiation in yearly data in which the wet and dry season data were delineated to develop all sky condition LW_d radiation models
    - Compare factors (such as cloud and land use) affecting LW_d based on the dry season data.

- Develop new land adapted all-sky LW_d radiation models based on dry and wet season data.

2. Water Budget on various Land use areas at regional scales in Florida (*Chapter 3*).

- Investigate the water balance on various land uses (Lake, wetland, agriculture, forest, and urban) at regional scale.

  EI Niño-Southern Oscillation (ENSO), which is one of the most studied patterns of the world's climate, includes a strong natural inter-annual climate signal that affects the surface climate in numerous regions, including Florida.

- Understand how drought events, EI Niño, La Niña, and seasonal and inter-annual variations in climatic variables affect the hydrologic cycle over different land use areas

3. Energy Budget on various Land use areas at regional scales in Florida (*Chapter 4*).

- Investigate the energy balance on various land uses (Lake, wetland, agriculture, forest, and urban) at regional scale.
- Understand how drought events, EI Niño, La Niña, and seasonal and inter-annual variations in climatic variables affect the energy budget over different land use areas.

4. Develop a Regional Land Use Adapted Drought index (Chapter 5).

- Understand local ENSO patterns on the regional scale and develop a new land use drought index in Florida based on the North American Regional Reanalysis (NARR) data set.

References

Allen, R.G., Pereira, L.S., Raes, D., Smith, M., 1998, Crop evapotranspiration – Guidelines for computing crop water requirements, FAO Irrigation and drainage paper 56, Food and Agriculture Organization of the United Nations, Rome

Allen, R.G., Walter, I.A., Elliot, R.L., Howell, T.A., 2005b, ASCE Standardized Reference Evapotranspiration Equation, American Society of Civil Engineers, Reston, Virginia

Alley, W.M., 1984, The Palmer drought severity index: limitation and assumptions, J. Climate Appl. Meteor, 23, 1100–1109

Alley, W.M., 1985; The Palmer drought severity index as a measure of hydrologic drought, Water Resour. Bull, 21, 1, 105–114

Angstrom, A, 1918, A study of the radiation of the atmosphere, Smithson Misc Collect 65, 1–159

ASOS, Program, 1998, ASOS User's Guide, http://www.nws.noaa.gov/asos/pdfs/aumtoc.pdf

Aubinet, M., Grelle, A., Ibrom, A., Rannik, Ü., Moncrieff, J., Foken, T., Kowalski, A.S., Martin, P.H., Berbigier, P., Bernhofer, C., Clement, R., Elbers, J., Granier, A., Grünwald, T.,

Morgenstern, K., Pilegaard, K., Rebmann, C., Snijders, W., Valentini, R., Vesala, T., 2000, Estimates of the annual net carbon and water exchange of forests: the EUROFLUX methodology, Adv Ecol Res, 30,113–175

Barr, A.G., Morgenstern, K., Black, T.A., McCaughey, J.H., Nesic, Z., 2006, Surface energy balance closure by the eddy-covariance method above three boreal forest stands and implications for the measurement of the CO 2 flux, Agr Forest Meteorol, 140:,322–337

Bastiaanssen, W.G.M., Menenti, M., Feddes, R.A., Holtslag, A.A.M., 1998a, A remote sensing surface energy balance algorithm for land (SEBAL): Part 1 formulation, J. of Hydrology, 198 – 212

Bastiaanssen, W.G.M., Pelgrum, H., Wang, J., Ma, Y., Moreno, J., Roerick, G.J., van der Wal, T., 1998b, The surface energy balance algorithm for land (SEBAL): Part 2 validation, J. of Hydrology, 212 – 213

Bates B. C., Kundzewicz Z. W., Wu S., Palutikof J. P., 2008, Climate Change and Water, IPCC, Geneva

Bhalme, H.N., Mooley, D.A., 1980, Large-scale droughts/floods and monsoon circulation, Mon. Wea. Rev, 108, 1197–1211

Bilbao, Julia, De, M., Argimiro, H., 2007, Estimation of daylight downward longwave atmospheric irradiance under clear-sky and all-sky conditions, American Meteorological Society, Boston, MA, ETATS-UNIS

Blanken, P.D., Black, T.A., Neumann, H.H., den Hartog, G., Yang, P.C., Nesic, Z., Staebler, R., Chen, W., Lee, X., 1998, Turbulent flux measurements above and below the overstory of a boreal aspen forest, Bound-Lay Meteorol, 89,109–140

Brenner, J., 1991, Southern oscillation anomalies and their relation to Florida wildfires, Fire Manage., Notes 52, 28–32

Brolley, J. M., O'Brien, J. J., 2007, Experimental drought threat forecast for Florida, Agricultural and Forest Meteorology, 145,1-2, 84-96

Burke, E. J., Brown, S. J., 2006, Modeling the recent evolution of global drought and projections for the twenty-first century with the Hadley Centre Climate Model, Journal of Hydrometeorology, 7,5, 1113-1125

Byun, H. R., Wilhite, D. A., 1999, Objective quantification of drought severity and duration, Journal of Climate, 12, 9, 2747-2756

Calder IR, 1998, Water use by forests, limits and controls, Tree Physiology, 18, 625–631

Calder I.R, Rosier P.T.W., Prasanna K.T., 1997, Eucalyptus water use greater than rainfall input – a possible explanation from southern India, Hydrology and Earth System Science, 1, 249–256

Canadell J., Jackson R.B., Ehleringer J.R., 1996, Maximum rooting depth of vegetation types at the global scale, Oecologia, 108, 583–595

Castellvi, F., Snyder, R.L., Baldocchi, D.D., 2008, Surface energy-balance closure over rangeland grass using the eddy covariance method and surface renewal analysis, Agr Forest Meteorol, 148,1147–1160

Chang, N. B., Yang, Y. J. Goodrich, J. A., 2008, The development of water availability index (WAI) under global climate change impacts with the aid of remote sensing technologies. J. Environmental Management.

Crawford T.M., Duchon C.E., 1999, An improved parameterization for estimating effective atmospheric emissivity for use in calculating daytime downwelling longwave radiation. J Appl Meteorol, 38, 4, 474-480

Dai, A., Trenberth, K. E., Karl, T.R., 1998, Global variations in droughts and wet spells: 1900–1995. Geophys. Res. Lett. 25, 17, 3367–3370

Dale, V. H., 1997, The relationship between land-use change and climate change, ecological applications, 7, 3, 753-769

Douglas, E. M., Jacobs, J. M., 2009, A comparison of models for estimating potential evapotranspiration for Florida land cover types, Journal of Hydrology, 373, 3-4, 366-376

Eltahir, E. A. B., Bras, R. L., 1994, Precipitation recycling in the Amazon basin. Quart. J. Roy. Meteor. Soc., 120, 861–880., and, 1996: Precipitation recycling. Rev. Geophys., 34, 367–378

Federal Emergency Management Agency (FEMA), 1995, National mitigation strategy—partnerships for building safer communities, FEMA, Washington, D.C., 26

Findell, K., LShevliakova, E., 2007, Modeled impact of anthropogenic land cover change on climate, Journal of Climate, 20,14, 3621-3634

Gholz, H.L., Clark, K. L., 2002, Energy exchange across a chronosequence of slash pine forests in Florida. Agricultural and Forest Meteorology, 112, 87–102

Gibbs, W.J., Maher, J.V., 1967, Rainfall deciles as drought indicators. Bureau of Meteorology Bulletin, 48, Commonwealth of Australia, Melbourne

Guttman, N.B., 1998, Comparing the Palmer drought index and the standardized precipitation index, J. Amer. Water Resour. Assoc., 34, 113-121

Guttman, N.B., Wallis, J.R., Hosking, J.R.M., 1992, Spatial comparability of the Palmer drought severity index, Water Resour. Bull., 28, 1111-1119

Hayes, M., 2003, Drought Indices. Nebraska, National Drought Mitigation Center

Heddinghaus, T.R., Sabol, P., 1991, A review of the Palmer drought severity index: where do we go from here? Proceedings, 7th Conf. on Appl. Climatol., 10-13 September, Boston: American Meteorological Society, 242-246

Heim, Jr., R.R., 2000, Drought indices: A review, chapter 11. In drought: A global assessment (Donald A. Wilhite, ed.), (Routledge Hazards and Disasters Series, volume 1), Routledge, London, 159-167

Hernandez-Ramirez, G., Hatfield, J., 2010, Energy balance and turbulent flux partitioning in a corn–soybean rotation in the Midwestern US, Theoretical and Applied Climatology, 100,1, 79-92

Humes, K. S. Norman, J. M., Moran, M. S., 1996, Single and dual-source modeling of surface energy fluxes with radio metric surface temperature. J. Appl. Meteor., 35, 110–121

Jackson, R.B., Jobbagy, E.G., Avissar, R., 2005, Trading water for carbon with biological carbon sequestration, Science, 1944–1947

Jarosz, N., Brunet, Y., Lamaud, E., Irvine, M., Bonnefond, J.M., Loustau, D., 2008, Carbon dioxide and energy flux partitioning between the understorey and the overstorey of a maritime pine forest during a year with reduced soil water availability, Agr Forest Meteorol, 148,1508–1523

Jones, J.W., Allen, L.H., Shih, S.F., Rogers, J.S., Hammond, L.C., Smajstrala, A.G., Martsolf, J.D., 1984, Estimated and measured evapotranspiration for Florida climate, crops, and soils. Bulletin 840, University of Florida Institute of Food and Agricultural Services, Gainesville, Florida

Karl, T., Quinlan, F., Ezell, D.S., 1987, Drought termination and amelioration: its climatological probability, J. Climate Appl. Meteor., 26, 1198–1209

Karl, T.R., 1983, Some spatial characteristics of drought duration in the United States, J. Climate Appl. Meteor., 22, 1356-1366

Katz, R.W., Glantz, M.H., 1986, Anatomy of a rainfall index. Mon. Wea. Rev., 114, 764–771

Kelliher F.M., Leuning R., Schulze E.D., 1993, Evaporation and canopy characteristics of coniferous forests and grasslands, Oecologia, 95, 153–163

Kipp and Zonen, 2000, CNR1 Net radiometer instruction manual, Delft, The Netherlands

Kite, G.W., Droogers, P., 2000, Comparison evapotranspiration estimates from satellites, hydrological models and field data, J. of Hydrology, 229, 3 – 18

Kogan, F.N., 1995, Droughts of the late 1980s in the United States as derived from NOAA polar-orbiting satellite data, Bull. Am. Meteor. Soc. 76 (5), 655–668

Konzelmann, T., van de Wal, R. S. W., Greuell, W., Bintanja, R., Henneken, E. A. C., Abe-Ouchi, A., 1994, Parameterization of global and longwave incoming radiation for the Greenland Ice Sheet, Global and Planetary Change, 9, 1-2, 143-164

Kumar, V., Panu, U., 1997, Predictive assessment of severity of agricultural droughts based on agro-climatic factors, J. Am. Water Resour. Assoc, 33, 6, 1255–1264

Liu, Y., Stanturf, J., Lu, H., 2008, Modeling the potential of the Northern China forest shelterbelt in improving hydroclimate conditions, J. of the American Water Resources Association, 44, 5, 1176–1192

Lockwood, J. G., 1999, Is potential evapotranspiration and its relationship with actual evapotranspiration sensitive to elevated atmospheric CO2 levels? Climatic Change, 41, 193–212

Massman, W.J., Lee, X., 2002, Eddy covariance flux corrections and uncertainties in long-term studies of carbon and energy exchanges, Agr Forest Meteorol, 113,121–144

Mauder, M., Liebethal, C., Göckede, M., Leps, J-P., Beyrich, F., Foken, T.., 2006, Processing and quality control of flux data during LITFASS-2003, Boundary-Layer Meteorol, 121,67–88

Mavromatis, T., 2007, Drought index evaluation for assessing future wheat production in Greece, International Journal of Climatology, 27, 7, 911-924

McKee, T.B., Doesken, N.J., Kleist, J., 1993, The relationship of drought frequency and duration to time scales. In: Proceedings of the 8th Conference on Applied Climatology. AMS, Boston, MA, 179–184

McKee, T.B., Doesken, N.J., Kleist, J., 1995, Drought monitoring with multiple time scales. In: Proceedings of the 9th Conference on Applied Climatology. AMS, Boston, MA, 233–236

McPherson, R. A., 2007, Review of vegetation, atmosphere interactions and their influences on Mesoscale phenomena, Progress in Physical Geography, 31, 3

Meir, P., 2006, The influence of terrestrial ecosystems on climate, Trends in Ecology & Evolution, 21,5, 254-260

Niemeyer, S., 2006, New drought index, Isora Italy, Institute for environment and Sustainability

Nkemdirim, L., Weber, L., 1999, Comparison between the droughts of the 1930s and the 1980s in the Southern Prairies of Canada, J. Climate, 12, 2434–2450

Oke T.R, 1987, Boundary Layer Climates, 2nd edn. Methuen and Co. Inc, New York, 435

Palmer, W.C., 1965. Meteorological Drought Research Paper No. 45, US Weather Bureau, Washington, DC

Palmer, W.C., 1968, Keeping track of crop moisture conditions, nationwide: the Crop Moisture Index. Weatherwise 21, 156–161

Penman, H.L.,1948, Natural evaporation from open water, bare soil and grass, Proc. Roy. Soc. London, A193, 120-146

Penman, H.L., 1956, Evaporation: An introductory survey, Neth. J. Agr. Res., 4, 1, 9-29

Pielke, R. A., Adegoke, J., Beltrán-Przekurat, A., Hiemstra, C. A., Lin, J., Nair, U. S., Niyogi, D., Nobis, T. E., 2007, An overview of regional land-use and land-cover impacts on rainfall, Tellus B, 59,3, 587-601

Pielke, R.A., Adegoke, J., Beltra´n-Przekurat, A., Hiemstra, C.A., Lin, J., Nair, U.S., Niyogi, D., Nobis, T.E., 2007, An overview of regional land-use and land-cover impacts on rainfall, 2007. Tellus B, 59, 3, 587–601

Powell, T. L., Starr, G., Clark, K. L., Martin, T. A., Gholz, H. L., 2005, Ecosystem and understory water and energy exchange for a mature, naturally regenerated pine flatwoods forest in North Florida, Canadian Journal of Forest Research, 35, 7, 1568–1580

Priestley, C. H. B., Taylor, R. J., 1972, On the assessment of surface heat flux and evaporation using large-scale parameters, Monthly Weather Review, 100, 81-92.

Restrepo, N.C., Arain, M.A., 2005, Energy and water exchanges from a temperate pine plantation forest, Hydrological Processes, 19, 27–49

Rizou, M., Nnadi, F., 2007, Land use feedback on clear sky downward longwave radiation: a land use adapted model, Int. J. of Climatol., 27(11): 1479-1496.

Rizou, M., Nnadi, F., Sumner, D.M., 2008, Controls and parameterizations of evapotranspiration at a grassland in Florida, Agric. Forest Meteorol.

Sakamoto, C. M., 1978, The Z-index as a variable for crop yield estimation, Agric. Meteor., 19, 305–313

Sapanov M. K., 2000, Water uptake by trees on different soils in the Northern Caspian region. Eurasian soil science, 33, 1157–1165

Schenk H.J., Jackson R.B., 2002, The global biogeography of roots. Ecologial Monographs, 72, 311–328

Schuurmans, J.M., Troch, P.A., Veldhuizen, A.A., Bastiaanseen, W.G.M., Bierkens, M.F.P., 2003, Assimilation of remotely sensed latent heat flux in a distributed hydrological model, Advances in Water Resources, 26, 151 – 159

Sellers, P.J., Rasool, S.I., Bolle, H.J., 1990, A review of satellite data algorithms for studies of the land surface. Bull. Am. Meteorol. Soc. 71, 10, 1429-1447

Shuttleworth, W.J., 1993, Chapter 4: Evaporation. In: Maidment D.R., Handbook of Hydrology. McGraw-Hill Inc., USA

Soule, P.T., 1992, Spatial patterns of drought frequency and duration in the contiguous USA based on multiple drought event definitions. Int. J. Climatol. 12, 11–24

Strommen, N., Krumpe, P., Reid, M., Steyaert, L., 1980, Early warning assessments of droughts used by the U.S. agency for international development, In: Pocinki, L.S., Greeley, R.S., Slater, L. (Eds.), Climate and Risk. The MITRE Corporation, McLean, VA, 8–37

Sugita, M., Brutsaert, W., 1993, Cloud effect in the estimation of instantaneous downward longwave radiation, Water Resour. Res., 29

Sun, G., Noormets, A., 2010, Energy and water balance of two contrasting loblolly pine plantations on the lower coastal plain of North Carolina, USA, Forest Ecology and Management, 259, 7, 1299-1310

Teixeira, A.H.C., Bastiaanssen, W.G.M., Moura, M.S.B., Soares, J.M., Ahmad, M.D., Bos, M.G., 2008, Energy and water balance measurements for water productivity analysis in irrigated mango trees, Northeast Brazil, Agr Forest Meteorol, 148,1524–1537

Thornthwaite, C. W., 1948, An approach toward a rational clas-sification of climate. Geogr. Rev., 38, 55–94

Titlow, J.K., 1987, A precipitation-based drought index for the Delaware river basin. Publications in Climatology 40, C.W. Thornthwaite Associates, Centerton, NJ

Trenberth, K.E., Smith, L., Qian, T.T., Dai, A.G., Fasullo, J., 2007, Estimates of the global water budget and its annual cycle using observational and model data, J. Hydrometeorol, 8, 4, 758-769

Tsakiris G, Vangelis H, 2005, Establishing a drought index incorporating evapotranspiration, Eur Water, 9–10,1–9

Twine, T.E., Kustas, W.P., Norman, J.M., Cook, D.R., Houser, P.R., Meyers, T.P., Prueger, J.H., Starks, P.J., Wesely, M.L,. 2000, Correcting eddy covariance flux underestimates over a grassland, Agr Forest Meteorol, 103,279–300

Van Rooy, M.P., 1965, A rainfall anomaly index independent of time and space, Notos 14, 43–48

Verma, S.B., Kim, J., Clement, R.J., 1992, Momentum, water vapor and carbon dioxide exchange at a centrally located prairie site during FIFE, J Geophys Res, 97, 8629–18639

Walter, I.A., Allen, R.G., Elliott, R., Mecham, B., Jensen, M.E., Itenfisu, D., Howell, T.A., Snyder, R., Brown, P., Echings, S., Spofford, T., Hattendorf, M., Cuenca, R.H., Wrigh., J.L, Martin, D., 2000, ASCE Standardized Reference Evapotranspiration, Reston, Virginia

Wever, L.A., Flanagan, L.B., Carlson, P.J., 2002, Seasonal and interannual variation in evapotranspiration, energy balance, and surface conduc tance in northern temperate grassland, Agr Forest Meteorol, 112,31–49

Wilhite D. A, Knutson C. L, 2008, Drought management planning: conditions for success. Options Mediterraneennes Series A, 80, 141–148

Wilhite, D.A., Rosenberg, N.J., Glantz, M.H., 1986, Improving federal response to drought, J. Climate Appl. Meteor, 25, 332– 342

Wilhite. DA, 2000, Drought: A Global Assessment. London: Routledge Publishers

Wilson, K.B., Goldstein, A., Falge, E., Aubinet, M., Baldocchi, D., Berbigier, P., Bernhofer, C., Ceulemans, R., Dolman, H., Field, C., Grelle, A., Ibrom, A., Law, B.E., Kowalski, A., Meyers, T., Moncrieff, J., Monson, R., Oechel, W., Tenhunen, J., Valentini, R., Verma, S., 2002, Energy balance closure at FLUXNET sites, Agr Forest Meteorol, 113,223–243

World Meteorological Organization, (WMO), 1975, Intercomparison of conceptual models used in operational hydrological forecasting, WMO Oper. Hydrol. Rep., 7, WMO 429, Geneva

CHAPTER 2:

PREDICTING DOWNWARD LONGWAVE RADIATION FOR VARIOUS LAND USE IN ALL SKY CONDITION: NORTHEAST FLORIDA

This chapter has been submitted for publication with the following citation: C. H., Cheng and F., Nnadi. The Open Atmospheric Science Journal (In review, October, 2011).

2.1 Introduction

Accurate estimate of downward longwave radiation flux density (LW_d) is necessary for calculating the net radiation, which in turn modulates the magnitude of the surface energy budgets, including latent heat (Crawford et al., 1999). This knowledge is also required for (a) forecasting of temperature variation, frost occurrence and cloudiness, (b) estimation of climate variability and global warming, and (c) design of radiant cooling systems; (Crawford et al., 1999; Intergovernmental Panel on Climate Change [IPCC], 2001).

The downward longwave radiation is a thermal infrared energy (in the wavelength of 4.0 -100 μm), mainly controlled by water vapor and aerosols such as cloud water droplets, CO_2 and O_3 molecules (Niemelä et al., 2001). The longwave radiation is more difficult and expensive to measure than shortwave radiation because it is not a conventional measurement and thus its measurement is rarely included in meteorological stations (Kruk et al., 2009). Moreover, due to

poor vertical resolution of water vapor data and difficulties associated in the atmospheric emissivity and temperature, many reasonably successful techniques have been developed in recent decades that estimate LW_d based on the screen-level humidity and air temperature measurements. Ångström (1918) first observed an empirical relationship between downward longwave clear-sky irradiance and vapor pressure. Following his pioneering work, several parameterizations have been developed for LWd using synoptic observations (Idso and Jackson, 1969; Maykut and Church, 1973; Jacobs, 1978; Culf and Gash, 1993; Aubinet, 1994; Dilley and Brien, 1998; Duarte et al., 2006; Lhomme et al., 2007, Rizou and Nnadi, 2007)

The major drawback of previous studies is that their methods did not perform well in other locations, since they utilized local empirical coefficients. This is mainly caused by the significant variation of the coefficients in those models, due to the variability of air temperature and water vapor pressure, which were in turn resulted from the spatial change in land use pattern and temporal change in atmospheric circulation. At land scale, human activities affect regional climate by changing the land use characteristics that impact the distributions of ecosystem, energy (latent and sensible heat), and mass fluxes (e.g. water vapor, trace gases and particulates). These contrasting land use patterns induce convection and circulation that affect the cloud formation and precipitation. For example, when large areas of forest are cleared, reduced transpiration results in less cloud formation, less rainfall, and increased drying of the earth surface (Dale, 1997). Previous studies on measurement of some radiation components (incoming shortwave radiation or net energy balance) focused on specific land use type, such as grass, short

vegetation, bare soil, forest and few crops but disregarded urban areas and water-covered areas (Kessler, 1985; Kessler and Jaeger, 1999; Barr and Sisterson, 2000)

Therefore, a long term monitoring and modeling of radiation components, especially longwave radiation on various land use types including urban and wetland areas rather than agricultural and rangeland areas only are essential and critical. Rizou and Nnadi (2007) developed a land use-adapted model which superpositioned nonlinear temperature effects and water vapor in one equation, to account for the net impact on clear sky emissivity. Their model was robust and adaptable for different land use areas. The statistical parameters, including normalized Mean Bias Errors (MBE) and Root Mean Square Errors (RMSE), are smaller than those of other existing models, which showed the model's good performance relative to others. In their study, three months data in spring 2004 at current study area were analyzed but the seasonal variation and cloud effect were not considered on the various land use effects.

Culf and Gash (1993) in considering a sinusoidal variation between wet and dry season showed that the leading coefficients of LW_d regression model were different. This is similar to other meteorological variables, such as temperature, solar radiation, and water vapor pressure. In the dry season, the lapse rate of water vapor is lower than a standard atmosphere. On the other hand, the wet season is more humid and has a higher water vapor lapse rate. Other studies suggested that seasonal analysis and adjustment of LW_d model is necessary and critical in long-term analysis (Crawford et al., 1999; Duarte et al., 2006; Kruk et al., 2009).

Rizou and Nnadi (2007) indicated that the clouds would result in more noise in diurnal pattern of radiation, while Crawford and Duchon (1999) argued that the utility of most techniques

applicable to clear sky has great limitations. Previous studies also suggested that cloud cover plays an important role to prevent radiation deficit. These studies stated that thick clouds primarily reflect solar radiation and cool the surface of the earth, while high and thin clouds mainly transmit incoming solar radiation. However, it was also suggested that thick clouds trap some of the outgoing infrared radiation emitted by the earth and radiate it back downward, thereby warming the surface of earth. Therefore, several researchers have proposed locally adjusted equations for LW_d fluxes in cloudy condition, such as Jacobs (1978) for Baffin Island, Canada, Maykut and Church (1973) for Alaska, United States, Sugita and Brutsaert (1993) for Kansas, United States, Konzelmann et al., (1994) for Greenland, and Crawford et al., (1999) for Oklahoma, United States.

Thus, in this study, the effects of seasonal variation and cloud cover on LW_d were considered and a new land use adapted model developed. The objectives of this paper are: (1) to analyze a yearly in-situ downward longwave data and seasonal variation of LW_d in yearly data based on wet and dry season for clear and all sky LW_d radiation models; (2) to compare as cloud and land use factors as they affect LW_d based on the dry season data; and (3) to develop land use adapted all-sky LW_d models based on dry and wet season data.

2.2 Parameterization Schemes

2.2.1 Basic Emissivity Model

Rizou and Nnadi (2007) developed a land use-adapted model based on slab emissivity by Elachi (1987)

$$\varepsilon_s = 1 - I_0 e^{-\alpha D} \tag{2.1}$$

Where I_0 is the incoming wave intensity, α is the total extinction coefficient (including absorption and emission), and D is the slab thickness. The term D is usually called the optical thickness or depth.

In their study, the authors suggested that either temperature or humidity parameters can capture all LW_d over a wide range of climatic condition because of the compensating effects of temperature and water vapor. Therefore, the following equation, which superpositioned the two effects in one equation, was generated for the daily LW_{dc}.

$$LW_{dc} = (1 - C_1 e^{\frac{-T_0}{C_2}} + C_3 e^{\frac{-e_0}{C_4}})\sigma T^4 \tag{2.2-a}$$

$$\varepsilon_s = (1 - C_1 e^{\frac{-T_0}{C_2}} + C_3 e^{\frac{-e_0}{C_4}}) \tag{2.2-b}$$

where C_1, C_2, C_3, and C_4 are site-specific constants, ε_s is the emissivity of the atmosphere, σ (= $5.67\times10^{-8} W/m^2K^4$) is the Stefan-Boltzman constant, e_o is the actual water vapor pressure at the

surface, T_0 is the surface or screen-level air temperature. With the use of multiple nonlinear regression analysis, the values of the parameters were obtained for all sites. Because temperature and water vapor variation affect cloud cover, the present study developed a form of equation (2.2-a) by considering seasonal variation and cloud effects.

2.2.2 Existing All Sky Parameterizations

The presence of clouds results in warmer air temperatures and also increases the amount of long wave radiation reaching the earth surface. Therefore, various studies considered cloud effect in estimating downward longwave radiation, (Crawford and Duchon, 1999; Duarte, 2006; Lhomme, 2007; Kruk, 2009). Most of their approaches adjusted εs for the fraction of cloud cover, C, to compute the increase in radiation. Equations (2.3-a) through (2.3-d) in Table 2.1 were developed for estimating all sky downward longward radiation in which the cloud cover, C was based on human observations. In determining C, the sky condition was divided into 10 sectors and the fraction of 10 was used to estimate the cloud fraction (Duarte, 2006). However, in some study areas, the cloud cover data were absent due to lack of observers (Crawford and Duchon, 1999; Duarte, 2006; Lhomme, 2007; Kruk, 2009). In their later study, Crawford and Duchon (1999) generalized the effect of clouds, as shown in Equation (2.3), by introducing a cloud fraction term clf, defined as, clf = 1 − s, in which s is the ratio of the measured solar irradiance to the clear-sky irradiance.

$$LW_d = \left\{clf + (1 - clf)(1.22 + 0.66 \times \sin\left[(m + 2)\frac{\pi}{6}\right](\frac{e_d}{T})^{\frac{1}{7}}\right\}\sigma T^4 \qquad (2.3)$$

where m is the numerical month (e.g., January = 1), e_d is the vapor pressure (mbar)

Table 2.1: Existing LW_d Model for All Sky Condition

Parameterization	**Experimental site**	**Equation**
Maykut and Church(1973)		
$LW_d = LW_{dc} \times (1 + 0.22 \times C^{2.75})$	Alaska(USA)	(2.3-a)
Jacobs(1978)		
$LW_d = LW_{dc} \times (1 + 0.26 \times C)$	Baffin Island(Canada)	(2.3-b)
Sugita and Brutsaert (1993)		
$LW_d = LW_{dc} \times (1 + 0.0496 \times C^{2.45})$	Kansas (USA)	(2.3-c)
Duarte (2006)		
$LW_d = LW_{dc} \times (1 + 0.242 \times C^{0.583})$	Southern Brazil	(2.3-d)

A general limitation and drawback of this approach is that it can only be used during the daylight hours. In order to avoid this limitation, this study uses the cloud fraction data of Automated Surface Observing System (ASOS) for developing the all sky LW_d model. The cloud amount is determined by a laser beam ceilometer with a vertical range of 3600 m where the beam's width is 18 m. The ASOS cloud senor has a 0.9 microns wavelength, a nominal pulse frequency of 770 Hz, and sampling frequency of 30 s with an average interval of 30 min. Thus the daily average cloud cover is based on 30 min internal cloud cover. The cloud fraction is recorded in oktas with a maximum error of 5 % (ASOS program 1998).

Table 2.2 shows ASOS cloud gradation used in this study to develop cloud cover fractions. Laser beam ceilometers have an advantage over human observers. Traditionally, observers must wait for their eyes to adapt to the dark before they are able to accurately distinguish nighttime sky condition, while Laser beam can adapt to night conditions. Another advantage of laser beam ceilometers is that it reports the onset of lower stratus moving over the ceilometer within 2 min and the formation/dissipation of a low ceiling within 10 min (ASOS program, 1998).

Table 2.2: ASOS Cloud Amount Report

ASOS measured amount in % of sky	Equivalent in oktas	Cloud Cover Fraction	ASOS note
00 to ≦05	0	0	Clear
>05 to≦25	>0 to 2/8	0.125	Few
>25 to ≦50	>2/8 to≦4/8	0.375	scattered
>50 to ≦87	>4/8 to≦8/8	0.75	Broken
>87 to 100	8/8	1.0	overcast

The Equivalent Oktas as defined by ASOS was further reduced to cloud cover fractions based on the average values (Table 2.2). Using the cloud cover fractions developed, the general form of all sky LW_d adjusted equation is given as

$$Lw_d = Lw_{dc}(\alpha + C^{\beta}) \tag{2.4}$$

where C is cloud cover fractions and α, β in general depend on cloud characteristics, with the use of multiple nonlinear regression analysis, the values of the parameters were obtained for all sites.

2.3 Data Collection

Daily data of year 2004 were utilized for model development. The data comprising of weather data (air temperature, dew point temperature, and cloud cover) were collected from, National Climatic Data Center of National Oceanic and Atmospheric Administration (NOAA, accessed March 2005, http://www.ncdc.noaa.gov/oa/ncdc.html), and LW radiation from Net Radiometer (CNR1) at four sites within Saint Johns River Water Management District (SJRWMD). The LW radiation sites spread over latitudes of 27.58 °N to 30.32 °N and longitudes of 80.60 °W to 82.07 °W and represent different land uses (urban, agricultural, rangeland, forest, open water, and wetland), as shown in Figure 2.1. The weather data were collected from NOAA's weather stations in the vicinity of the CNR1 locations. The proximity of the weather stations to the CNR1 locations varies by 1'–17' latitude. The CNR1 considered in this study are located in Deland, Orange Creek, Ocklawaha, and Lindsey Citrus. The Deland radiation station, which is located at a wastewater treatment plant surrounded by a paved road, grass, and shrubs, represents an urban land use. Orange Creek, which is covered by bahia grass, oak and pine trees, represents a rangeland land use type. Ocklawaha is a wetland covered by willow, saw grass, cattail, lily pads, and wiregrass. Lindsey Citrus is an agricultural site with short grass beneath the tree canopy, which is under regular irrigation schedule.

At these sites, the longwave and shortwave radiation fluxes were measured by pyrgeometer (CG3 radiometers with spectral range 5–50 μm, by Kipp and Zonen) and pyranometers (CM3

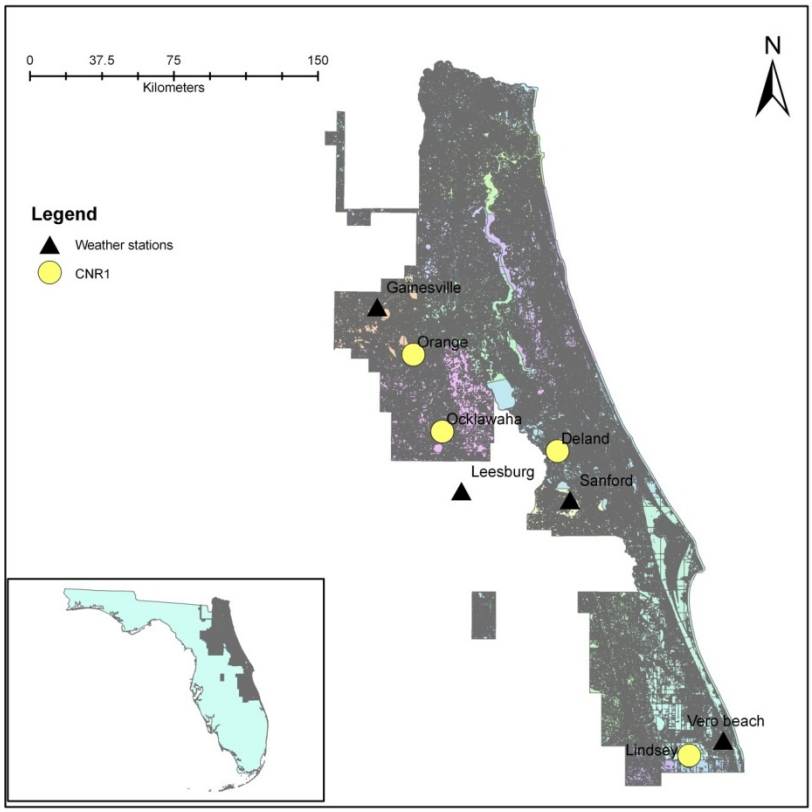

Figure 2.1: Location of the CNR1 and weather stations in the SJRWMD region

radiometers, by Kipp and Zonen), respectively. The expected accuracy of the CG3 sensor has a limit of ± 10% for daily totals and ± 20 W/m^2 for individual measurements as provided by the manufacturer (Kipp and Zonen, 2000). The ASOS HO-83 hygrothermometer was used for temperature measurements, which uses a resistive temperature device (Root Mean Square Errors (RMSE): 0.5 °C, max error: 1 °C) to measure air temperature, and a chilled mirror device (RMSE: 0.6–2.6 °C, max error: 1.1–4.4 °C) to measure dew point temperature. The sampling frequency for both devices is one minute with averaging interval of 5 minutes. Water vapor

pressure data were obtained by daily averaging of the dew point temperature from NOAA data. The water vapor pressure at the surface was calculated using Equation (2.5) (Shuttleworth, 1993).

$$e_0 = 6.1078 \times 10^{\frac{7.5T_d}{T_d+287.3}} \quad (2.5)$$

where e_o (hPa) is the actual water vapor pressure at the surface and T_d (°C) is the dew point temperature.

Model validation data were obtained from SURFace eXchange (SURFX) sites located at Bondville, Illinois (40.01 °N, 88.29 °W), which represents an agricultural setting with corn and soybeans. SURFX sites are part of Global Energy and Water cycle EXperiment (Gewex) America Prediction Project (GAPP) program for an agricultural area. Data collected at the SURFX sites, which include energy fluxes, carbon and surface meteorology were obtained from, http://www.joss.ucar.edu/ghp/ceopdm/archive/eop1_data for July through September 2001. The cloud cover data were obtained from the nearest NOAA station located at Champaign/Urbana Willard Airport and has an elevation of 230 m a.s.l. (Rizou and Nnadi, 2007).

2.4 Model Downward Longwave Radiation Modeling for All Sky Condition

2.4.1 Seasonal Variation

The wet season in Florida starts from end of May to middle of October while the rest is classified as dry season. The longwave radiation is higher and stable during wet season and lower with relative large variation during the dry season. Figure 2.2 shows the observed

downward longwave radiation seasonal variation for all land uses. The LW_d ranges from 230 to 440 Wm^{-2} in the four sites in the study area during the year 2004. The LW_d ranged from 381 to 441Wm^{-2}, 363 to 432 Wm^{-2}, 359 to 431 Wm^{-2}, and 349 to 436 Wm^{-2}, in Deland, Orange Creek, Ocklawaha Prairie, and Lindsey Citrus, respectively during the wet season. The LW_d in city of Deland (urban area), Orange Creek (rangeland), Ocklawaha Prairie (wetland), and Lindsey Citrus (agriculture), varied from 233 Wm^{-2} to 441Wm^{-2}, 224 Wm^{-2} to 431 Wm^{-2}, 219 Wm^{-2} to 432 Wm^{-2}, and 241 Wm^{-2} to 438 Wm^{-2}, respectively during the dry season. Figure 2.3 presents the LW_d and cloud cover in the four land use sites during wet season, while Figure 2.4 provides the LW_d and cloud cover of the four sites over the study period in dry season. LW_d in all the four sites showed positive correlation to the cloud cover in wet season; however, this relationship is not as significant as that of dry season because there are only few clear sky days during wet season, as shown in Table 2.3, while there were more than 20 days of clear sky (c=0) during the dry season. It can be seen that the cloud cover strongly affects LW_d, while in clear sky condition; the LW_d had lower values, which dropped significantly and approached its lowest value. This variation is obviously much smaller in wet season than the dry season.

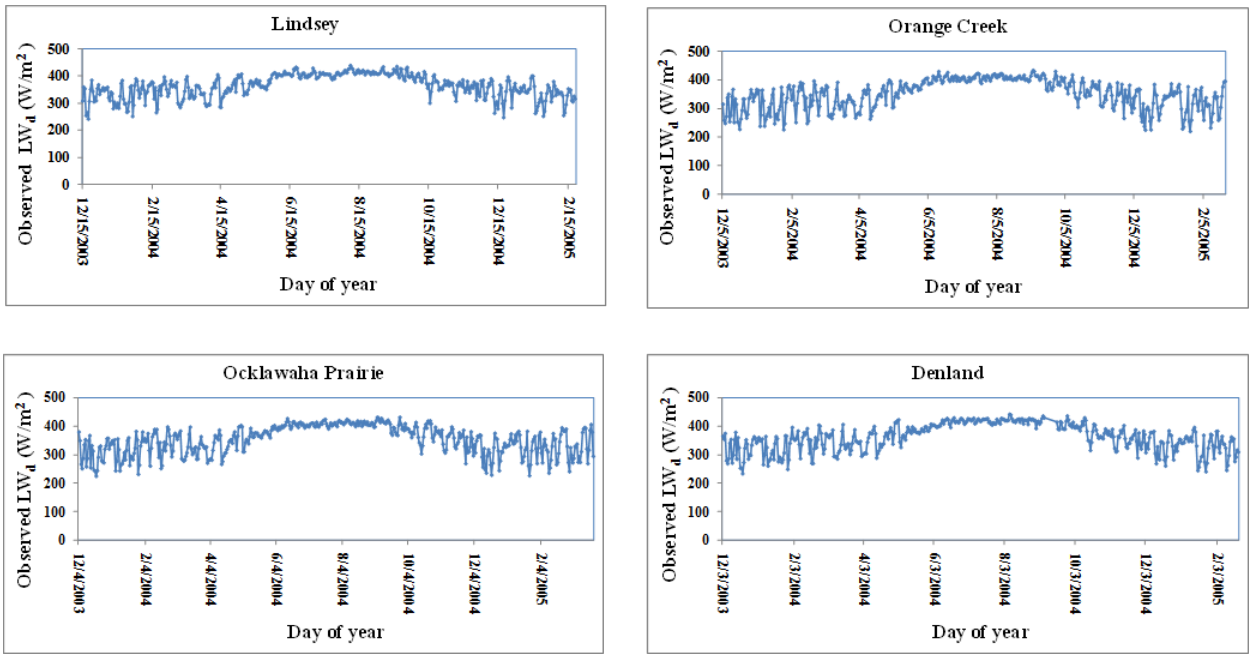

Figure 2.1: Seasonal Variation of LW_d

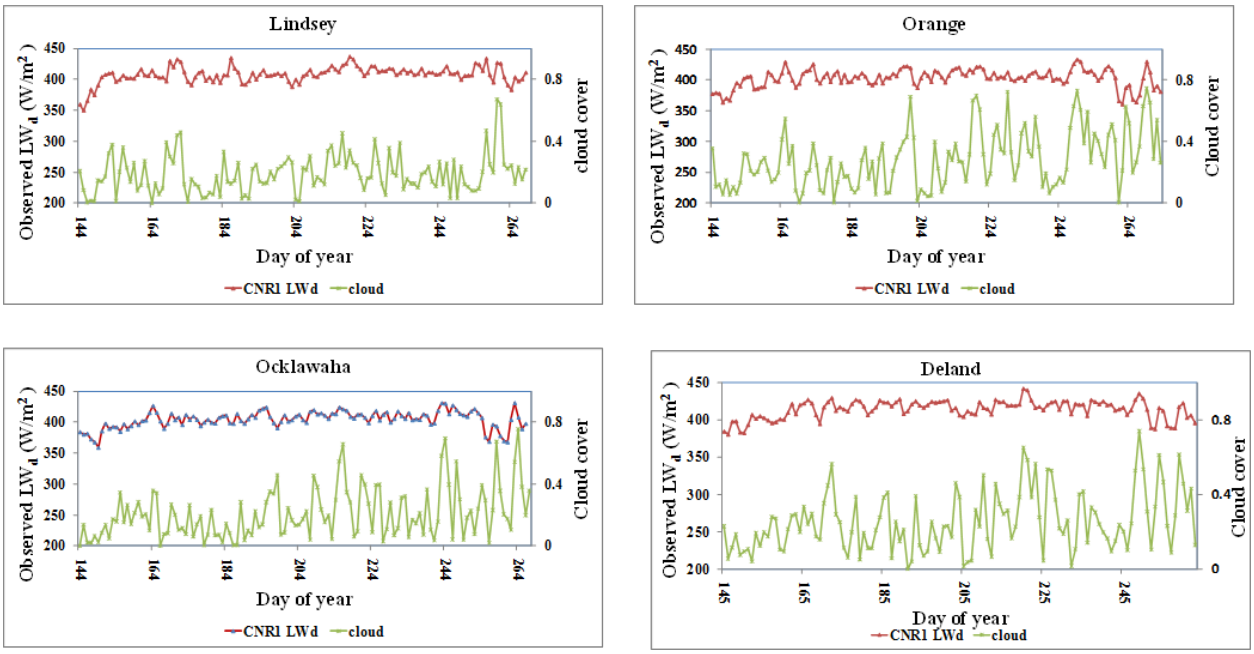

Figure 2.2: LW_d and Cloud Cover during Wet Seaso

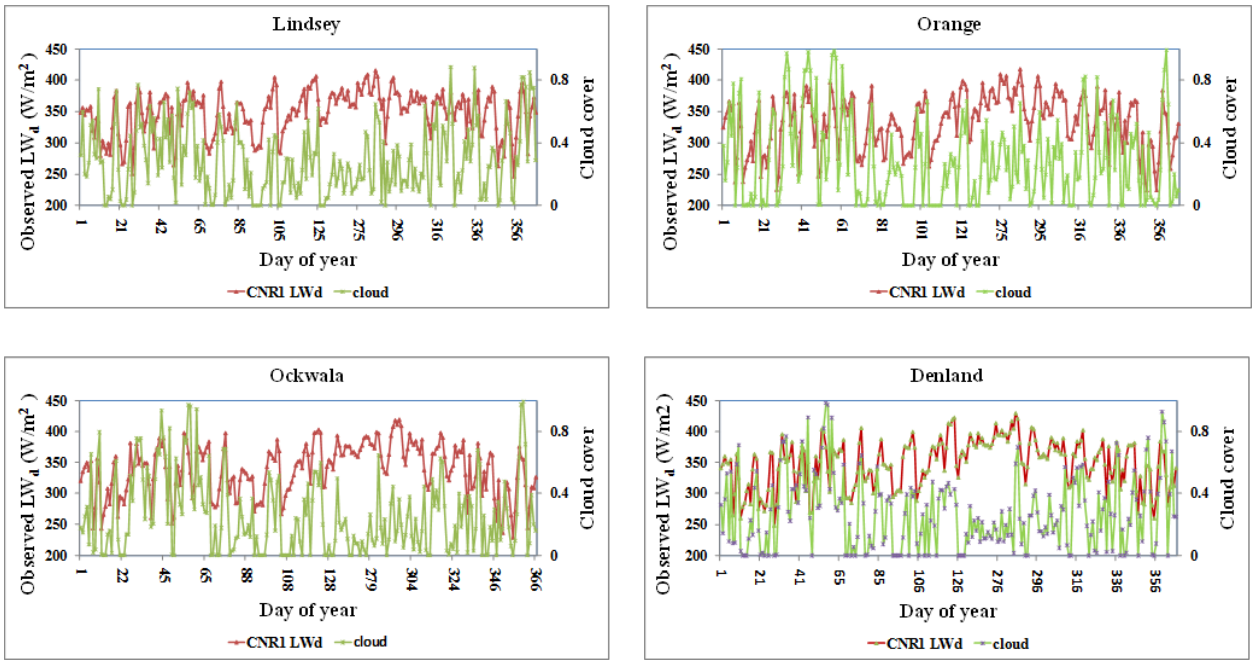

Figure 2.3: LW_d and Cloud Cover during Dry Season.

Table 2.3: Comparison of LWd and Cloud Cover Days in Wet and Dry Season

Dry season (Total days = 231)				
Site	Deland	Ocklawaha	Lindsey	Orange
Land Use Type	Urban (medium density)	Wetland	Agriculture	Rangeland
Average LW_d radiation of all days (Wm^{-2})	349.10	338.81	349.09	332.86
average cloud cover of all days	0.27	0.26	0.28	0.28
Number of clear days	36 days	41 days	20 days	44 days
Wet season (Total days = 126)				
Site	Deland	Ocklawaha	Lindsey	Orange
Land Use Type	Urban (medium density)	Wetland	Agriculture	Rangeland

Average LW_d radiation of all days (Wm^{-2})	414.13	404.32	407.55	402.55
average cloud cover of all day	0.32	0.31	0.31	0.35
Number of clear days	0 days	1 day	1 day	0 days

2.4.2 Factors Affecting Downward Longwave Radiation in Dry Season

The average air temperature and water vapor pressure on cloudy days were observed to be higher than those in clear sky days. Figure 2.5 and 2.6 show the average daily air temperature and water vapor pressure, respectively at the study sites during the dry season. During the clear sky days, the wetland had the smallest surface albedo (about 0.03~0.1 for small zenith angle, Oke, 1987), which resulted in the highest temperature and water vapor pressure. However, as cloud cover is a kind of albedo (0.6~0.9, Oke, 1987), when combined with the other surface albedo can affect surface air temperature. Thus the agricultural area shows highest temperature and water vapor pressure in cloud days. This could be explained by the facts that under cloudy condition, albedo of soils and vegetation are decreased thus resulting in higher temperature and water vapor. High albedo of the rangeland area (0.26, Oke, 1987) resulted in low temperature and low water vapor pressure under all-sky conditions.

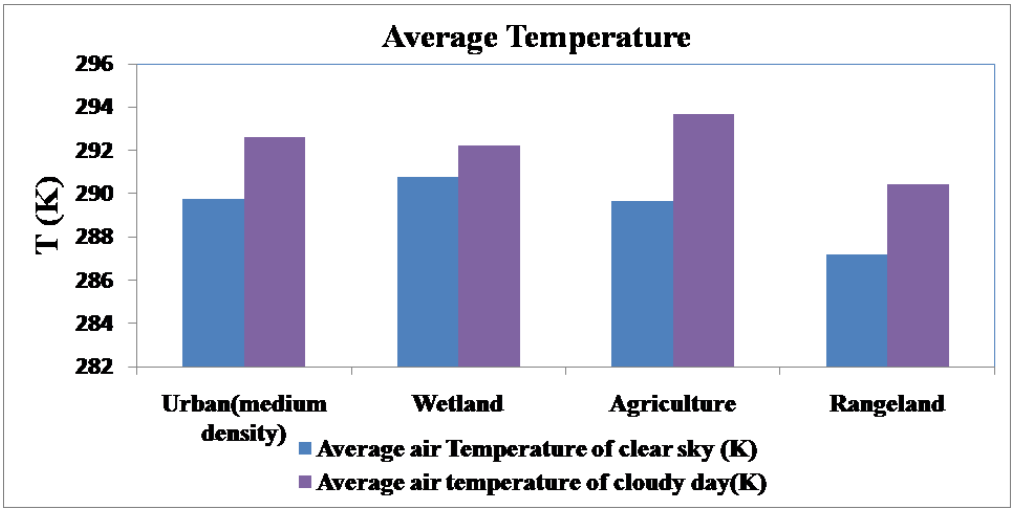

Figure 2.4: Average Daily Temperature in dry season.

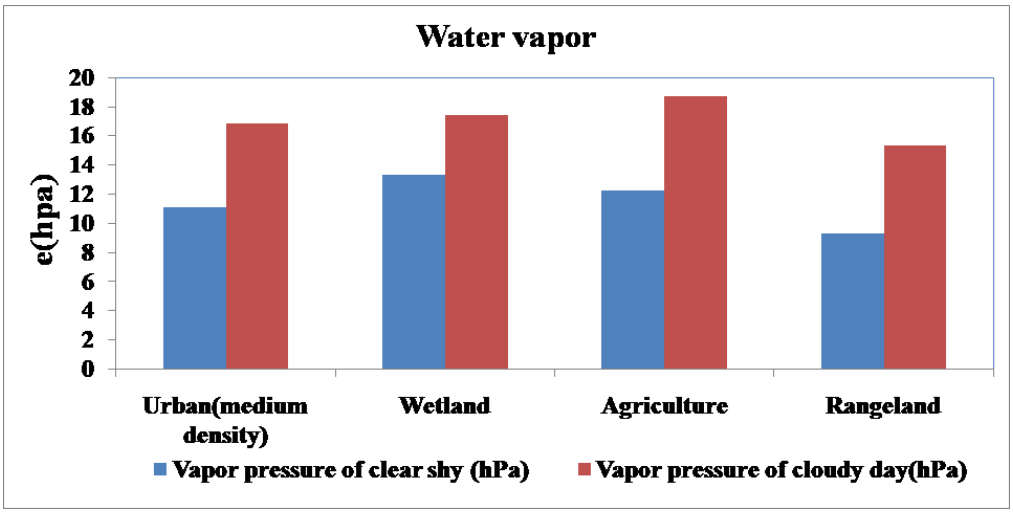

Figure 2.5: Average Water Vapor in dry season

Also in Figure 2.6 the relationship between water vapor and LW_d under clear sky condition suggests that though the water vapor in the urban area was lower than the other areas, but LW_d was larger. This suggests that: (1) the geometry of city streets absorbs more shortwave radiation

and makes longwave radiation be exchanged between buildings rather than lost to the sky; (2) the concrete structures especially paved roads as well as the high density of industrial processes in the urban environment are favorable for pollution and dust release; and (3) longwave radiation trapped in the polluted urban atmosphere leads to the urban greenhouse effect (Sieghardt et al., 2005).

Figure 2.7 shows the LW_d from four different land use sites in the dry season with the largest on the urban area and smallest on the rangeland area in both clear sky and cloudy conditions. Considering the effect of outward longwave radiation (LW_o), which is the solar radiation absorbed by the Earth that causes the planet to heat up and emit radiation, is can be observed that the agriculture area had the largest LW_o while rangeland area had the smallest LW_o. Figure 2.8 compares LW_o and LW_d on the four different land use sites in dry season, while Figure 2.9 shows the ratio of LW_d to LW_o. Because under clear sky condition a significant fraction of the longwave radiation emitted from the surface is absorbed by trace gases and suspended particles in the air, therefore the urban area had the largest value of LW_d /LW_o, compared to the other three land use areas. This condition results in atmospheric greenhouse effect.

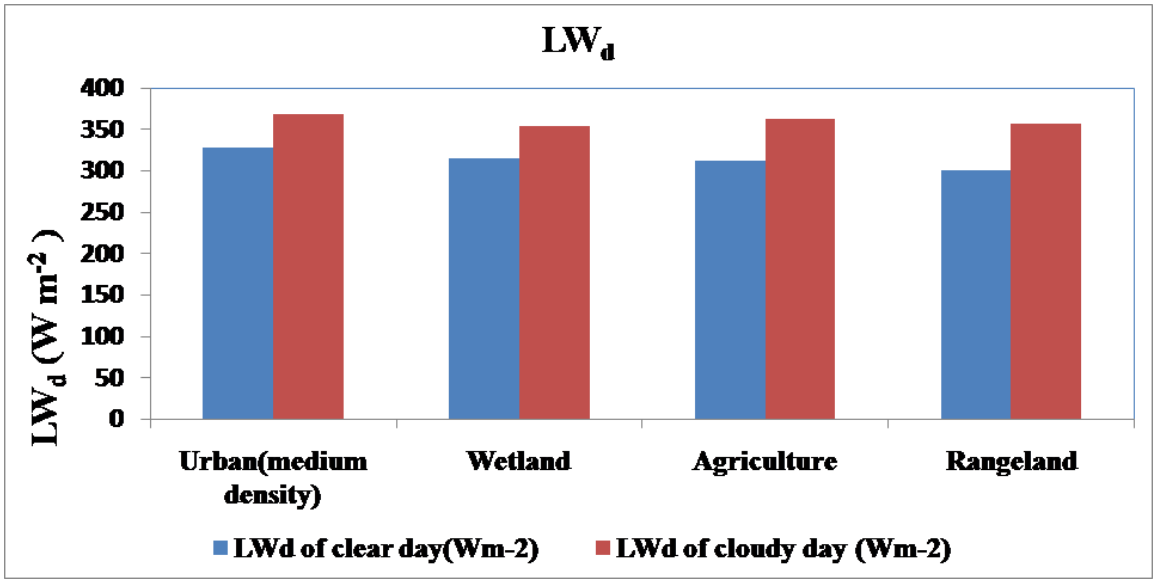

Figure 2.6: LW_d of different landuse sites in the dry season.

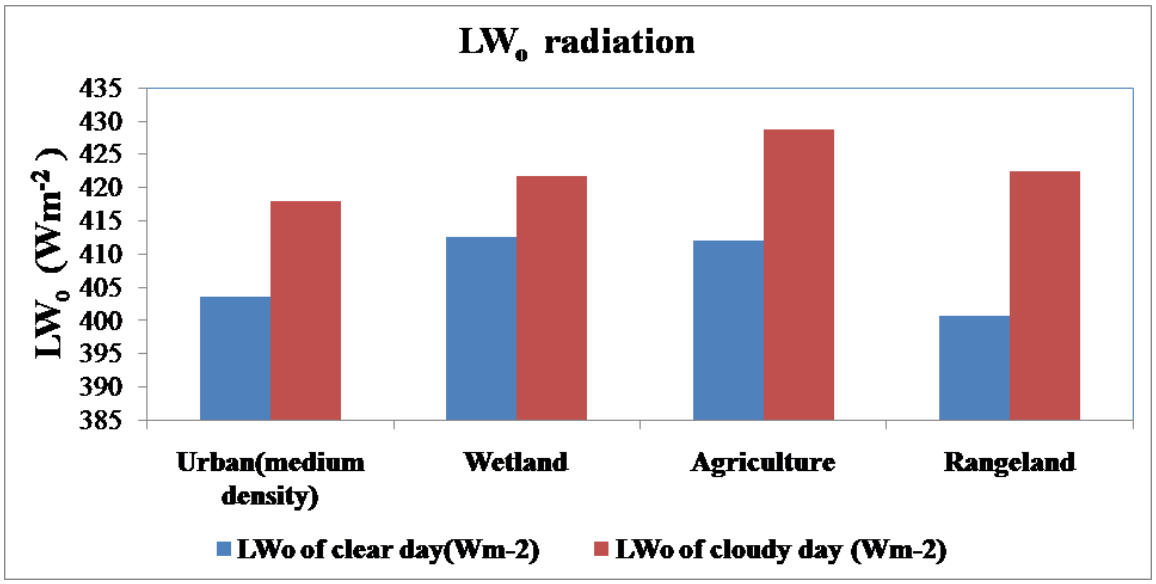

Figure 2.7: LW_o in Dry Season.

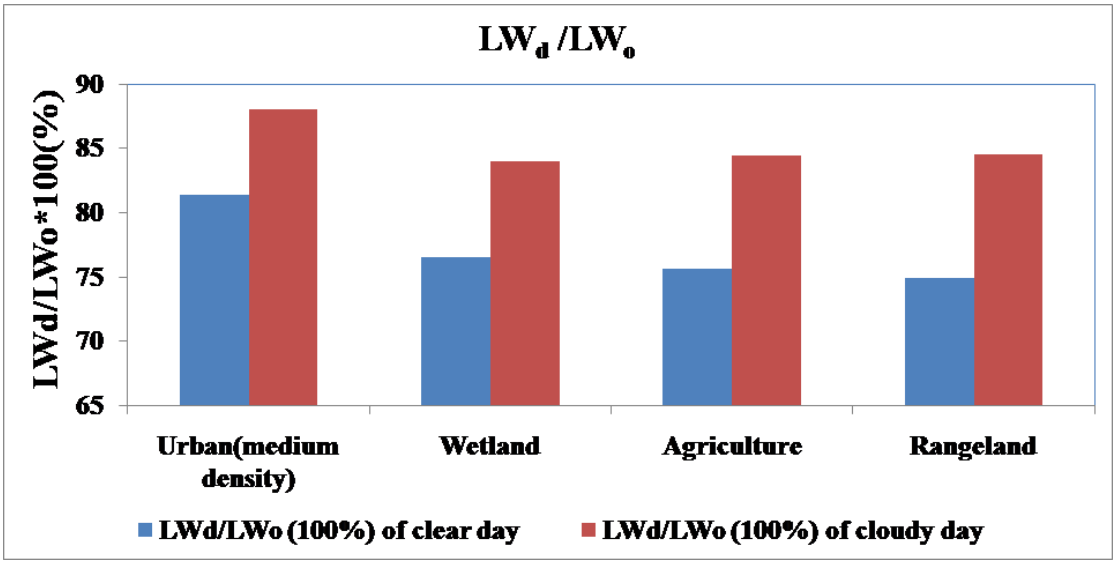

Figure 2.8: Ratio of LW_d to LW_o in Dry Season

2.4.3 All sky LWd Model Calibration for Dry Season

In this section, the general form of land use-adapted model, Equation (2.4) was used in developing all-sky LW_d at the land use sites in the dry season. Clear sky data obtained from CNR1 were used determined the coefficients for LW_{dc} in Equation (2.2-a). Using observed data for all sky condition during dry season, and Equation (2.2-a) with cloud cover data the coefficients α and β were determined from Equation (2.4) for all land use areas as shown in Equations (2.6) through (2.13) in Table 2.4. In Figure 2.10 the new all sky LW_d model is verify by comparing LW_d data obtained from measurements over the study area. The results show that the new all sky LW_d models closely predict the measured data with R^2 values between 0.88 and 0.92 for all land use areas studied.

Table 2.4: New All Sky LW_d Equations for four land use Sites During Dry Season

Parameterization	Experimental site	Equation
$Lw_{dc} = (1— \left(-4.575 \times e^{\frac{-T_0}{e^{94.856}}} + 0.576 \times e^{\frac{-e_0}{42.409}}\right) \sigma T^4$		(2.6)
$LW_d = LW_{dc} \times (1 + 0.222 \times C^{1.753})$	City of Deland(USA)	(2.7)
$Lw_{dc} = (1— (-19.087 \times e^{\frac{-T_0}{66.064}} + 0.658 \times e^{-\frac{e_0}{36.520}}) \sigma T^4$		(2.8)
$LW_d = LW_{dc} \times (1 + 0.249 \times C^{1.884})$	Orange Creek(USA)	(2.9)
$Lw_{dc} = (1— (-61.037 \times e^{\frac{-T_0}{58.424}} + 0.905 \times e^{-\frac{e_0}{44.482}}) \sigma T^4$		(2.10)
$LW_d = Lw_{dc} \times (1 + 0.194 \times C^{1.425})$	Ocklawaha Prairie(USA)	(2.11)
$Lw_{dc} = (1— (-100.719 \times e^{\frac{-T_0}{43.942}} + 0.555 \times e^{-\frac{e_0}{34.988}}) \sigma T^4$		(2.12)
$LW_d = Lw_{dc} \times (1 + 0.219 \times C^{1.556})$	Lindsey Citrus(USA)	(2.13)

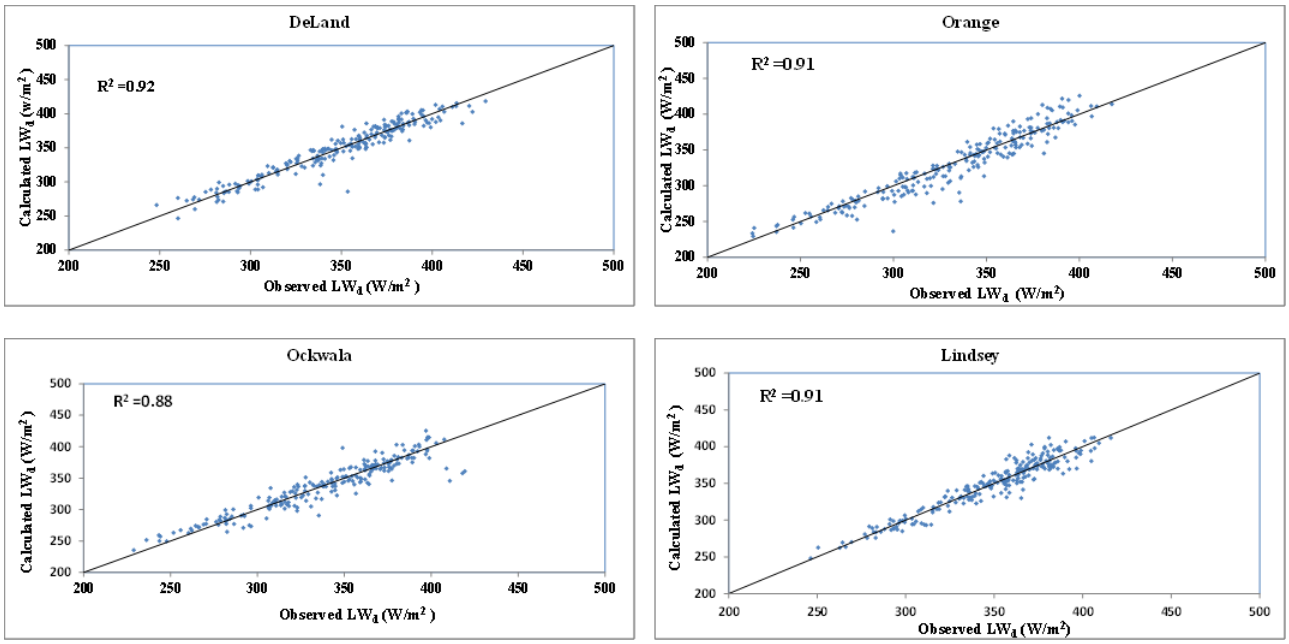

Figure 2.9: Comparison of New LW_d Models for All Sky and Observed Data in Dry Season.

These models were compared to four existing models for all sky condition (Jacobs, 1978; Maykut and Church, 1973; Sugita and Brutsaert, 1993; and Duarte, 2006) as shown in Table 2.5. In this comparison LW_{dc} for all models were calculated using Equation (2.2-a). This is to form a baseline for better appreciation of the effect of the coefficients since earlier study, Rizou and Nnadi (2007) also used in the current study have shown that their LW_{dc} model is better than those in Jacobs (1978), Maykut and Church (1973), Sugita and Brutsaert (1993), and Duarte (2006). Statistical evaluation of the performance of these models, suggested that the new all sky model gave the smallest values for the Bias (BIAS), Root Mean Square Error (RMSE), Mean Absolute Error (MAE), Percent Mean Relative Error (PMRE) (Table 2.5). Amongst the four

existing models, Jacobs (1969)'s model had the best performance on the rangeland area but the worst on the urban area, while Maykut and Sugita's model had the best performance on the urban but the worst on the rangeland area and Duarte (2006)'s model had the worst performances of the four different land use areas.

Table 2.5: Comparison of Model Predictions with Observed All Sky LW_d Data in Dry Season

Statistical performance	**Model**				
	New	**Maykut and Church (1973)**	**Jacobs(1978)**	**Sugita and Brutsaert (1993)**	**Duarte (2006)**
			City of Deland		
BIAS(Wm^{-2})	-0.18	-5.42	7.05	-10.09	22.37
RMSE(Wm^{-2})	10.81	12.78	13.86	18.54	27.86
MAE(Wm^{-2})	8.00	9.26	10.99	13.15	24.00
PMRE(%)	2.30	2.64	3.14	3.70	6.77
			Orange Creek		
BIAS(Wm^{-2})	-2.61	-8.06	2.78	-14.10	16.35
RMSE(Wm^{-2})	14.45	16.22	15.99	23.71	25.85

MAE(Wm^{-2})	10.64	12.27	12.31	16.90	20.48
PMRE(%)	3.19	3.67	3.63	4.95	5.91
			Lindsey Citrus		
BIAS(Wm^{-2})	-0.07	-7.27	6.01	-11.76	22.33
RMSE(Wm^{-2})	10.53	13.86	12.64	19.44	26.66
MAE(Wm^{-2})	8.03	10.55	9.93	14.40	22.97
PMRE(%)	2.27	2.95	2.81	4.00	6.46
			Ocklawaha Prairie		
BIAS(Wm^{-2})	-0.62	-6.10	4.60	-10.94	18.45
RMSE(Wm^{-2})	13.97	15.71	15.27	20.81	25.86
MAE(Wm^{-2})	9.76	11.10	11.58	14.99	21.72
PMRE(%)	2.87	3.41	3.23	4.30	6.34

In validating the new all sky models, an agricultural land use area under all sky conditions at Bondville, Illinois was selected. The new agricultural land use clear sky model (Equation (2.12) in Table 2.4) was used to determine LW_{dc} and the cloud coverage data was obtained from the nearest NOAA station, located at Champaign/Urbana Willard Airport, while Equation (2.13) was used to calculate all sky LW_d. Figure 2.11 shows that the new all-sky model had a very good fit with the data with R^2 value of 0.93. The four existing models were also compared to the observed data from Bondville, Illinois. The statistical results show that these models performed poorly as shown in Table 2.6. The poor performance existing models could be attributed to the

fact that land use they effects were not consider in their development. Hence land use is an important factor in developing all sky LW_d.

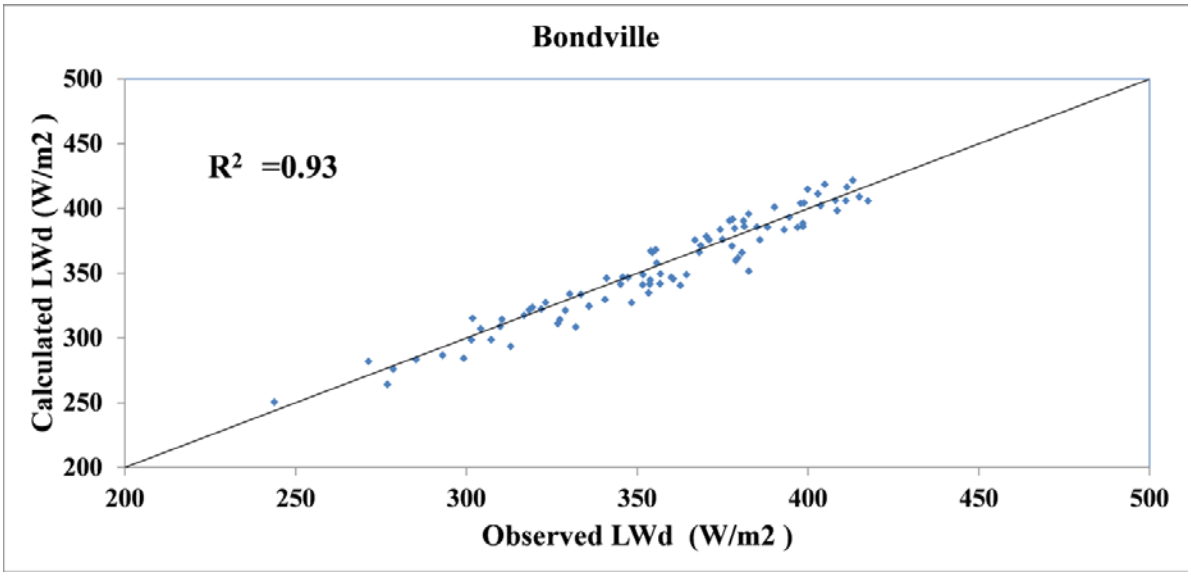

Figure 2.10: Validation of All Sky LW_d at Bondville, IL.

Table 2.6: Statistical Analysis for Model Verification and Validation

Statistical performance	Model				
	New	Maykut and Church (1973)	Jacobs (1978)	Sugita and Brutsaert (1993)	Duarte (2006)

			City of Bondville		
BIAS(Wm^{-2})	-2.80	-9.10	2.86	-12.54	18.58
RMSE(Wm^{-2})	10.82	14.90	10.95	19.24	22.95
MAE(Wm^{-2})	8.91	12.01	8.95	15.44	19.58
PMRE(%)	2.51	3.36	2.50	4.27	5.35

Figure 2.2 and Table 2.3 show that in the wet season, the LW_d was higher with much fewer days of clear sky compared to the dry season. The fact that there was only one or no clear sky day at all the four sites during wet season indicate that it was unnecessary and impossible to calculate the LW_{dc} accurately. However, LW_{dc} is needed for the calculation of LW_d under all sky condition, as shown in Equation (2.4). In order to overcome this difficulty, the initial approach was to substitute the values of temperature and water vapor in wet season into dry season model under clear sky condition to come up with LW_{dc} and then substitute in the LW_d model to generate wet season model under all sky conditions using Equation (2.4). The statistical results of this analysis are presented in Table 2.7. It can be seen that the error were higher than those obtained in dry season condition.

Table 2.7: Statistical Performance of the LW_d Dry Season Models Tested for Wet Season

Statistical performance	**Model**
	Dry season model
	City of Deland
BIAS(Wm^{-2})	4.38
RMSE(Wm^{-2})	10.46
MAE(Wm^{-2})	8.05
PMRE(%)	1.94
	Orange Creek
BIAS(Wm^{-2})	11.58
RMSE(Wm^{-2})	17.14
MAE(Wm^{-2})	13.94
PMRE(%)	3.46
	Lindsey Citrus
BIAS(Wm^{-2})	-3.19
RMSE(Wm^{-2})	10.43

MAE(Wm^{-2})	6.46
PMRE(%)	1.61
	Ocklawaha Prairie
BIAS(Wm^{-2})	2.94
RMSE(Wm^{-2})	18.54
MAE(Wm^{-2})	10.25
PMRE(%)	2.52

2.4.4 All Sky LWd in Wet Season

Another approach was proposed in this study where a term called pseudo-LW_{dc} was introduced. The pseudo-LW_{dc} is defined as a longwave radiation value during wet season when the cloud coverage equals to a certain cut-off value that is small enough but can assure enough observation data for the regression of Equation (2.2), for example 10 percentile of the whole observation cloud coverage data such that Equation (2.4) would be applicable to cases where cloud coverage is larger than the cut-off value for the pseudo-LW_c. In this study, a cut-off cloud coverage value of 0.1 was used to define the pseudo-LW_{dc} giving clear sky days in the observed data to be 22, 24, 30, and 39 days for agriculture, rangeland, wetland, urban area, respectively. The all-sky LW_d models for wet season generated based on pseudo-LW_{dc} are given in Equation 2.14 through 2.21 for all land use areas considered as shown in Table 2.8.

The results and the statistical analysis are presented in Figure 2.12 and Table 2.9, respectively. The statistics by the new model following the pseudo-LW_{dc} approach gave the smallest values when compared to the existing four models as shown in Table 2.9, therefore suggesting that this approach provided a better prediction except for the agricultural area. The discrepancy could be attributed to improperly selection of the cut-off value of cloud coverage for the pseudo-LW_{dc}. As addressed above the modified Equation (2.4) is mainly applicable when the cloud cover is larger than the cut-off value. As shown in Figure 2.3, Lindsey Citrus site has fewer days with cloud coverage larger than the cut-off value in wet season hence the amount of data used to estimate pseudo-LW_{dc} is limited. This in turn gave a weak prediction of LW_d at this site. However, sites with more days with cloud cover have better prediction.

Table 2. 8: All Sky LW_d Parameterizations for Wet Season

Parameterization	Experimental site	Equation
$\text{pseudo Lw}_{dc} = (1 - \left(-21.29 \times e^{\frac{-T_0}{e^{52}}} + 0.30 \times e^{\frac{-e_0}{15}}\right)\sigma T^4$		(2.14)
$\text{LW}_\text{d} = \text{LW}_\text{dc} \times (1 + 0.087 \times \text{C}^{1.665})$	The city of Deland(USA)	(2.15)
$\text{pseudo Lw}_{dc} = (1 - \left(-22.43 \times e^{\frac{-T_0}{e^{88.24}}} + 1.19 \times e^{\frac{-e_0}{82.68}}\right)\sigma T^4$		(2.16)
$\text{LW}_\text{d} = \text{LW}_\text{dc} \times (1 + 0.173 \times \text{C}^{3.83})$	Orange Creek(USA)	(2.17)

$$\text{pseudo Lw}_{dc} = (1 - \left(-182.78 \times e^{\frac{-T_0}{e^{60.12}}} + 1.63 \times e^{\frac{-e_0}{151.02}}\right)\sigma T^4 \quad (2.18)$$

$$\text{LW}_\text{d} = \text{LW}_\text{dc} \times (1 + 0.037 \times \text{C}^{1.969}) \quad \text{Ocklawaha Prairie(USA)} \quad (2.19)$$

$$\text{pseudo Lw}_{dc} = (1 - \left(-46379.70 \times e^{\frac{-T_0}{e^{25}}} + 1.12 \times e^{\frac{-e_0}{28.18}}\right)\sigma T^4 \quad (2.20)$$

$$\text{LW}_\text{d} = \text{LW}_\text{dc} \times (1 + 0.098 \times \text{C}^{0.845}) \quad \text{Lindsey Citrus(USA)} \quad (2.21)$$

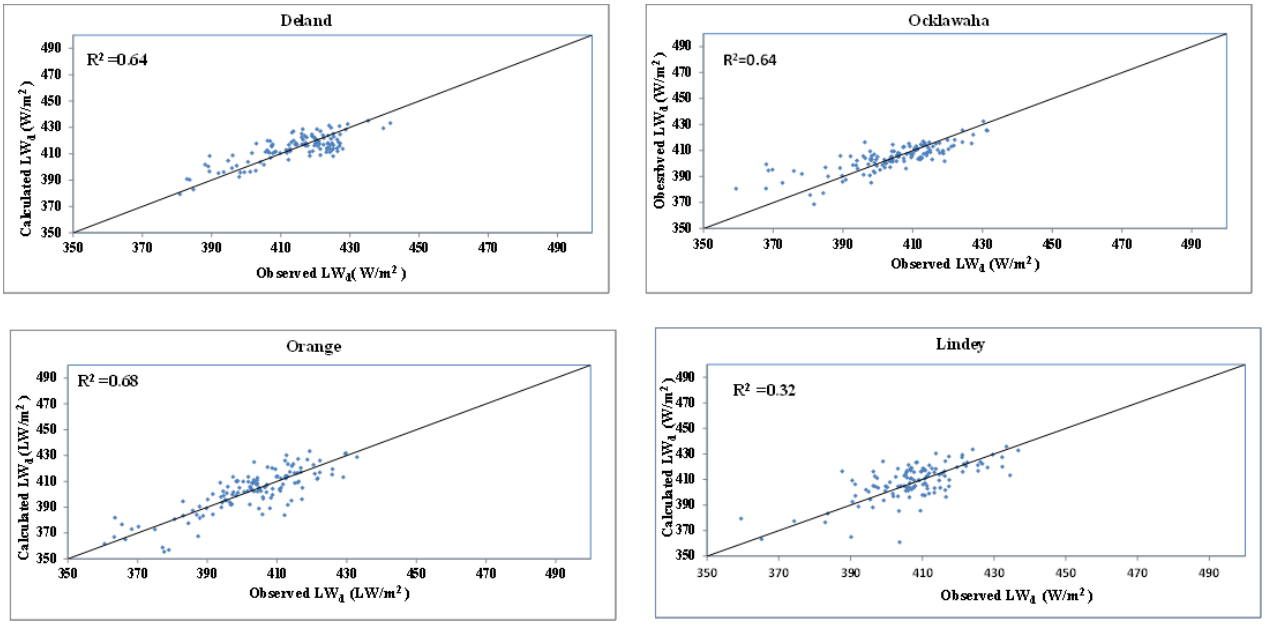

Figure 2.11: Comparison of New LWd Models for All Sky and Observed Data in Wet Season.

2.5 Summary and Conclusions

Analysis of the observed LW_d data in 2004 showed seasonal variation on different land use; suggesting that LW_d has higher values and are stable during wet season and lower values with relatively large variation during dry season. Because of the variation in the dry season, the LW_d data was used to compare factors affecting LW_d radiation such as temperature, water vapor pressure, cloud cover and land use. Since different land use has different albedo in relation to energy and water budget, the effects of temperature and water vapor pressure on various land use evaluated using the albedo. The results of the analysis suggested that; (1) the wetland area had the smaller albedo resulting in the higher temperature and water vapor pressure in the clear sky condition; whereas the rangeland had the higher albedo leading to lower temperature and water vapor pressure in all sky conditions; and (2) the LW_d at the four sites investigated varied with larger values in the urban area and smaller value in the rangeland in both clear and cloud sky conditions.

Based on the seasonal variation dry and wet season data were separated and used for developing LW_d models for different land use under all sky conditions. This approach enhanced the models suitable for dry season and wet season prediction. The dry season models for the land use areas investigated performed better that existing models for LW_d under all sky condition as indicated by the statistical analysis of the results. However, the wet season models did not do as well as the dry season models. The low performance of the wet season models could be explained by the presence of one or no clear sky day condition at all the four sites, which made it

difficult to calculate the LW_{dc} accurately, therefore developing a wet season model for LW_d was challenging. To overcome this difficulty, a term, pseuso-LW_{dc}, was introduced to replace LW_{dc} in all sky model, Equation (2.4). This effort improved the model with an R^2 values ranging from 0.32 to 0.68. However, more work is required to further improve the wet season models for the land use areas investigated.

References

Angstrom, A., 1918, A study of the radiation of the atmosphere, Smithson Misc. Collect, 65 (3): 1–159.

ASOS Program, 1998, ASOS User's Guide", http://www.weather.gov/asos/pdfs/aumttoc.pdf.

Aubinet, M., 1994, Longwave sky radiation parameterizations, Sol Energy, 53: 147-154

Barr, S., Sisterson, D. L., 2000, Locale Analysis Report for the Southern Great Plains, ARM-00-001, Atmospheric Radiation Measurement Program, U.S. Department of Energy, http://www.arm.gov/publications/site reports/sgp/sgp2000.pdf.

Bilbao, Julia, De, M., Argimiro, H., 2007, Estimation of daylight downward longwave atmospheric irradiance under clear-sky and all-sky conditions, American Meteorological Society, Boston, MA, ETATS-UNIS..

Brutsaert, W., 1975, On a derivable formula for long-wave radiation from clear skies, Water Resources Research, 11(5): 742–744.

Crawford, T.M., Duchon, C.E., 1999, An improved parameterization for estimating effective atmospheric emissivity for use in calculating daytime downwelling long-wave radiation, J. Appl. Meteorol. 38: 474–480.

Culf, A.D., Gash, J.H.C., 1993, Long-wave radiation from clear skies in Niger: a comparison of observations with simple formulas, J. Appl. Meteorol., 32: 539–547.

Dale, V., H., 1997, The relationship between land-use change and climate change, Ecological Applications, 7(3): 753-769.

Dilley, A.C., O'Brien, D.M., 1998, Estimating downward clear sky long-wave irradiance at the surface from screen temperature and precipitable water, Q. J. R. Meteorol. Soc., 124: 1391–1401.

Duarte, H.F., Dias, N.L., Maggiotto, S.R., 2006, Assessing daytime downward long-wave radiation estimates for clear and cloudy skies in Southern Brazil. Agric, Forest Meteorol., 139: 171–181.

Elachi C., 1987, Introduction to the Physics and Techniques of Remote Sensing. John Wiley and Sons: USA.

Flerchinger, G. N., Xaio, W., Marks, D., Sauer, T. J., Yu, Q., 2009. Comparison of algorithms for incoming atmospheric long-wave radiation, Water Resour. Res., 45

Idso, S.B., Jackson, R.D., 1969, Thermal radiation from the atmosphere, J. Geophysical Res. 74 (23): 5397–5403.

Intergovernmental Panel on Climate Change [IPCC], 2001, Intergovernmental Panel On Climate Change [IPCC], 2001. In: J.T. Houghton et al. (Eds.), Climate Change 2001: The Scientific Basis, Cambridge University Press, New York.

Jacobs, J.D., 1978, Radiation climate of Broughton Island. In: Barry, R.G., Jacobs, J.D. (Eds.), Energy Budget Studies in Relation to Fast-ice Breakup Processes in Davis Strait. Inst. of Arctic and Alp. Res. Occas. Paper No. 26. University of Colorado, Boulder, CO, 105–120.

Kessler, A., 1985, Heat balance climatology, World survey of climatology, Vol. 1A, Elsevier, Amsterdam

Kessler, A., Jaeger, L., 1999, Long-term changes in net radiation and its components above a pine forest and a grass surface in Germany. Int. J. Climatol, 19, 211–226.

Kipp, Zonen, 2000, CNR1 Net Radiometer Instruction Manual, Delft: The Netherlands.

Konzelmann, T., Van, De, Wal, R.S.W., Greuell, W., Bintanja, R., Henneken, E.A.C., Abeouchi, A.,1994, Parameterization of global and long-wave incoming radiation for the Greenland ice sheet, Global Planet Change, 9: 143–164.

Kruk, N., Vendrame, Í., da Rocha, H., Chou, S., Cabral, O., 2009, Downward longwave radiation estimates for clear and all-sky conditions in the Sertãozinho region of São Paulo, Brazil. Theor Appl Climatol. 99 (1): 115-123.

Lhomme, J.P., Vacher, J.J., Rocheteau, A., 2007, Estimating downward long-wave radiation on the Andean Altiplano, Agric For Meteorol., 145 (3-4): 139-148.

Maykut, G.A., Church, P.E., 1973, Radiation climate of Barrow, Alaska, 1962–1966, J. Appl. Meteorol. 12: 620–628.

Niemela, S., Raisanen, P., Savijarvi, H., 2001, Comparison of surface radiative flux parameterizations, Part I: Long-wave radiation. Atmos. Res. 58: 1–18.

Oke, T.R., 1987, Boundary Layer Climates, 2rd edn, Methuen and Co. Inc, New York, 435

Rizou, M., Nnadi, F., 2007, Land use feedback on clear sky downward longwave radiation: a land use adapted model, Int. J. of Climatol., 27(11): 1479-1496.

Shuttleworth W.J., 1993, Chapter 4: evaporation. In Handbook of Hydrology, Maidment DR (ed.). McGraw-Hill Inc.: USA.

Sieghardt, M., Mursch-Radlgruber, E., Paoletti, E., Couenberg, E., Dimitrakopoulus, A., Rego, F., Hatzistathis, A., Randrup, T.B., 2005, The abiotic urban environment: 281-323.

Sugita, M., Brutsaert, W., 1993, Cloud effect in the estimation of instantaneous downward long-wave radiation, Water Resour. Res., 29, 599–605.

Swinbank, W.C., 1963, Long-wave radiation from clear skies. Quarterly Journal of the Royal Meteorological Society, 89, 339–348.

CHAPTER 3:

WATER BUDGET OF VARIOUS LAND USE AREAS IN FLORIDA USING NARR REANALYSIS DATA

This chapter has been submitted for publication with the following citation: C. H., Cheng and F., Nnadi. Advances in Meteorology (Accepted, December, 2011).

3.1 Introduction

The catchment water cycle, assuming steady state, consists of precipitation (P), discharge (Q), and evapotranspiration (ET) (Lee et al., 2010). More specifically, estimations of water cycle components include; (1) atmosphere budget, which consists of sources (surface evaporation and evapotranspiration) and sinks (rainfall and cloud) as well as the transports between them, and (2) terrestrial water budget, which includes the soil moisture storage, surface/ subsurface runoff, precipitation and evapotranspiration (Pan et al., 2006).

Terrestrial water cycle are intrinsically coupled and linked through evapotranspiration and precipitation (Hutjes et al., 1998; Kucharik et al., 2000; Arora, 2002). Precipitation and snowmelt influence plant-available moisture during the growing season, which impacts water and energy cycles through vegetation canopy controls on transpiration, plant atmosphere exchanges of water vapor and the partitioning of net radiation energy into sensible and latent heat fluxes (Trenberth et al., 2007).

Humans are an active and increasingly significant component of the hydrologic cycle (NRC, 1992). For example, land clearance for waste disposal and other activities, such as agriculture, urbanization and the conversion of native grasslands cause significant hydrological disruptions that adversely impact the water resources of the locality and beyond. Moreover, human activities are significantly changing the global environment and climate, in variety of diverse ways beyond the effects of human emissions of greenhouse gases. Within the context of global climate change, land use change and climate change are interrelated, and there is a mounting need for predicting watersheds response to these changes (NRC, 1992). Therefore, better understanding of the terrestrial water budget would improve our knowledge of the current climate, global hydrological cycle and its dynamics, and thus improve our skills in modeling, foresting, and analyzing the land-atmosphere system.

The widely used approaches to evaluate the terrestrial water cycle can be divided into three categories: (1) Observations based on in situ measurements; direct observation is the most traditional approach for water budget estimates and considered reliable at the scale of measurement. However, several basic atmospheric hydrological variables, such as evaporation, precipitation and runoff are poorly or/and sparsely measured (Pan et al., 2006). At regional to continental scales - dense networks of instruments are too expensive and long-term observation data are always limited. (2) Derived estimates based on spatially-remote sensed observations; remote sensing and the corresponding retrieval techniques have come of age as a viable source of data collection, particularly in parts of the world where in-situ data networks are sparse. Many hydrological state variables and fluxes can be estimated through satellite remote sensing, but still

are inadequate (Pan et al., 2008). (3) Estimates based on land surface models; observations can fail to provide relevant required information with sufficient space and time resolution. High resolution climate or land use model could be a constitutive tool to generate hydrological cycle components that are difficult to measure. An advantage of these model-derived data is their self-consistency and they can be used by many to model the land surface water and energy balances. However, a drawback of a model-only approach for water budget estimation is that models are not perfectly parameterized and calibrated as errors and biases exist and propagate through time (Pan et al., 2006).

Moreover, hydrological processes strongly rely on surface processes, topography and meso-scale atmospheric circulations. Investigating water budget on various land use is necessary and critical. However, in previous studies, models have related land use effects/ changes in regional water cycles (Dickinson and Henderson-Sellers, 1988; Chase et al., 1996; Copeland et al., 1996; Bonan, 1997, 1999; Pielke et al., 1999; Tracy et.al., 2004; Coe et al., 2007), but a disproportional majority water budget studies have been in grasslands and forests, and only few studies have been assessed in agricultural, wetland and lake areas (Wayne et al., 2009).

To improve these situations, in this study, North American Regional Reanalysis (NARR) data, which include model- based four- dimensional data assimilation procedures, were used for investigating water budget on various land uses. Data assimilation techniques, the integration of the virtues of observations and modeling by fusing them together, have been studied and used for decades in meteorological and oceanic applications (Ming et al., 2006). The NARR data sets may provide a great possibility for more accurate evaluation of interactions of the land surface-

atmosphere. Therefore, the first objective of this study is investigating the water balance on various land uses (Lake, wetland, agriculture, forest, and urban) at regional scale. Moreover, EI Niño-Southern Oscillation (ENSO), which is one of the most studied patterns of the world's climate, includes a strong natural inter-annual climate signal that affects the surface climate in numerous regions. The effect of ENSO on the U.S. surface temperature has been documented in previous studies (Ropelewski and Halpert, 1986, 1987; Kiladis and Diaz, 1989; Hoerling et al., 1997; Larkin and Harrison, 2005; Wang et al., 2007; Lau et al., 2008). However, few studies have investigated the role of ENSO on the individual terms of the surface water balance and descriptions of changes in hydrologic cycle over different land uses. Hence, the second objective of this study is using the NARR data to understand how drought events, EI Niño, La Niña and seasonal, inter-annual variations in climatic variables affect the energy and water exchange between atmosphere and land use.

3.2 Data set

This study employs the NARR dataset developed at the Environmental Modeling Center (EMC) of the National Centers for Environmental Prediction (NCEP). This dataset is based on the April 2003 frozen version of the operational Eta Model and its associated Eta Data Assimilation System (EDAS), and uses many observed quantities in its data assimilation scheme, including gridded analyses of rain gauges precipitation over the continental United States (CONUS), Mexico, and Canada (Luo et al., 2005). Hence, this regional reanalysis is produced at high

spatial and temporal resolutions (32-km, 45 layer, 3 hourly) and spans a period of 25 years from October 1978 to December 2003. Full details on the NARR products can be found online at http://www.emc.ncep.noaa.gov/mmb/rreanl/.

The EDAS is successful with downstream effects, including two-way interaction between precipitation and the improved land-surface model (Ek et al., 2003). Mitchell et al., (2004) demonstrated significant regional improvements in a number of variables when using precipitation assimilation over the CONUS. Therefore, it is expected that this dataset will be useful not only for energy and water budget studies, but also for analysis of atmosphere- land relationships. However, NARR still carries important, but unavoidable, model dependence. Hence, we still need to verify how well the water cycles are presented in NARR dataset in this study.

NARR variables in this study are basically a function of the model parameterizations; these include soil moisture, runoff, actual surface evaporation and precipitation. The study applied 11-year period of NARR dataset from 1992 through 2002, while utilizing monthly averages of the data.

3.3 Study area

This study examined the water balance on various land use sites in Florida. The climate in Florida is humid subtropical with a rainy wet season extending from May through October. Most areas in Florida receive at least 1270 mm of rainfall annually. The long-term annual mean temperature is 22.4°C based on historical records of a weather station located in

Kissimmee, Florida (Southeast Regional Climate Center, http://www.sercc.com/climate). Florida has varied annual precipitation as floods in one year may be followed by drought the next (Black, 1993).

In Florida, EI Niño-Southern Oscillation (ENSO) often influences temperature, precipitation, and upper-level wind, which in turn result in drought and wildfires (Brenner, 1991). These impacts are stronger during winter and spring months than during the summer months. Hence, a strong EI Niño phenomenon occurred in fall and winter of 1997-1998 when rainfall was above normal for most of the state and temperature were cooler. By late 1998, a strong La Niña event was in effect, which continued through 2001 (Richard et al., 2002). During 1998 - 2002, Florida experienced multiple high-pressure systems with higher temperatures and dry weather that brought a La Niña effect during part of the period. Hence, lower than normal precipitation caused a severe statewide drought in Florida during that period. The drought was one of the worst ever to affect the state based on precipitation and steam-flow data. Wildfire statistics show that 25,137 fires burned 1.5 million acres between 1998 and 2002 (Florida Division of Forestry: Part A, (undated)). Finally, rainfall occurred in late 2002, 2003, and from a tropical storm and four hurricanes in 2004 ended this drought period.

In this study, five different land uses in six areas were selected based on Florida's different climatic zones and land use /land cover data. Figure 3.1 presents the six selected 32×32 km regional study areas along with land-use/ land cover data from the 1992 National Land Cover Dataset. Three different land uses, urban, forest and agriculture, are located in Northeast Florida, while the other three are lake, wetland and agriculture located in South Florida. Figure 3.2 shows

the map of Florida depicting the four regions of the state. The climate of Northeast Florida is somewhat cooler and receives abundant precipitation between 1000 and 1500 mm annually. The combination of long frost-free periods of more than 240 days and plentiful water has historically enabled the production of specialized crops (Drummond and Loveland, 2010). For example, the citrus industry focused its intensive orange grove production on the southern interior and southeastern coast of Northeast Florida. Pastureland in Northeast Florida has also been an important agriculture resource. Hence a regional agriculture land use, which is located west Alachua (Figure 3.1) and devoted to forage, hay production and silage corn, was selected for studying the water budget. Moreover, extensive pine plantations, employed for timber production, are a relative common use of forests in North Florida. Almost one- third of Florida's forestland is commercial pine harvested and regenerated at a relatively fast pace (Carter and Jokela, 2002). Therefore, investigating land use effects on the water balance on the forest area is very important. In this study, Ocala National Forest, which is covered by sand pine scrub forest, presents a regional forest land use. Furthermore, substantial population growth has occurred, causing an expansion of urban and developed land. Within 30 years, the population increased by more than 140 percent, from 4.2 million to 10.3 million people. Larger urban areas are prevalent on the Florida peninsula, including Orlando, St. Petersburg, Tampa and Jacksonville. Hence, Jacksonville, which is the largest city in the State of Florida, was selected for a regional urban land use.

South Florida, exposed to onshore breezes, enjoys comfortable temperatures most of the year. The climate is generally frost-free and subtropical and annual rainfall is about 1400 mm. The

main regional characteristics in South Florida are wetland, lake, agriculture and urban areas (Fig. 3.1). The Everglades region is a subtropical wetland, the only one of its kind in the U.S (Munson and Leeper, 2005). Historically, it covered much of South Florida, comprising over 4000 square miles stretching from Lake Okeechobee in the north to the Florida Bay at the southern end of the peninsula (The South Florida Everglades Restoration Project). Hence, a regional 32×32 km grid of wetlands in the South Florida was selected for a study area. Lake Okeechobee (Fig 3.1) is a large, shallow, eutrophic lake located in south central Florida, and frequently hit by hurricanes. The Lake is the second largest freshwater lake in the U.S and covers a surface area of 1800 square km, with an average depth of 2.7 m. As the central part of a larger interconnected aquatic ecosystem in South Florida and as the major surface water body of the Central and Southern Florida Flood Control Project, Lake Okeechobee provides a number of societal and environmental service functions including water supply for agriculture, urban areas, and the environment (Folks, 2005). Therefore, investigating long-term water budgets of Lake Okeechobee is very critical and necessary. Finally, the Everglades Agriculture area (EAA), which presents an agriculture land use type in this study, is a small portion of the Everglades region, consisting of artificially rich organic soil. EAA have built a thriving agriculture industry with annual benefits around $500 million (Snyder, 1987), attributable for the most part to sugarcane and winter vegetables.

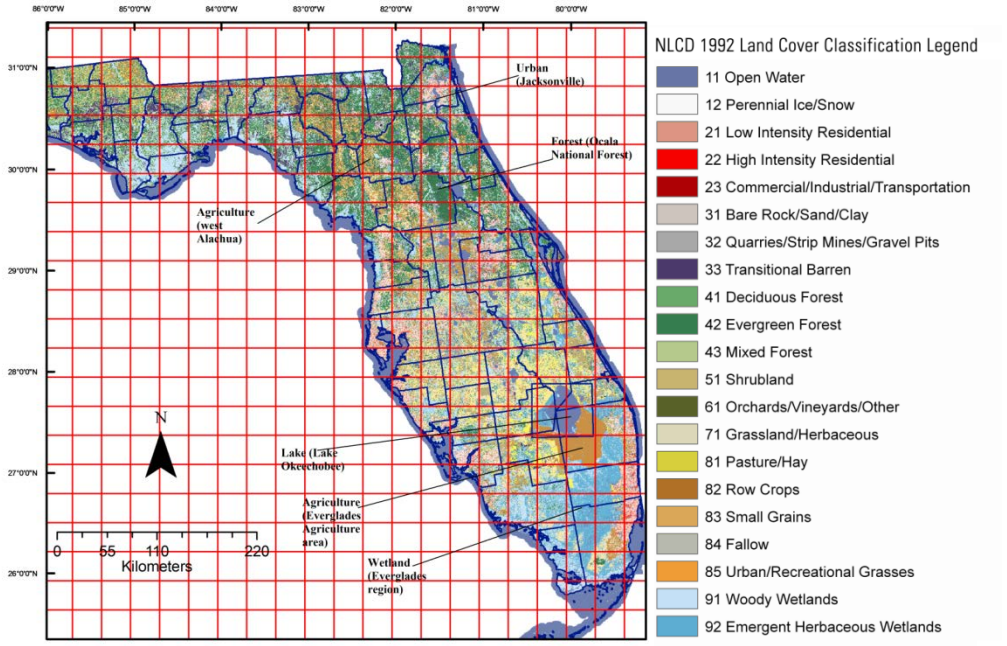

Figure 3.1: Six selected 32×32 km^2 regional study areas along with land-use/ land cover from the 1992 National Land Cover Dataset

Figure 3.2: Map of Florida depicting the four regions of the State (Richard et al. 2002)

Figure 3.3 showed the six selected 32×32 km regional study areas along with land use/ land cover data from the 2001 National Land Cover Dataset. Comparing National Land cover Dataset of two different periods of 10 years interval, the land use changes could be monitored and detected. The regional agriculture land use, which is located in west Alachua, changed the land use from row crop in 1992 to pasture hay in 2001, but other land use areas didn't change a lot within the 10 year period. This land use change may change energy balance, ET rate and rainfall and affects water budget and regional climate. Therefore, in this study, land use change effects also could be observed by examining long-term water budgets on various land uses in Florida.

3.4 Results and Discussions

In this study, monthly data set from 1992 through 2002 NARR data, which includes precipitation, actual and potential surface evaporation, soil moisture and runoff, was utilized for studying water budgets on various land uses by using the water balance equation expressed as:

$$P=E+\Delta S+R \tag{3.1}$$

where P is the precipitation; E is the evaporation; R is the sum of surface and subsurface runoff; S is the water content from snow accumulation, soil moisture, and canopy water.

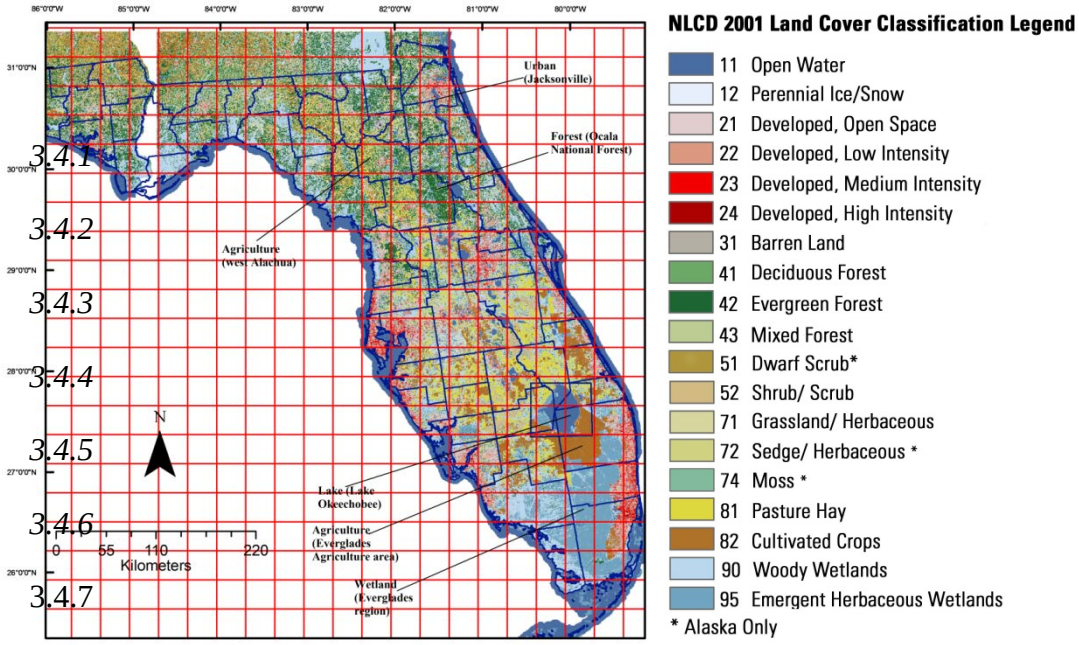

Figure 3.3: Six selected 32×32 km^2 regional study areas along with land-use/ land cover from the 2001 National Land Cover Dataset

3.4.1 Rainfall Variations

Rainfall varies in annual amounts, seasonal distributions and locations. Figure 3.4 and 3.5 shows the average annual precipitation on various land uses in Northeast and South Florida, respectively. In the Northeast, the average annual rainfall was lowest in 2000 for all land uses, while urban and forest areas had the highest values in 1994 with the agriculture area in 1997. The highest values of average annual rainfall were about 4.31, 3.70 and 3.74 mm/day, on the forest, urban and agriculture, respectively, whereas the lowest values were about 2.62 mm/day on the

three land uses. In South Florida, the three land uses experienced the highest average annual rainfall in 1994, but the lowest values were in 2000. The highest average values of annual rainfall were 3.66, 4.5 and 4.1 mm/day, while the lowest values were 2.27, 2.97, 2.28 mm/day on lake, wetland and agriculture, respectively.

Seasonal precipitation patterns in Florida vary between summer convective thunderstorms and winter fronts. Figure 3.6 and 3.7 present the average monthly rainfall in Northeast and South Florida, respectively. In the Northeast Florida, three land uses had the highest average monthly rainfall in June, with values of 5.00, 6.26 and 5.88 mm/day and the lowest values exhibited in May, with values of 1.37, 1.78 and 1.53 mm/day on the urban, forest and agriculture respectively. In South Florida, three land uses had the highest average monthly precipitation in June, with values of 6.26, 8.37, 6.96 mm/day and the lowest values were in December, with values of 1.54, 1.38, and 1.40 mm/day on lake, wetland and agriculture, respectively.

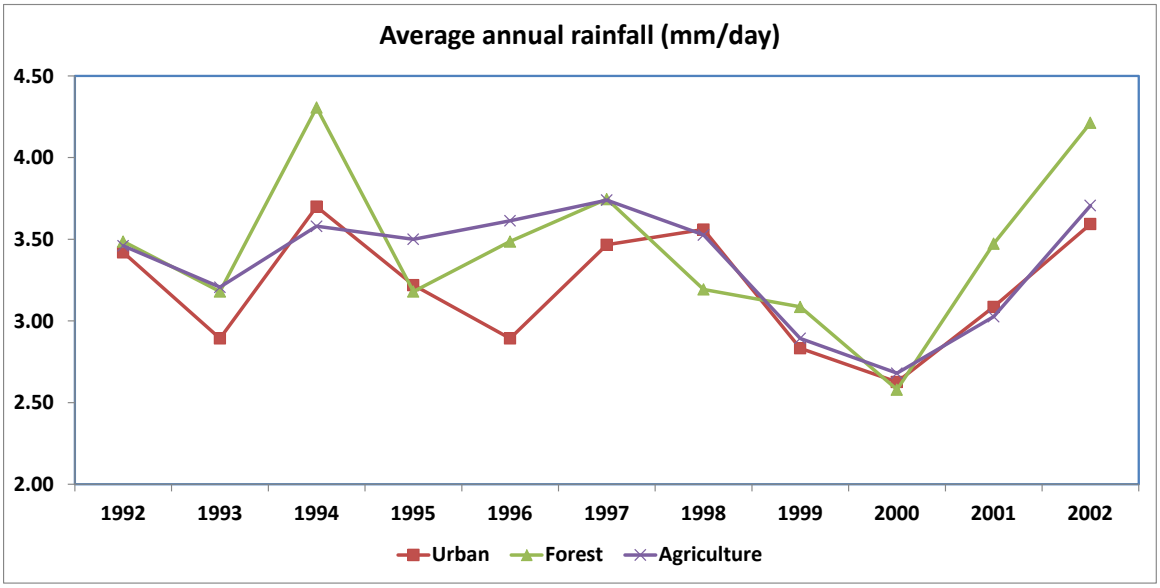

Figure 3.4: The average annual rainfall in Northeast Florida

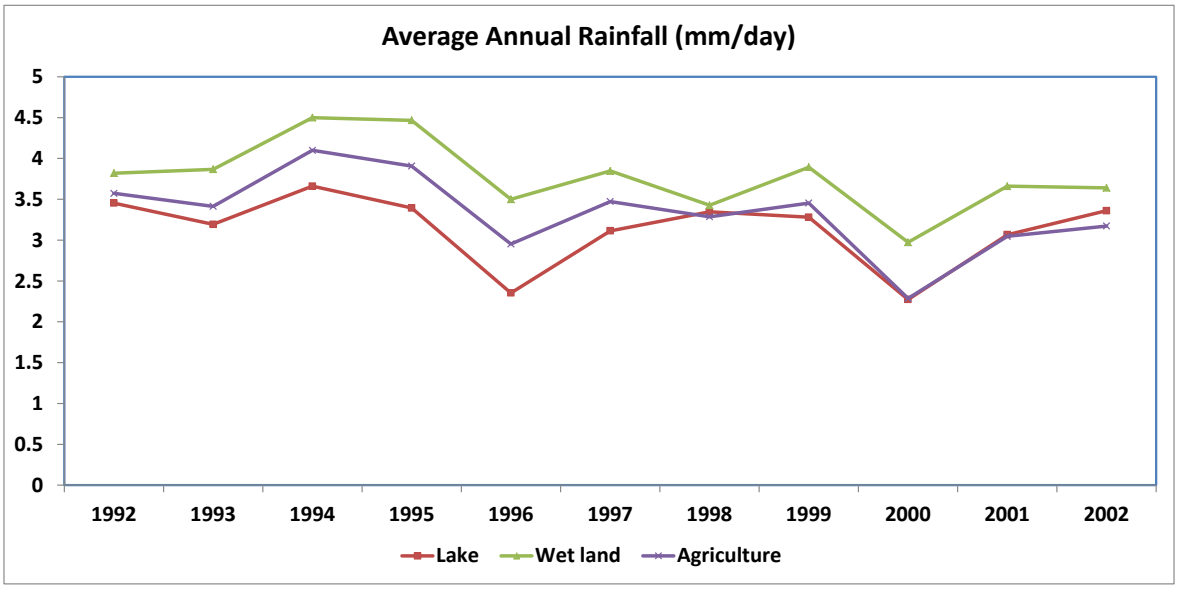

Figure 3.5: The average annual rainfall in South Florida

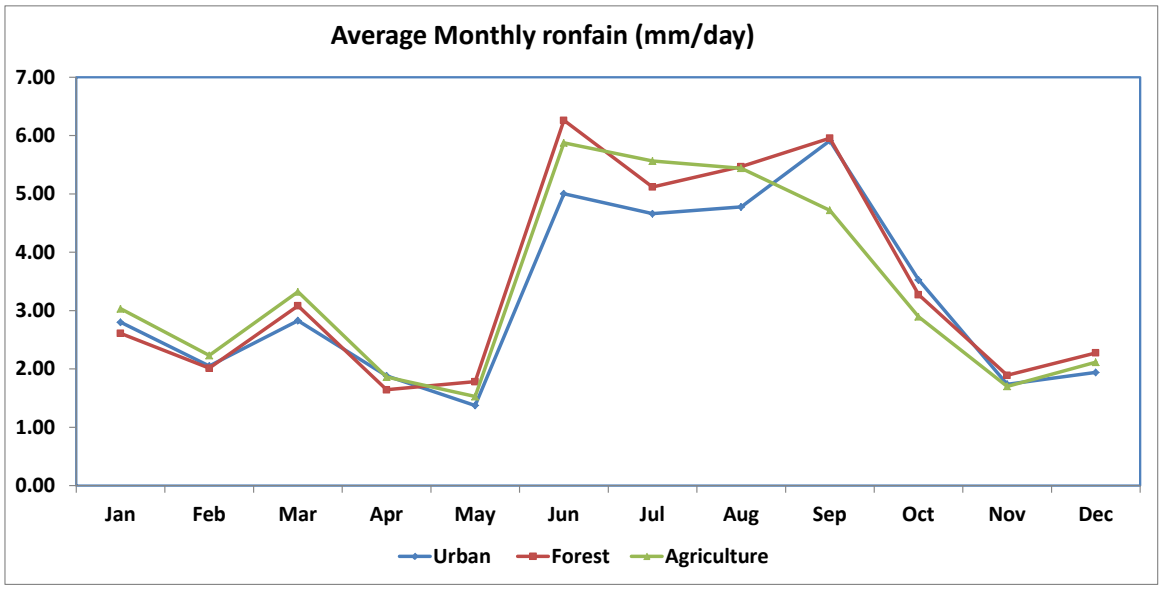

Figure 3.6: The average monthly rainfall in Northeast Florida

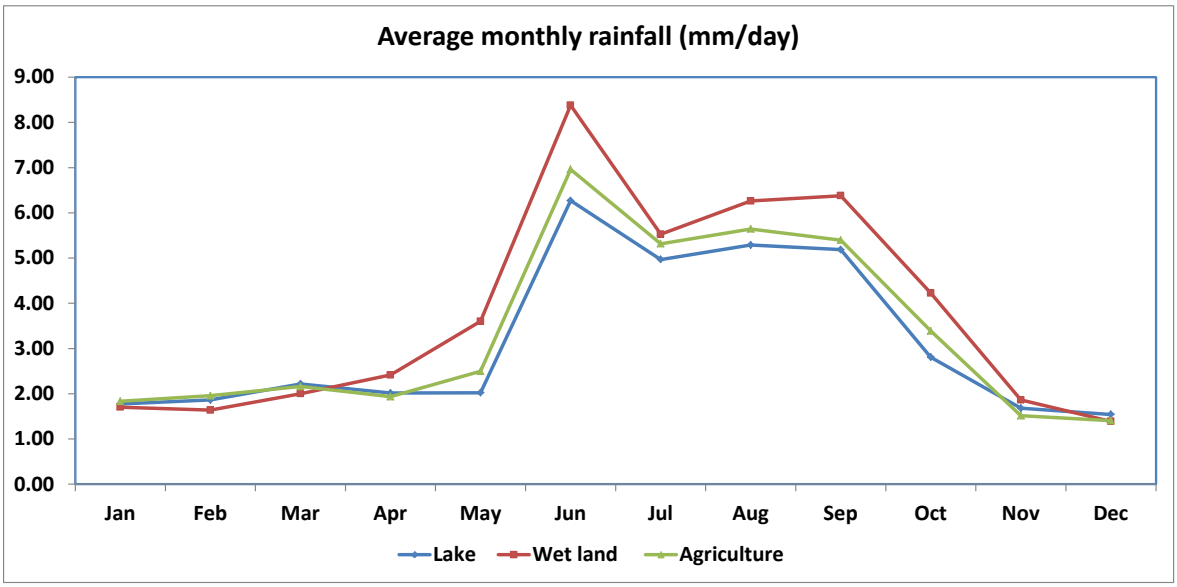

Figure 3.7: The average monthly rainfall in South Florida

3.4.2 Monthly Rainfall Anomaly

To determine anomaly patterns during the study period, 11 year monthly averages of climatology parameters were developed. Individual monthly anomaly was calculated as percent departure from the 11 years average of monthly averages using Equation 2:

$$P_a = \left(\frac{P_o - P_m}{P_m}\right) \times 100 \qquad (3.2)$$

where P_a is the respective monthly percent anomaly; P_o is the monthly parameters such as precipitation, soil moisture, actual evaporation, potential evaporation and runoff; P_m is the long-term average of parameters. Figure 3.8 and 3.9 show the time series monthly precipitation anomaly patterns for Northeast and South Florida, respectively. Winter of 1997-1998 represents a strong EI Niño phenomenon with rainfall anomalies more than 95 % above normal occurred on the three land uses in October 1997 and February 1998. By in late 1998, a strong La Niña event was in effect, which continued through 2001. On the three land uses, precipitation anomalies decreased to negative anomaly values between -30% and -87% from October to May in 1999, 2000 and 2001. However positive anomalies occurred on the three different land uses in March 2001. Hurricanes and thunderstorms are the main sources of rain in Florida. Their frequency and intensity were usually higher in June and August. For example, rainfall anomalies were more than 80% above normal on the three land use areas in August 1992, because hurricane Andrew. Thunderstorms also caused rainfall anomalies more than 70% above normal in June 1992, 1994, 2001 and 2002 on the three areas. In South Florida, rainfall anomalies were higher than 8%

above normal in December 1997 and 35% above normal in February 1998 on the three land uses because of EI Niño effects. During a drought period, rainfall anomalies decreased to negative anomaly values between -50% and -100% from November to May on the three areas. Moreover, hurricane Andrew and thunderstorms in June caused the rainfall anomalies more than 100% above normal on the three land use areas in 1992, 1995, 1999 and 2002, respectively.

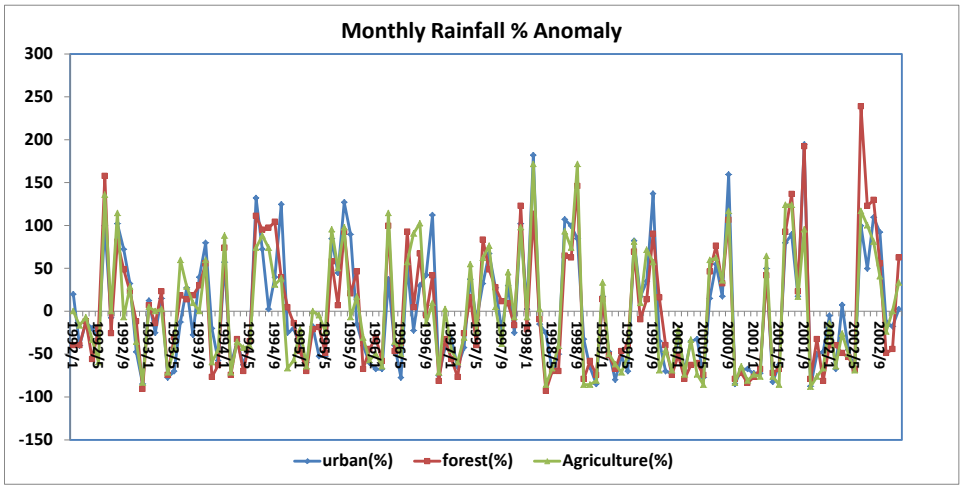

Figure 3.8: The time series monthly rainfall anomaly patterns for Northeast Florida

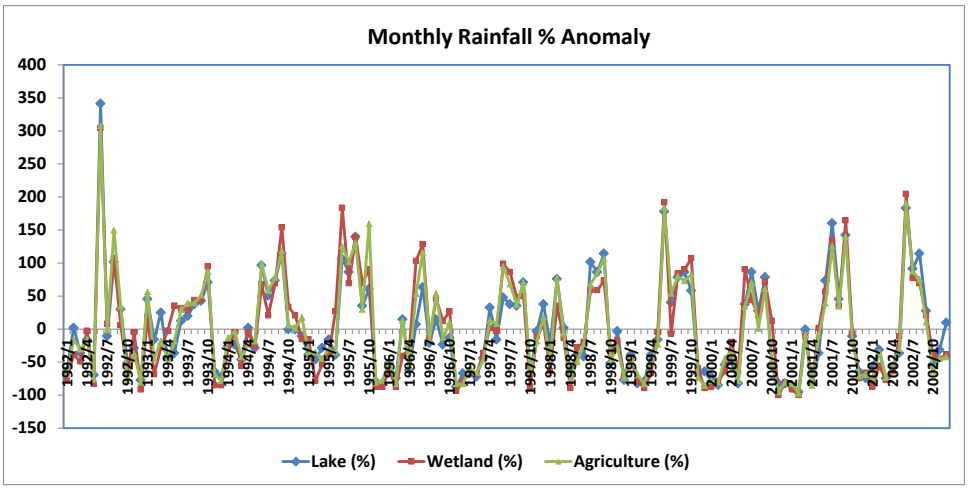

Figure 3.9: The time series monthly rainfall anomaly patterns for South Florida

3.4.3 Evaporation Variations

In the hydrologic budget of Florida, ET is the second most important component after precipitation (Knowles, 1996). It is influenced by seasonal changes in climate and can vary considerably among within basins with different types of vegetation or different proportions of water surface. Hence, in this study, seasonal, inter-annual variations and land use effects would be considered in using 11 years actual evaporation reanalysis data. Figures 3.10 and 3.11 show the average annual actual evaporation from 1992 to 2002 on various land uses in Northeast and South Florida, respectively. In Northeast Florida, the highest average of annual evaporation on the urban area was occurred in 1992 of with a value of 3.2 mm/day and the lowest value was in 2001 of with a value of 2.88 mm/day. On the forest and agriculture areas, the highest average values of annual evaporation were in 1996 of for 3.11 mm/day and 3.23 mm/day, and while the lowest values were in 2000 of for 2.66 mm/day and 2.54 mm/day, respectively. In South Florida, the highest values of average annual evaporation were in 1999 for 3.53 mm/day on the lake area, in 1993 for 2.69 mm/day on the wetland and in 1995 for 3.34 mm/day on the agriculture. The lowest values were in 2001 for 3.08 mm/day, 2.33 mm/day and 2.48 mm/day on the lake, wetland and agriculture areas, respectively.

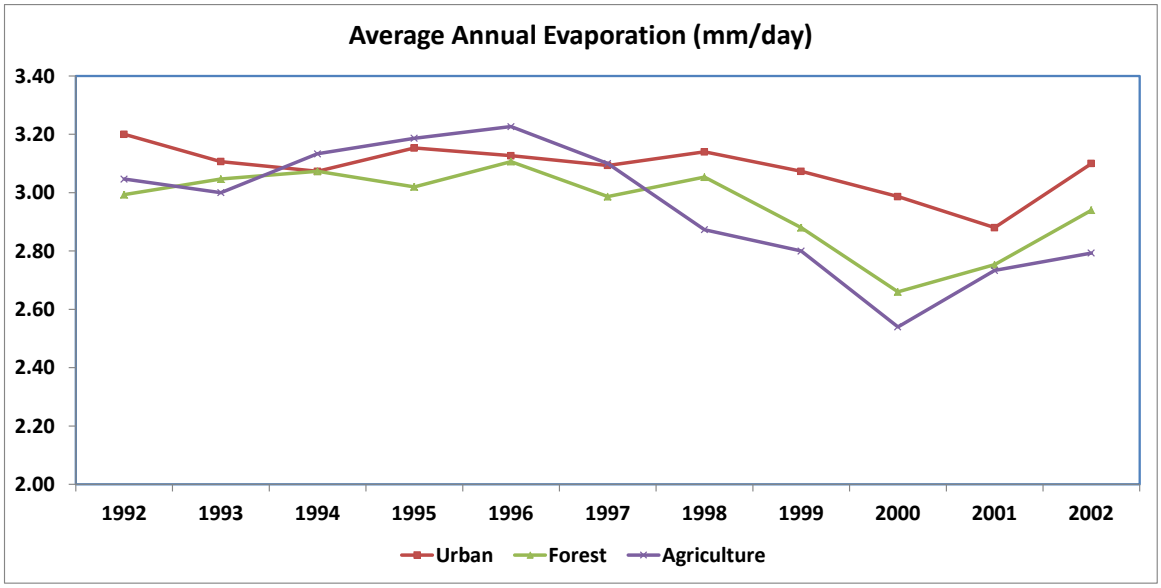

Figure 3.10: The average annual actual evaporation in Northeast Florida

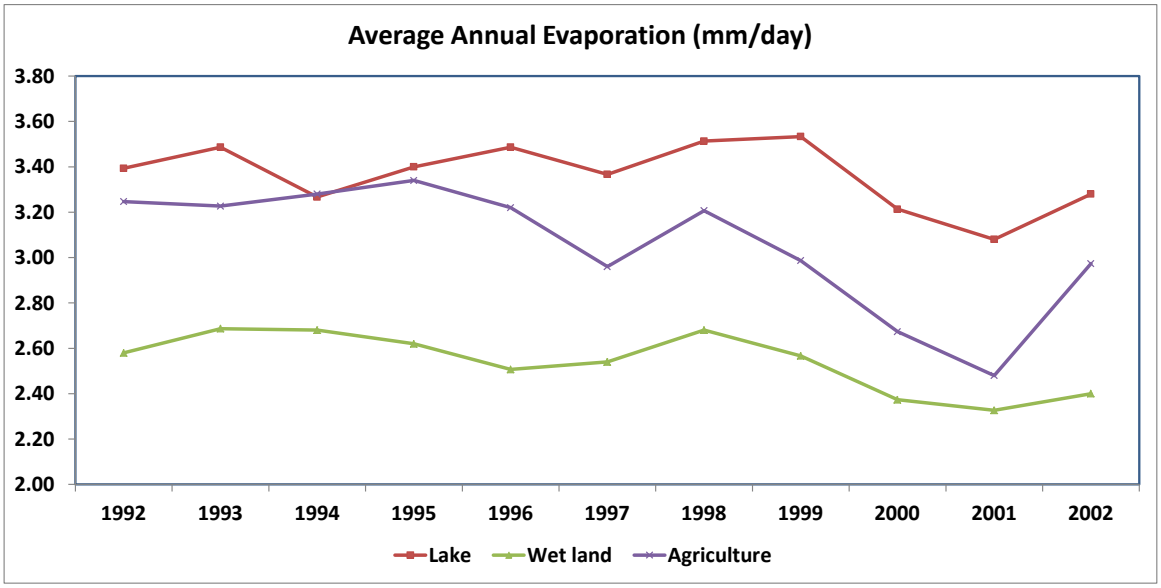

Figure 3.11: The average annual actual evaporation in South Florida

Seasonal variations of the average monthly evaporation in Northeast and South Florida are shown on Figures 8a and 8b, respectively. In Northeast Florida, the higher average values were seen to occur during April - September on the urban and forest areas, with values between 3.25 mm/day and 4 mm/day. However, on the agriculture area, the lowest average monthly evaporation was in May, with the value of 2.94 mm/day, and the highest in July with a value of 4.35mm/day. In South Florida, the wetland area, which is located in the Everglades, had the highest values of the average monthly evaporation in June, with the value of 3.43 mm/day. It has been suggested that much of the rainfall in South Florida is based on the evaporation in the Everglades (Pielke et al., 1999). Pielke et al., (1999) also suggested that the effect of water vapor movement to the north due to wind action from the ocean induces evaporation in the Lake Okeechobee area and the surrounding agriculture area (Figure 3.1) with higher values of evaporation in July and August. These values range from 4.21 mm/day to 3.83 mm/day for lake and agriculture respectively.

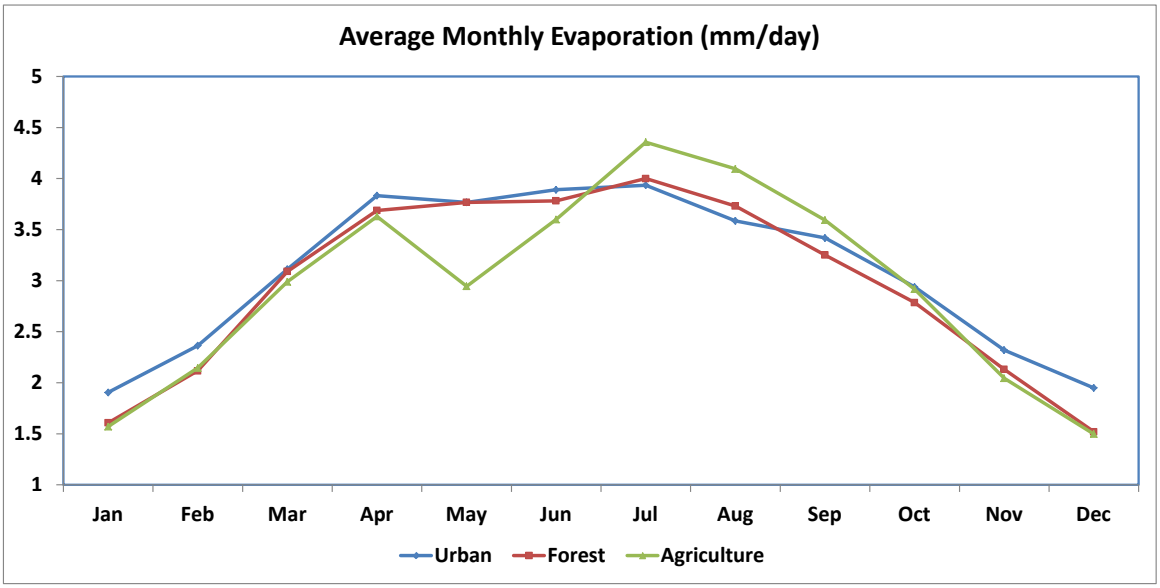

Figure 3.12: Seasonal variations of the average monthly actual evaporation in Northeast Florida

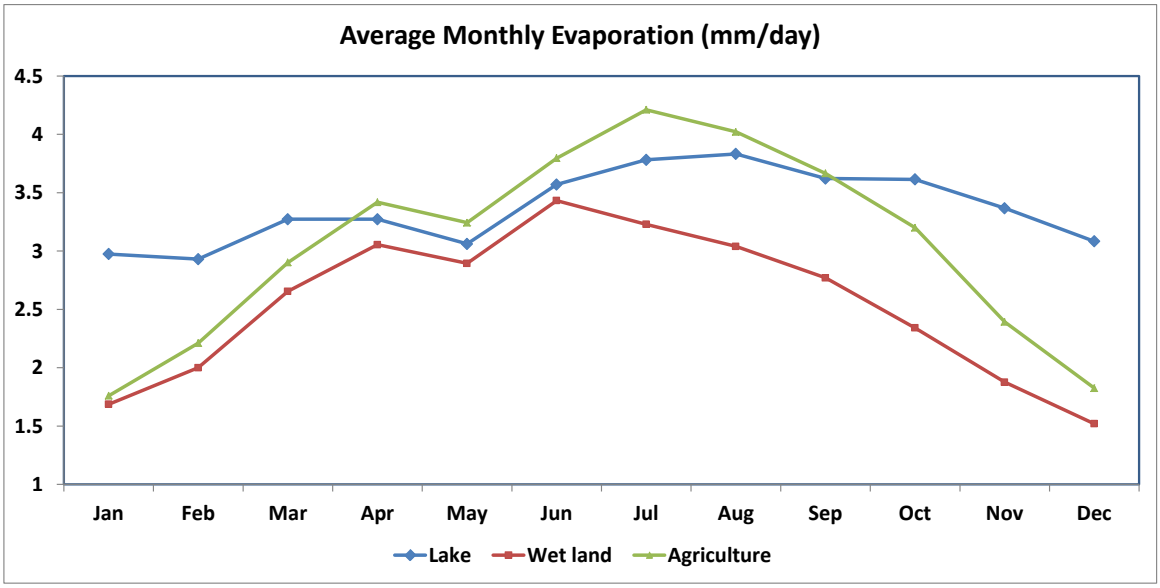

Figure 3.13: Seasonal variations of the average monthly actual evaporation in South Florida

3.4.4 Monthly Evaporation Anomaly

Inter-annual variations in monthly evaporation in Northeast and South Florida were shown on Figures 14 and 15, respectively. In Northeast Florida, monthly evaporation anomalies were positive from March to September with the values between 0.39 % and 57.37 % above the normal for all three land uses. However, during the drought years, anomalies were negative on the three land uses in March 2000 and 2001. Different land use types are strongly affected by evaporation and also had different responses to the drought events. For example, on the agriculture area, the negative anomalies were shown in April 2000, May of 1999 through 2002, and June 1998, but the forest and urban areas had positive values in these months. In South Florida, the positive anomalies were shown on all three land use areas from March to October, but the lake area had the negative values in May. During the drought years, the negative anomalies for the land uses were from December to May of 1999 through 2002, which varies between -7.29% and -86.90 %, except for the positive values in April 2000 and 2002 on the wetland and agriculture areas.

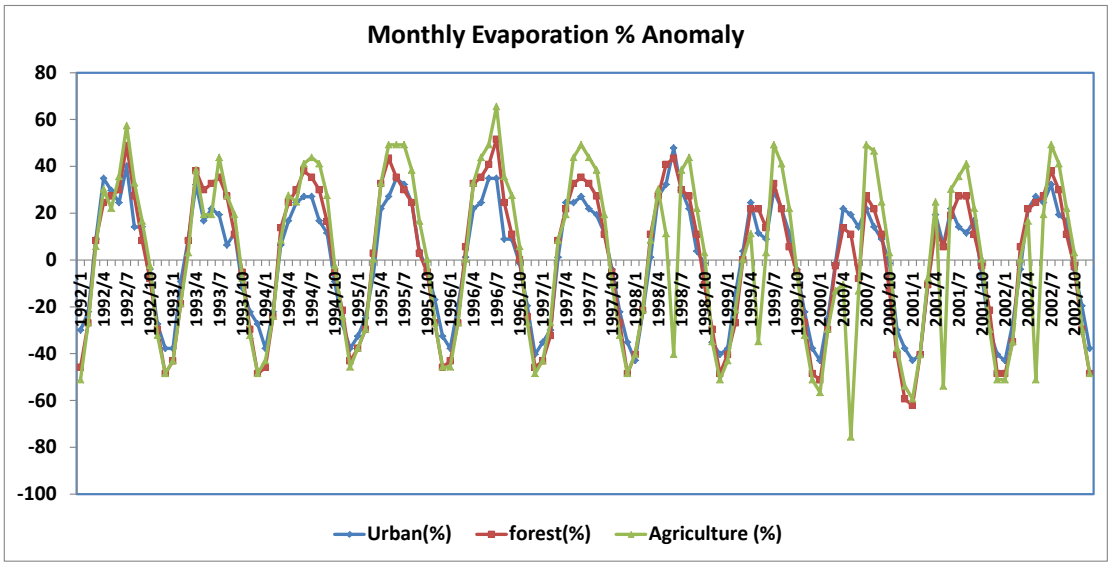

Figure 3.14: Inter-annual variations in monthly evaporation in Northeast Florida

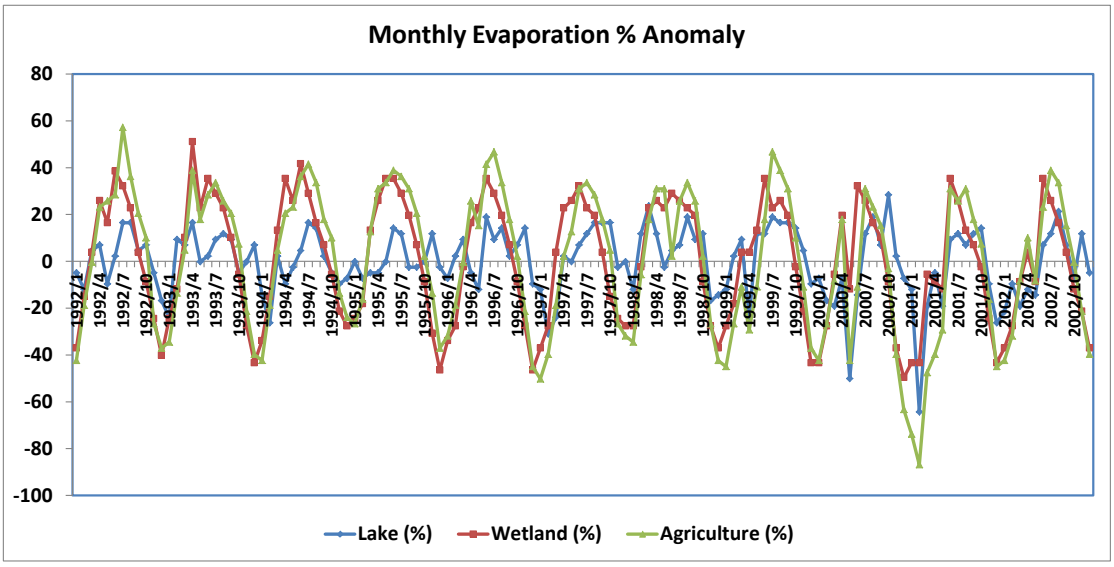

Figure 3.15: Inter-annual variations in monthly evaporation in South Florida

3.4.5 Monthly Soil Moisture Variations

Soil moisture reflects past precipitation and evaporation, infiltration and runoff. In turn, the soil moisture acts as a strong control on the partitioning between sensible heat flux and latent heat flux at the surface modulating precipitation over a given basin (Luo et al., 2007). Figures 16 and 17 show a range of 0 - 200 mm monthly soil moisture anomalies for agriculture, forest and wetland areas in Northeast and South Florida, respectively. The urban and lake areas where not evaluated due to the monthly soil moisture reanalysis data were not available. In Northeast Florida, in the winter 1997-1998, the higher rainfall led to the higher soil moisture, with anomalies between 20% and 41% above the normal on the forest and agriculture areas. Wetter soil moisture caused an enhance moisture flux into the atmosphere from the surface leading to greater specific humidity, and enhancing precipitation over regions. Hence, the positive soil moisture anomalies were shown from 1992 to May 1998, which resulted in the higher rainfall; while negative anomalies occurred during the drought event over the regions. Under drier conditions, the availability of soil moisture becomes the primary source of ET, and differences in capacity of plants access water, often dictated by the rooting depth, can result in contrasting evaporative losses across vegetation types (Calder, 1998). Trees tend to have deeper roots than herbaceous plants (Canadell et al., 1996; Schenk and Jackson, 2002), and hence could maintain higher ET than crops or grasslands when the supply declines (Calder et al., 1997; Sapanov, 2000). Therefore, the forest area had lower soil moisture anomalies, but higher evaporation anomalies than the agriculture area in the Northeast during the drought event. In South Florida, the

agriculture area had negative soil moisture anomalies during the drought event, from February 2000 to July 2001, with the values between -14.95 % and -35.63 %, while the wetland area had higher soil moisture or positive anomalies from July 2000 to October 2000. This can be explained by the fact that a wetland soil is saturated with moisture either permanently or seasonally and can slowly release large volumes of water. Hence as water resources become more and more scarce, wetland provides drought relief for stock and habitat for a range of threatened plants and animals (Green, 1997).

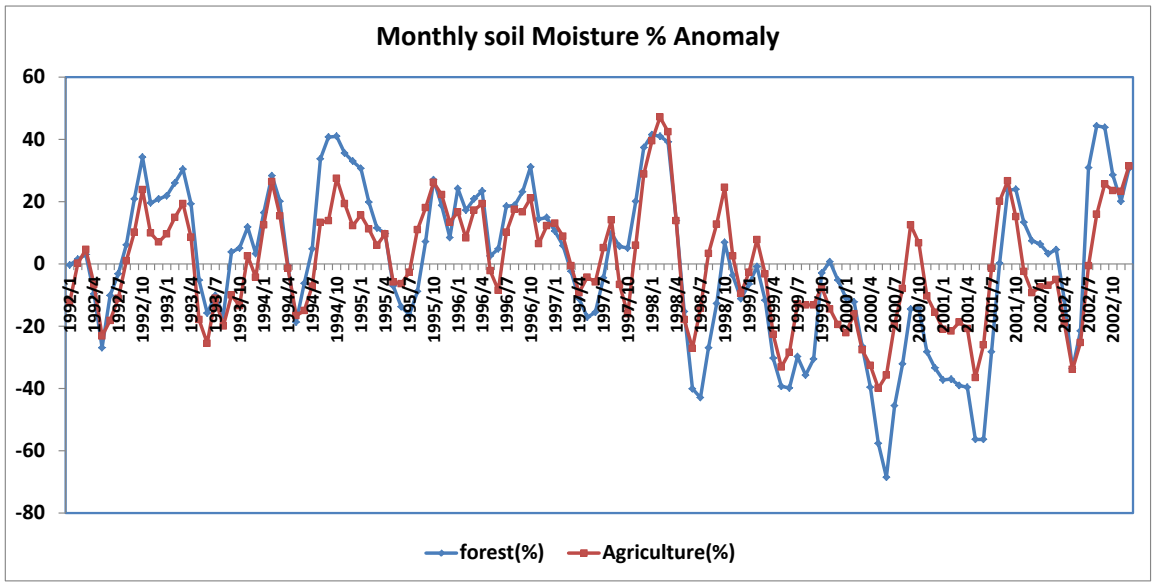

Figure 3.16: The monthly 0-200 mm soil moisture anomalies in Northeast Florida

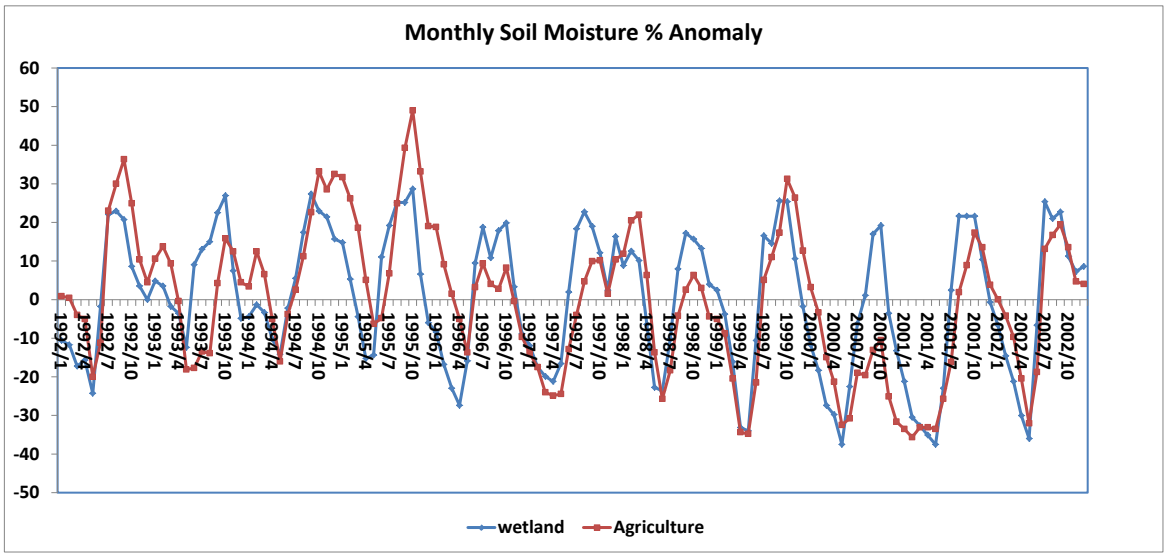

Figure 3.17: The monthly 0-200 mm soil moisture anomalies in South Florida

3.4.6 Water budget balance

Tables 3.1 and 3.2 presented the mean water budget on various land uses in Northeast and South Florida, respectively. Runoff and potential evaporation were calculated from the dataset while the local soil moisture (dw/dt) is the residual of the surface water balance (i.e. dw/dt=P-E-R). However, runoff was not calculated for urban and lake areas due none availability data. Potential evaporation (PE) or potential evapotranspiration (PET) defined as the amount of evaporation that would occur if sufficient water source were available. Hence, the difference

between potential evaporation and actual evaporation (PE-E) was used as a measure of water and energy availability. Regions with larger values of PE-E imply abundance of energy for evaporation, but not enough water available for evaporation, while smaller values imply regions of abundance of water sufficient to satisfy evaporative demand.

In the Northeast, the forest area had the higher rainfall, actual evaporation, potential evaporation, local soil moisture, PE-E, and the lower runoff than the agriculture area, because forests could contain more soil moistures for evaporation and result in the higher rainfall and lower runoff. The urban area located at St. Jones River had the higher evaporation as most of rainfall was returned to the atmosphere locally by evaporation, hence the ratio of evaporation/rainfall was closed to unity. In South Florida, hydric soils in wetlands slowly evaporate large volumes of water on surface. Hence, the wetland area had the higher local soil moisture, potential evaporation, rainfall and PE-E, but lower evaporation and runoff. In the lake area, evaporation loss exceeded the amount gained from rainfall, and abundance of water was sufficient to satisfy evaporative demand, hence the ratio of Evaporation/Rainfall (E/R) close to unity and the value of PE-E is smaller. Moreover, the previous researches showed that annual lake evaporation for the Lake Okeechobee area was approximately 129.5 cm per year (3.54 mm/day) (Viessman et al., 1977). Waylen and Zorn (1998) also presented an annual evaporation estimation map that showed the Lake Okeechobee area with an annual value of approximately 126 cm (3.45 mm/day). Hence, the NARR data set could provide the valuable analysis for estimating evaporation of Lake Okeechobee.

Table 3.1: Annual mean (1992-2001) water budget for various land uses in Northeast Florida

Water budget	Urban	Forest	Agriculture
Precipitation , P (mm/day)	3.208	3.448	3.358
Evaporation, E (mm/day)	3.085	2.956	2.948
Runoff, R (mm/day)	N/A	0.013	0.015
*dW/dt	N/A	0.480	0.394
E/P	0.961	0.857	0.878
Potential Evaporation, PE (mm/day)	5.444	5.668	5.387
P/PE	0.589	0.608	0.623
PE-E	2.359	2.712	2.439

*dW/dt: soil moisture change with time (W = 0-200 mm soil moisture)

Table 3.2: Annual mean (1992-2001) water budget for various land use areas in South Florida

Water budget	Lake	Wetland	Agriculture
Precipitation , P (mm/day)	3.14	3.78	3.33
Evaporation, E (mm/day)	3.37	2.54	3.05
Runoff, R (mm/day)	N/A	0.04	0.09
*dW/dt	N/A	1.20	0.19
E/P	1.07	0.67	0.92
Potential Evaporation, PE (mm/day)	4.90	6.00	5.72
P/PE	0.64	0.63	0.58
PE-E	1.54	3.46	2.67

*dW/dt: soil moisture change with time (W = 0-200 mm soil moisture)

3.5 Summary and Conclusions

Better understanding of the terrestrial water budget on various land uses is necessary and critical for improving our knowledge of current climate, global hydrological cycle and its dynamics. However, traditional observations, including in-situ data and satellite images, have deficiencies in limited long-term records for many hydrologic variables. Moreover, the

drawbacks of model-only approaches are (1) models are not perfectly parameterized and calibrated and (2) models were used in limited land uses like forest, grassland and agriculture. Hence, in this study, the 1992 to 2002 dataset from North American Regional Reanalysis (NARR) was employed to investigate the water budget on various land uses (Lake, wetland, agriculture, forest, and urban) at regional scale in Florida. In Table 3.1 and 3.2, the results showed that Lake Okeechobee and the urban area located at St. Johns River had higher evaporation, lower values of PE-E and E/R ratios closed to 1, while the wetland area had lower evaporation, E/R, and higher local soil moisture, PE and PE-E. Moreover, previous studies suggested that evaporation rate measurement at Lake Okeechobee was difficult, but the NARR data set provided valuable resource for estimating evaporation rate over water bodies. Comparing to the forest and agriculture areas, the tree had the deeper roots, which can sustain more soil moisture, to maintain the higher evaporation and lower the surface runoff.

It was observed that EI Niño years, tend to be cooler and wetter, while La Niña years tend to be warmer and drier than the normal in the fall through the spring, with the strongest effect in the winter. Above-normal rainfall were observed on the various land uses during the 1997/1998 EL Niño event, while the negative monthly rainfall anomalies showed on the various land uses during the 1999/2000 La Niña event. Hurricanes like Andrew and thunderstorms in summer also caused the positive rainfall anomalies more than 70% above normal on the study areas. La Niña drought events, seasonal and inter-annual variations of climatic variables affect the individual terms of surface water balance on various land uses in Florida. The results showed that during the drought years, lower average annual precipitation and evaporation were shown on land uses

in Florida. The northeast part of the state experienced two dry periods—one is from November to December and the other one is from April to May, while, in South Florida, the dry season occurred continuously from winter through spring.

Soil moisture reflects past precipitation, evaporation, infiltration and runoff and is related to land surface-atmosphere interactions with the behavior of the boundary layer and precipitation processes. The higher rainfall led to the higher soil moisture and the wetter soil moisture caused an enhance moisture flux into the atmosphere from the surface, leading to grater specific humidity and precipitation over regions. Hence, the higher soil moisture anomalies were shown from 1992 to May 1998, which resulted in the higher rainfall and evaporation over the forest, agriculture and wetland areas. Hence, the forest, which had the deeper roots, had the lower soil moisture anomalies, but higher evaporation anomalies than agriculture area during the drought event. Moreover, the wetland area had the higher or positive anomalies soil moisture and evaporation during the drought event, because wetland can contain and slowly release large volumes of water.

Based on these results, the North American Regional Reanalysis (NARR) could provide valuable, independent analysis of the water budget on various land uses in Florida.

References

Arora, V., 2002, Modeling vegetation as a dynamic component in soil–vegetation–atmosphere transfer schemes and hydrological models. Rev. Geophys. 40, 3.1–3.26

Bates, B. C., Kundzewicz, Z. W., Wu, S., Palutikof, J. P., 2008, Climate Change and Water, IPCC, Geneva

Black, R. J., Florida Climate Data 1, July: 1-4.

Bonan, 1999, Frost followed the plow: Impacts of deforestation on the climate of the United States. Ecol. Appl., 9, 1305–1315.

Bonan, G. B., 1997, Effects of land use on the climate of the United States. Climatic Change, 37, 449-486.

Brenner, J., 1991, Southern Oscillation anomalies and their relation to wildfire activity in Florida, Int. J. Wildland Fire, 1, 73–78

Calder, I.R., Rosier, P.T.W., Prasanna, K.T., 1997, Eucalyptus water use greater than rainfall input – a possible explanation from southern India, Hydrology and Earth System Science, 1, 249–256.

Calder, I.R., 1998, Water use by forests, limits and controls, Tree Physiology, 18, 625–631

Canadell, J., R.B., Jackson, and J.R., Ehleringer, 1996: Maximum rooting depth of vegetation types at the global scale, Oecologia, 108, 583–595

Carter, D.R., and E.J., Jokela, 2002: Florida's renewable forest resources, CIR1433: Gainesville: University of Florida, Institute of Food and Agricultural Sciences, Florida Cooperative Extension Service, 9.

Chase, T. N., Pielke, R. A., Kittel, T. G. F., Nemani, R. R., Running, S. W., 1996, Sensitivity of a general circulation model to global changes in leaf area index. J. Geophys. Res.,101 (D3), 7393–7408.

Copeland, J. H., Kittel, T. G. F., 1996, Potential climatic impacts of vegetation change: A regional modeling study. J. Geophys. Res., 101 (D3), 7409–7418

Dickinson, R. E., A. Henderson-Sellers, 1988: Modelling tropical deforestation: A study of GCM land-surface parametrizations. Quart. J. Roy. Meteor. Soc., 114, 439–462.

Drummond, M. A., Thomas R. L., 2010, Land-use Pressure and a Transition to Forest-cover Loss in the Eastern United States, BioScience, 60, 4, 286-298

Ek, M. B., Mitchell, K. E., Lin, Y., Rogers, E. P., Grunmann, V., Koran, G. G., Tarpley, J. D. 2003, Implementation of Noah land surface model advances in the National Cen- ters for Environmental Prediction operational Mesoscale Eta Model. J. Geophys. Res., 108, 8851

FASS, 1996, Florida agriculture: Vegetables winter acreage, Florida Agricultural Statistics Service, Florida Department of Agriculture and Consumer Services, January 19, 2.

Florida Division of Forestry, undated(a), Wildfire statistics for Florida: 1981-present: Accessed August 31, 2005, at http://www.fl-dof.com/wildfire/stats_fires_since1981.html.

Florida Wetlands, http://wetlandextension.ifas.ufl.edu/hydricsoils.htm

Folks, J. C., 2005, Lake Okeechobee TMDL: Technologies and Research. North Carolina State University College of Agriculture and Life Sciences, 1-12.

Green, Dayle L., 1997, WETLAND MANAGEMENT TECHNICAL MANUAL: Wetland Classification, Environmental Studies, 1.

Hanson, K., Maul, G. A. 1991, Florida precipitation and the Pacific El Nin˜o, 1985–1989, Florida Sci., 54, 160–168

Hansen, J.W., Jones, J.W., Kiker, C.F., Hodges, A.W., 2010, El Niño–Southern Oscillation Impacts on Winter Vegetable Production in Florida. October 92-102.

Hoerling, M., Kumar, P. A., Zhong, M., 1997, El Niño, La Niña, and the nonlinearity of their tele-connections, J. Climate, 10, 1769–1786

Hutjes, R. W. A., P. Kabat, S. W. Running, W. J. Shuttleworth, C. B. Field, B. Bass, M. A. F. da Silva Dias, R. Avissar, A. Becker, M. Claussen, A. J. Dolman, R. A. Feddes, M. Fosberg, Y. Fukushima, J. H. C. Gash, L Guenni, H. Hoff, P. G. Jarvis, I. Kayane, A. N. Krenke, C. Liu, M. Meybeck, C. A. Nobre, L. Oyebande, A. Pitman, R. A. Pielke Sr., M. Raupach, B. Saugier, E. D. Schulze, P. J. Sellers, J. D. Tenhunen, Valentini, R., Victoria, R. L., Vorosmarty, C. J. 1998, Journal of Hydrology, 212-213

Kiladis, G. N., Diaz, H., 1989, Global climatic anomalies associated with extremes in the Southern Oscillation. J. Climate, 2, 1069–1090.

Knowles, By Leel, 1996, Estimation of Evapotranspiration in the Rainbow Springs and Silver Springs Basins in North-Central Florida, Water Management

Kucharik, C.J., Foley, J.A., Delire, C., Fisher, V.A., Coe, M.T., Lenters, J.D., Young, C., Ramankutty, M. N., 2000, Testing the performance of a dynamic global ecosystem model:

water balance, carbon balance, and vegetation structure. Glob. Biogeochem. Cycles, 14, 795–825.

Larkin, N. K., Harrison, D. E. 2005, On the definition of El Niño and associated seasonal average U.S. weather anomalies, Geophys. Res. Lett., 32, L13705, doi:10.1029/2005GL022738.

Lau, N.C., Leetmaa, A., Nath, M.J., 2008, Interactions between the Responses of North American Climate to El Niño–La Niña and to the Secular Warming Trend in the Indian–Western Pacific Oceans. J. Climate, 21, 476–494.

Lee, D., J., Kim, K., Lee, S., Kim, S., 2010, Partitioning of catchment water budget and its implications for ecosystem carbon exchange, Biogeosciences, 7, 1903-1914,

Luo, Y., Ernesto H. B., Kenneth E. M., 2005, The Operational Eta Model Precipitation and Surface Hydrologic Cycle of the Columbia and Colorado Basins. J. Hydrometeor, 6, 341–370.

Luo, Y., Ernesto H. B., Kenneth E. M., Alan, K. B., 2007, Relationships between Land Surface and Near-Surface Atmospheric Variables in the NCEP North American Regional Reanalysis, J. Hydrometeorol, 8, 6, 1184

Mitchell, K., Coauthors, 2004, NCEP completes 25-year North American Reanalysis: Precipitation assimilation and land surface are two hallmarks. GEWEX News, 14, 2, International GEWEX Project Office, Sliver Spring, MD, 9–12

Munson, A. B., Joseph J. D., Douglas, A. L., 2005, Determining Minimum Flows and Levels: the Florida Experience. Journal of the American Water Resources Association 41, no. 1 (February): 1-10

National Research Council (NRC), 1992, Opportunities in the Hydrologic Sciences, 348, Natl. Acad. of Sci., Washington, D. C

Pan, M., Wood, E. F., Wójcik, R., McCabe, M. F., 2008, Estimation of regional terrestrial water cycle using multi-sensor remote sensing observations and data assimilation. Remote Sensing of Environment, 112(4), 1282-1294

Pan, M., Wood, E. F., 2006, Data Assimilation for Estimating the Terrestrial Water Budget Using a Constrained Ensemble Kalman Filter, J. Hydrometeor, 7, 534–547.

Pielke, R. A., Walko, R. L., Steyaert, L. T., Vidale, P. L., Liston, G. E., Lyons, W. A., Chase, T. N. 1999, The influence of anthro-pogenic landscape changes on weather in south Florida. Mon. Wea. Rev., 127, 1663–1673

Richard, B., J. Tomlinson, V. S., Marella, R., 2002, The Drought of 1998-2002: Impacts on Florida's Hydrology and Landscape Circular, 1295

Ropelewski C. F., Halpert, M. S., 1986, North American precipitation and temperature patterns associated with the El Niño/Southern Oscillation (ENSO). Mon. Wea. Rev., 114, 2352–2362.

Ropelewski, C. F., Halpert, M. S., 1987, Global and regional scale precipitation patterns associated with the El Niño/ Southern Oscillation. Mon. Wea. Rev., 115, 1606–1626.

Ruiz, B., Nigam, A. S., 2006, Great Plains Hydro-climate Variability: The View from North American Regional Reanalysis. J. Climate, 19, 3004–3010.

Sapanov M. K., 2000, Water uptake by trees on different soils in the Northern Caspian region, Eurasian soil science, 33, 1157–1165

Schenk H. J., Jackson, R. B., 2002, The global biogeography of roots. Ecologial Monographs, 72, 311–328.

Sittel, M. C., 1994a, Marginal probabilities of the extremes of ENSO events for temperature and precipitation in the southeastern United States, Tech. Rep. 94-1, Center for Ocean-Atmospheric Prediction Studies, 155

Snyder, G.H., 1987, Agricultural flooding of organic soils. Bulletin No. 570, Institute of Food and Agricultural Sciences, University of Florida, Gainesville.

The South Florida Everglades Restoration Project, http://www.ce.utexas.edu/prof/maidment/grad/dugger/GLADES/glades.html

Trenberth K. E., Smith L., Qian T., Dai A., Fasullo J., 2007, Estimates of the global water budget and its annual cycle using observational and model data. J. Hydrometeor, 8, 758–769

Twine, T. E., Kucharik, C. J., Foley, J. A., 2004, Effects of land cover change on the energy and water balance of the Mississippi River Basin. Journal of Hydrometeorology, 5, 640-655.

Wang, Z., Chang, C.P., Wang, B., 2007, Impacts of El Niño and La Niña on the U.S. Climate during Northern Summer, J. Climate, 20, 2165–2177

Wayne R. R., Jacqueline B., Peter D., Blanken, N. B., Claude R. D., Claire J. O., William M. S., Christopher S., 2006, The Influence of Lakes on the Regional Energy and Water Balance

of the Central Mackenzie River Basin. In: DiCenzo P (ed), Proc. 11 the Sci Workshop Mackenzie GEWEX Study , Ottawa ON Canada

Viessman, W., Klapp, J. W., Lewis, G. L., Harbaugh, T. E., 1977, Introduction to hydrology, Harper & Row, New Yor

CHAPTER 4:

ENERGY BUDGET OF VARIOUS LAND USE AREAS IN FLORIDA USING NARR REANALYSIS DATA

This chapter has been submitted for publication with the following citation: C. H., Cheng and F., Nnadi. Journal of Applied Meteorology and Climatology (in review, November, 2011)

4.1 Introduction

The energy budget on land surface is closely related to the hydrological cycle. It has been suggested that evapotranspiration (ET) or latent heat (LE) is a key component in both energy and water budgets (Yan Luo, 2006). Within the hydrological cycle, ET or LE are driven primarily by the evaporative power of the net radiation (energy budget). The partitioning of net radiation is dependent on the amount of available water on the surface. Hence, when soil moisture drops below a critical limit, the available soil water coupled with the available energy limit the evaporation rate and reduced rainfall thus affecting the water budget. Therefore, quantifying the energy budget above plant canopies is critical to the understanding of the water budget, and it can provide insight into improving the modeling of future regional and global climate regimes (Hernandez-Ramirez et al., 2009).

Land-atmospheric interactions also govern the energy balance at the land-atmosphere boundary layer, as it reflects the nature of the coupling between boundary conditions and rainfall

processes. Vegetation strongly influences the exchange of energy and moisture between land and atmosphere through (1) the vegetation's response to incoming radiation and its emission of longwave radiation (2) the vegetation's physical presence, and (3) the plant's transpiration (McPherson, 2007). These processes affect the daily temperature range in the atmospheric boundary layer, cloud cover, rainfall, differential heating, and atmospheric circulations. Hence, changing the vegetation cover can change the lower boundary conditions of the atmosphere and thereby impact the climate (Pielke et al., 1998).

Land use changes can have both immediate and long-lasting impacts on hydrological processes, by altering the balance between rainfall and evapotranspiration and the resultant runoff (K Li et al., 2007). For example, in short-term impacts, disruptive land use changes disrupt the hydrological cycle either by increasing the water yield or by diminishing or even eliminating the low flow in some circumstances (Croke et al., 2004; Pereira, 1992; Bruijnzeel, 1990). However, in long-term impacts, the reductions in evapotranspiration and water recycling arising from land use changes may initiate a feedback mechanism that results in reduced rainfall (Savenije, 1995). Hence, measuring the energy balance of various land uses could provide useful supports for decision making in land use planning and management, policies and the feedback of land use changes to climate change at the regional scale (Hernandez-Ramirez et al., 2009).

A larger number of observational and model studies conducted over the last few decades have demonstrated the importance of the interactions or feedbacks between land surface and atmospheric processes. At the field scale, eddy covariance (EC) and the Bowen ratio (BR), which are conventional techniques to measure ET over a homogenous surface, can provide not

only the overall water balance, but also insight into the processes controlling the coupled cycles of energy in ecosystems across seasons and under varying weather conditions (Leuning et al., 2005). Therefore, these conventional techniques have been applied to various land uses such as grassland (Verma et al., 1992; Twine et al., 2000; Wever et al., 2002; Castellvi et al., 2008), forests (Blanken et al., 1998; Aubinet et al., 2000; Massman and Lee, 2002; Barr et al., 2006; Jarosz et al., 2008), mango orchard (Azevedo et al., 2003), garlic (Vilalolobos et al., 2004), grapes (Yunusa and Walker, 2004), pecans (Sammis et al., 2004), citrus (Rana et al., 2005), peach (Paco, 2006), olives (Testi et al., 2006), grapes (Teixeira et al., 2007), and corn–soybean (Hernandez-Ramirez et al., 2009). However, a disproportionate majority of existing energy balance studies has been conducted in grasslands and forests, and only a few studies have assessed other land uses such as lakes and wetlands (Rouse et al., 2006). These conventional techniques do not provide spatial trends (or distribution) at the regional scale especially in regions with advective climatic conditions. Furthermore, characterization of the surface hydrologic cycle requires adequate long-term records of not only precipitation but also runoff and evaporation, however such records are lacking in observational data (Yan Luo, 2006).

Modeling studies have the advantages of extending scopes and overcoming the limitations of traditional field experiments, which is particularly true when addressing regional and global issues including land use and climate change impacts. Several modeling approaches have related land use changes to potential changes in regional climate (Costa and Foley, 1997, Dickinson and Henderson-Sellers, 1988; Chase et al., 1996; Copeland et al., 1996; Bonan 1997, 1999; Pielke et al., 1999; Twine et al., 2004; Li et al., 2007). Simulations have shown that replacing forests,

woodlands, and savanna with grassland over the Amazon river basin (Costa and Foley, 1997); replacing forests and grasslands with annual crops in the large Mississippi river basin (Twine, et al., 2004); or deforesting, overgrazing or logging the Columbia River Basin (Matheussen et al., 2000) and West Arica (Li et al., 2007) have led to increased stream-flow and reduced ET and rainfall. Therefore, hydrological models are increasingly used to address the hydrologic impacts of land use changes and the sensitivity of precipitation to the characteristics of surface conditions. However, most of these studies are on forest, grassland and agriculture areas.

The National Centers for Environmental Prediction (NCEP) North American Regional Reanalysis (NARR), which includes model- based four-dimensional data assimilation procedures, is a long-term, consistent, high-resolution climatic dataset for the North American domain (Mesinger et al., 2005). These datasets have great potential for more accurate evaluation s of the interactions of land surfaces and the atmosphere. Therefore, the objectives of this study are as follows: (1) to investigate the energy balance of various land uses (lake, wetland, agriculture, forest, and urban) at the regional scale using the NARR datasets. (2) to understand how drought events and seasonal and inter-annual variations in climatic variables affect the energy exchange between the atmosphere and various land uses; and. (3) to determine how well the energy cycles are presented in NARR datasets.

4.2. Dataset

This study employs the NARR dataset developed at the Environmental Modeling Center (EMC) of the National Centers for Environmental Prediction (NCEP). This dataset is based on the April 2003 frozen version of the operational Eta Model and its associated Eta Data Assimilation System (EDAS), and it uses numerous observed quantities in its data assimilation scheme, including gridded analyses of rain gauges precipitation over the continental United States (CONUS), Mexico, and Canada (Luo et al., 2005). Hence, this regional reanalysis dataset is produced at high spatial and temporal resolutions (32-km, 45 layers, 3 hourly) and spans a period of 25 years from October 1978 to December 2003. Full details of the NARR products can be found online at http://www.emc.ncep.noaa.gov/mmb/rreanl/.

The EDAS is successful with downstream effects, including two-way interaction between precipitation and the improved land-surface model (Ek et al., 2003). Mitchell et al., (2004) demonstrated significant regional improvements in a number of variables when using precipitation assimilation over the CONUS. Therefore, it is expected that this dataset will be useful not only for energy and water budget studies, but also for analysis of atmosphere-land relationships. However, NARR is still subject to important, but unavoidable, model dependence; hence, it was necessary to verify the energy budget as derived from the NARR dataset in this study.

The NARR variables used in this study are based on model parameterizations, which include surface evaporation, latent heat, sensible heat and surface temperature. The current study applied

an 11-yr period of NARR analyses from 1992 through 2002, while utilizing monthly averages of the data.

4.3Study area

This study examined the energy balance of various land use sites in Florida. The climate in Florida is humid subtropical with a rainy wet season extending from May through October. Most areas in Florida receive at least 1270 mm of rainfall annually. The long-term annual mean temperature is 22.4°C based on historical records of a weather station located in Kissimmee, Florida (Southeast Regional Climate Center, http://www.dnr.sc.gov/climate/sercc). Florida has varied annual precipitation: floods in one year may be followed by drought the next (Black, 1993).

In Florida, the EI Niño-Southern Oscillation (ENSO) often influences temperature, precipitation, and upper-level wind, which in turn result in drought and wildfires (Brenner, 1991). These impacts are stronger during the winter and spring months than the summer months. Hence, a strong EI Niño phenomenon occurred in fall and winter of 1997-1998 when the rainfall was above normal for most of the state and temperatures were cooler. By late 1998, a strong La Niña event was in effect, which continued through 2001 (Richard et al., 2002). During 1998 - 2002, Florida experienced multiple high-pressure systems with higher temperatures and dry weather, which brought a La Niña effect during part of the period. Hence, lower than normal precipitation caused a severe statewide drought in Florida during that period. The drought was one of the worst ever to affect the state based on precipitation and steam-flow data. Wildfire

statistics show that 25,137 fires burned 1.5 million acres between 1998 and 2002 (Florida Division of Forestry: Part A, (undated)). Finally, rainfall occurred in late 2002 and 2003, and a tropical storm and four hurricanes in 2004 ended this drought period.

In this study, five different land uses in six areas were selected based on Florida's different climatic zones and land cover data. Figure 4.1 presents the six selected 32×32 km regional study areas along with land use/land cover data from the 1992 National Land Cover Dataset. There are three different land uses (i.e., urban, forest and agriculture) in Northeast Florida, and there are three (i.e., lake, wetland and agriculture) in South Florida. Figure 4.2 shows the six selected 32×32 km regional study areas along with the land use/land cover data from the 2001 National Land Cover Dataset. By comparing the National Land cover Dataset of two different periods with a 10-year interval, the land use changes could be monitored and detected. The regional agriculture land use, which is located in west Alachua, changed the land use from row crop in 1992 to pasture hay in 2001, but the other land use areas did not change much within the 10-year period. This land use change could change the energy balance, ET rate and rainfall and could affect the water budget and regional climate. Therefore, in this study, land use change effects could also be observed by examining long-term water budgets on various land uses in Florida.

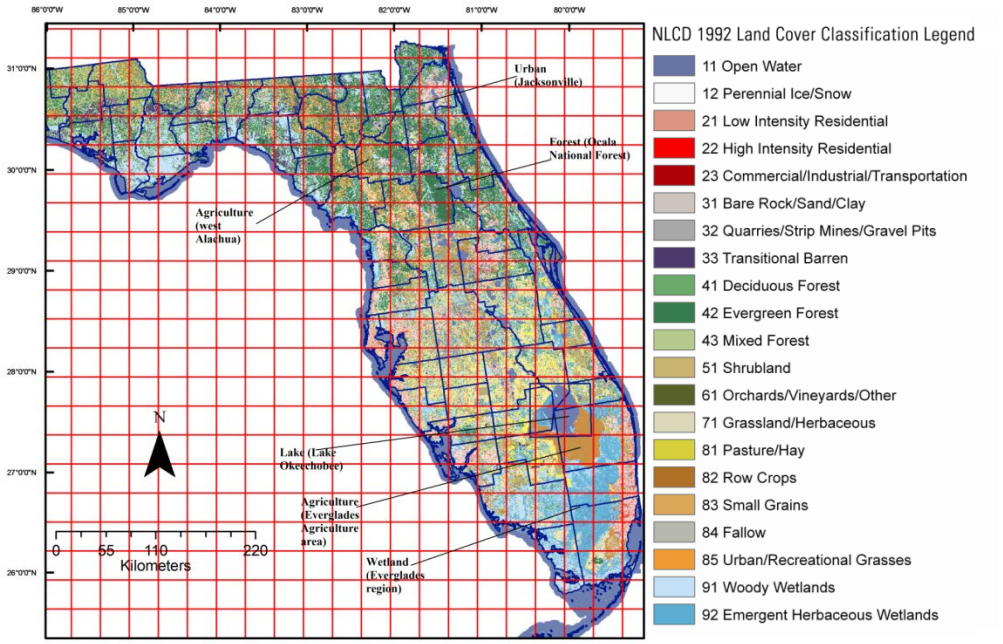

Figure 4.1: Six selected 32×32 km^2 regional study areas along with land-use/ land cover from the 1992 National Land Cover Dataset

The climate of Northeast Florida is somewhat cooler than South Florida and receives abundant precipitation between 1000 and 1500 mm annually. The combination of long frost-free periods of more than 240 days and plentiful water has historically enabled the production of specialized crops (Drummond and Loveland, 2010). For example, the citrus industry focused its intensive orange grove production on the southern interior and southeastern coast of Northeast region. Pastureland in the Northeast Florida has also been an important agriculture resource. Hence a regional agriculture land use, which is located west of Alachua (Figures 4.1 and 4.2) and is devoted to forage, hay production and silage corn, was selected to study the energy budget.

Extensive pine plantations, employed for timber production, are a relatively common use of forests in North Florida. Almost one-third of Florida's forestland is commercial pine harvested and regenerated at a relatively fast pace (Carter and Jokela, 2002). Therefore, investigating land use effects on the energy balance if forest areas is important. In this study, the Ocala National Forest, which is covered by sand pine scrub forest, represents a regional forestland use. Furthermore, within the past 30 years, the population of Florida has increased by more than 140 percent, from 4.2 million to 10.3 million, caused an expansion of urban and developed land. Large urban areas are prevalent on the Florida peninsula. These areas include Tallahassee, Tampa, St. Petersburg, Miami, Orlando, and Jacksonville. Jacksonville, located in the Northeast region is the largest city in the State of Florida, was selected for a regional urban land use.

South Florida, which is exposed to onshore breezes, enjoys comfortable temperatures most of the year. The climate is generally frost-free and subtropical with annual rainfall of approximately 1400 mm. The main regional characteristics in South Florida are wetland, lake, agriculture and urban areas (Figure 4.1). The Everglades is a subtropical wetland, and it is the only one of its kind in the U.S (Munson et al., 2005). Historically, the Everglades have covered much of South Florida, comprising over 4000 square miles and stretching from Lake Okeechobee in the north to the Florida Bay at the southern end of the peninsula (The South Florida Everglades Restoration Project). Hence, a regional 32×32 km grid of wetlands within the Everglades was selected as a study area in South Florida.

Lake Okeechobee (Figures 4.1 and 4.2) is a large, shallow, eutrophic lake located in south central Florida, and is frequently hit by hurricanes. Lake Okeechobee is the second largest

freshwater lake in the U.S covering a surface area of 1800 square km, with an average depth of 2.7 m. As the central part of a larger interconnected aquatic ecosystem in South Florida and as the major surface water body of the Central and Southern Florida Flood Control Project, Lake Okeechobee provides a number of societal and environmental service functions including water supply for agriculture, urban areas, and the environment (Folks, 2005). Therefore, investigating the long-term energy budgets of Lake Okeechobee is critical. Finally, the Everglades Agriculture Area (EAA), which represents an agriculture land use type in this study, is a small portion of the Everglades region, consisting of artificially rich organic soil. The EAA has built a thriving agriculture industry for the most part due to sugarcane and winter vegetables with annual revenues around $500 million (Snyder, 1987).

.

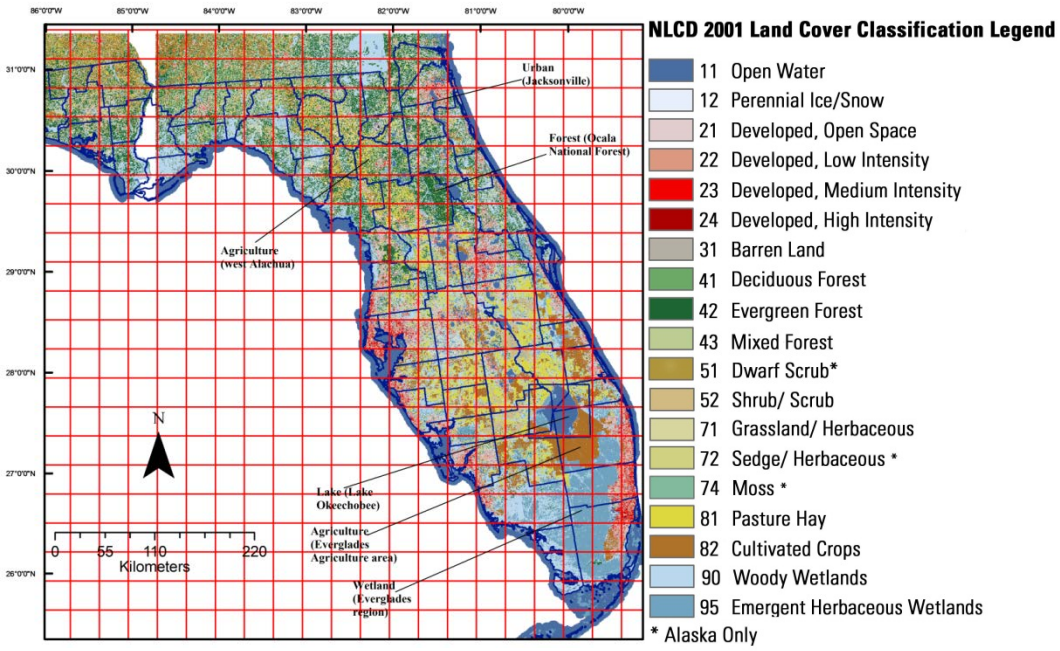

Figure 4.2: Six selected 32×32 km^2 regional study areas along with land-use/ land cover from the 2001 National Land Cover Dataset

4.4 Results and Discussions

Monthly data the from 1992 through 2002 NARR dataset, which include actual evaporation, latent heat, sensible heat and surface temperature data, were utilized to evaluate energy budgets on various land uses using the energy balance equation expressed as:

$$R_n=H+LE+G \quad (4.1)$$

where R_n is the net radiation flux at the interface between land cover and atmosphere; G is conductive soil heat flux; , H is sensible heat (heat exchange by convection); and LE is latent heat, (water vapor condensation or water evaporation from surfaces and plant transpiration). The conductive soil heat flux would be neglected in this equation because it is small (Douglas et al., 2009). The ratio of H to LE is used to calculate the Bowen ratio, B.

4.4.1 Actual Evaporation and Latent Heat Variations

In the hydrologic budget of Florida, ET is the second most important component after precipitation (Knowles, 1996), while latent heat flux is the heat energy transferred by the evaporation of water from the surface. ET and latent heat flux are influenced by seasonal changes in the climate and can vary considerably among basins with different types of vegetation or different proportions of water surface. Hence, in this study, seasonal, inter-annual variations

and land use effects were considered in the analyses of the 11 years NARR dataset. Figures 4.3 and 4.4 show the average annual actual evaporation and latent heat in Northeast Florida, respectively, while Figures 4.5 and 4.6 show those of South Florida. In Table 4.1, the maximum and minimum values of annual evaporation and latent heat on the selected land use areas in both regions are presented with the years of occurrence. From Table 4.1, we find that the selected areas had the lowest evaporation and latent heat during the drought years.

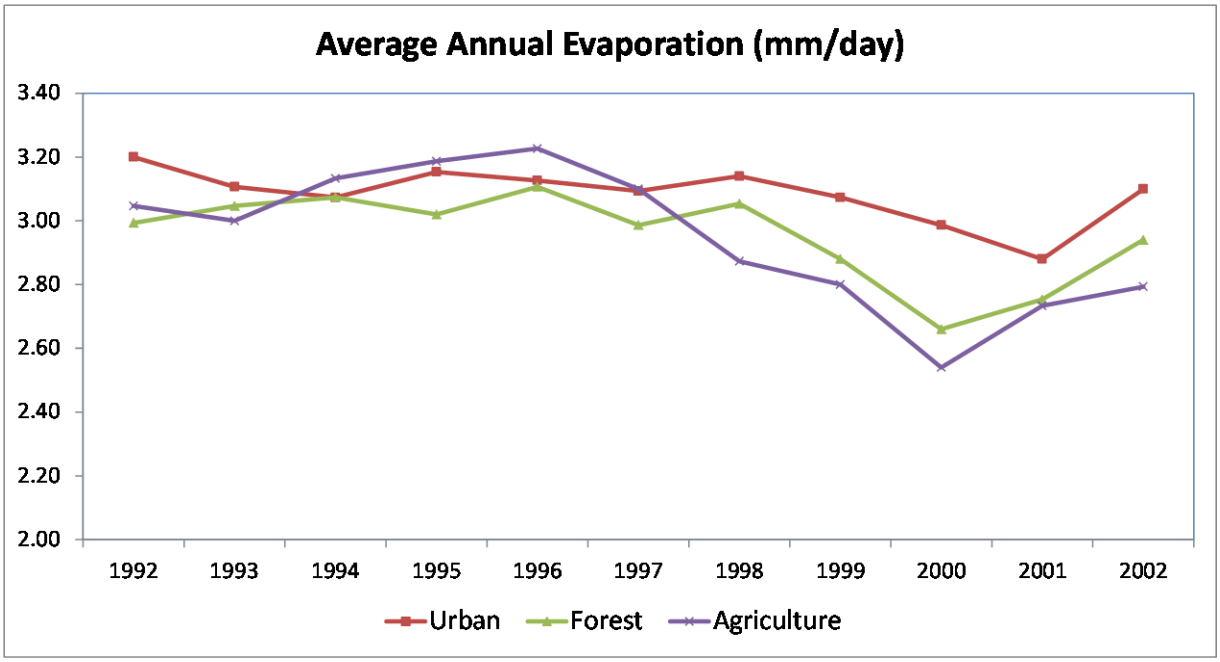

Figure 4.3: The average annual actual evaporation in Northeast Florida

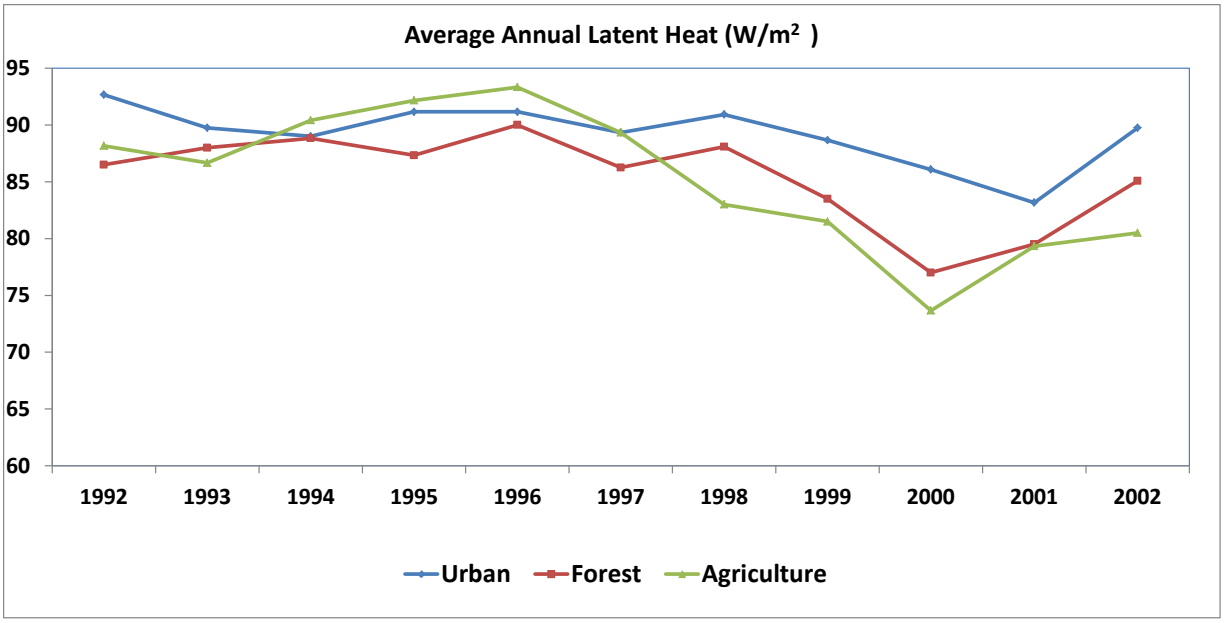

Figure 4.4: The average annual actual latent heat in Northeast Florida

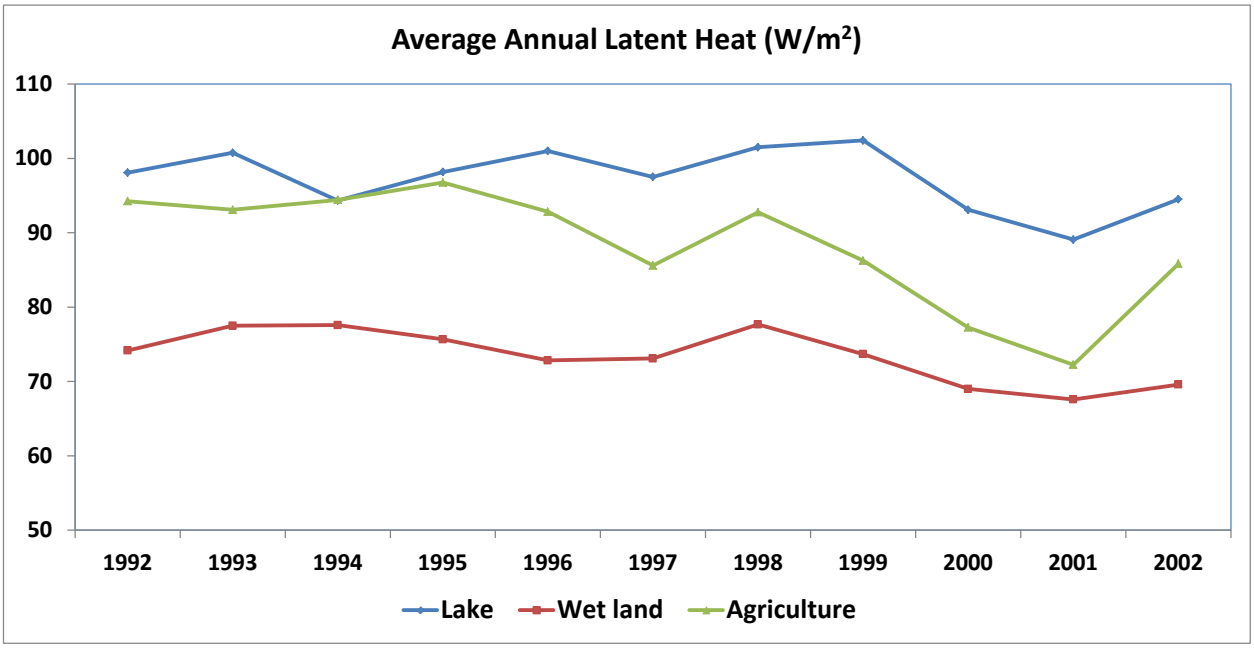

Figure 4.5: The average annual actual evaporation in South Florida

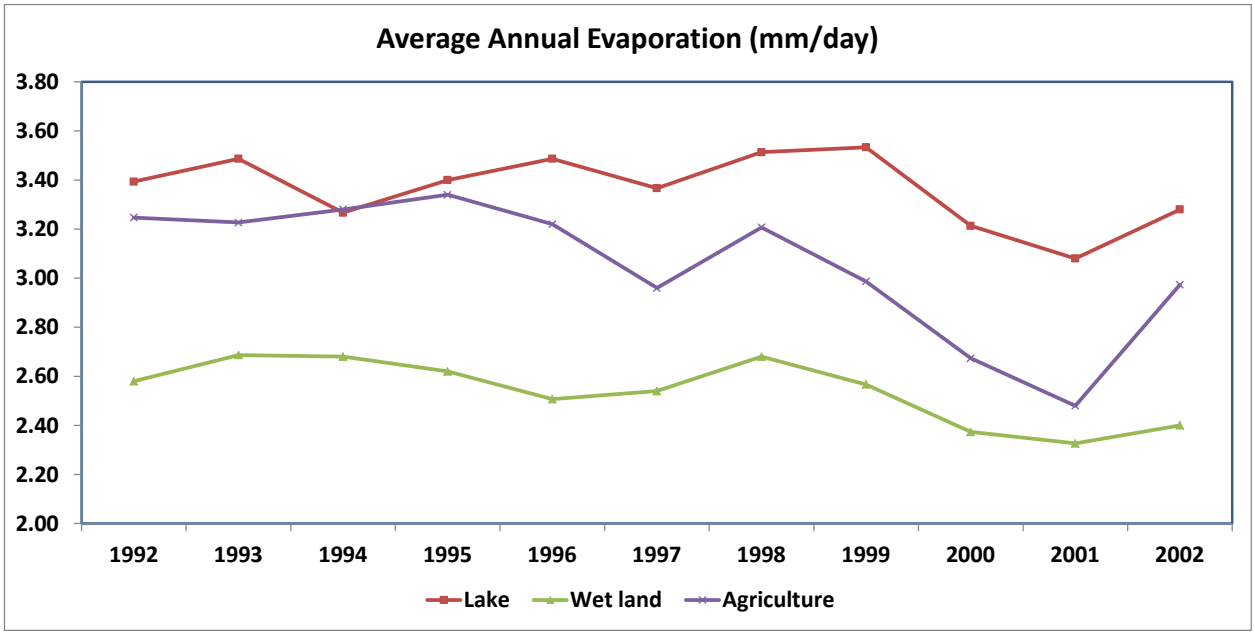

Figure 4.6: The average annual latent heat in South Florida

Table 4.1: Annual Variation of Actual Evaporation and Latent Heat Flux in the selected Land use Areas

Land use	Actual Evaporation (mm/d)		Latent Heat Flux (W/m^2)		Year Reported	
	Max	Min	Max	Min	Max	Min
Northeast Florida Region						
Urban	3.20	2.88	96.27	83.17	1992	2001
Forest	3.11	2.66	90.00	77.00	1995	2000
Agriculture	3.23	2,54	93.33	73.67	1995	2000

South Florida Region						
Lake	3.53	3.08	102.42	89.08	1999	2001
Wetland	2.69	2.33	77.50	67.58	1993	2001
Agriculture	3.34	2.48	96.75	72.25	1995	2001

The seasonal variations of the average monthly actual evaporation and latent heat in Northeast Florida are shown in figure 4.7 and 4.8, respectively; while those of South Florida are presented in Figures 4.9 and 4.10 respectively. In Northeast Florida, higher average values of monthly actual evaporation and latent heat were observed between April and September, in the urban and forest areas, while in the agriculture area, the higher values occur in July; lower values are observed in December and January. These variations are listed in Table 4.2 for the selected land use areasn South Florida, the wetland area, which is located in the Everglades, had the highest values of average monthly actual evaporation and latent heat in June, with values of 3.43 mm/day and 99.09 W/m^2, respectively. It has been suggested that much of the rainfall in South Florida is based on the evaporation in the Everglades (Pielke et al., 1999). Pielke et al., (1999) also suggested that the effect of water vapor movement from the ocean to the north due to wind action induces evaporation in the Lake Okeechobee area and the surrounding agriculture area (Figures 4.1 and 4.2), leading to higher values of actual evaporation in July and August. Lower values were observed in winter. These variations are listed in Table 4.2.

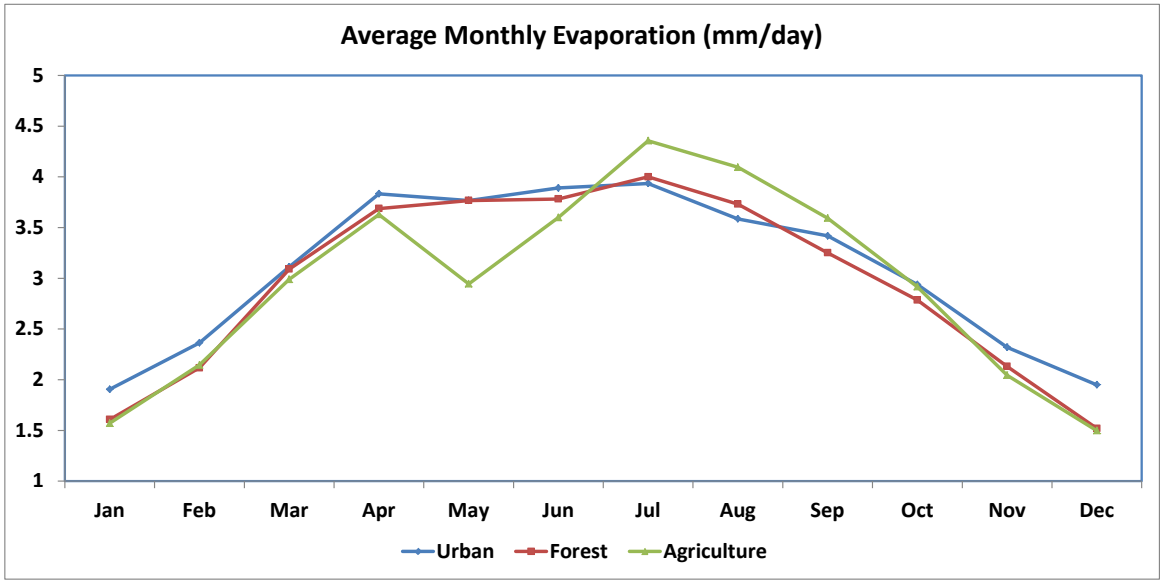

Figure 4.7: The average monthly actual evaporation in Northeast Florida

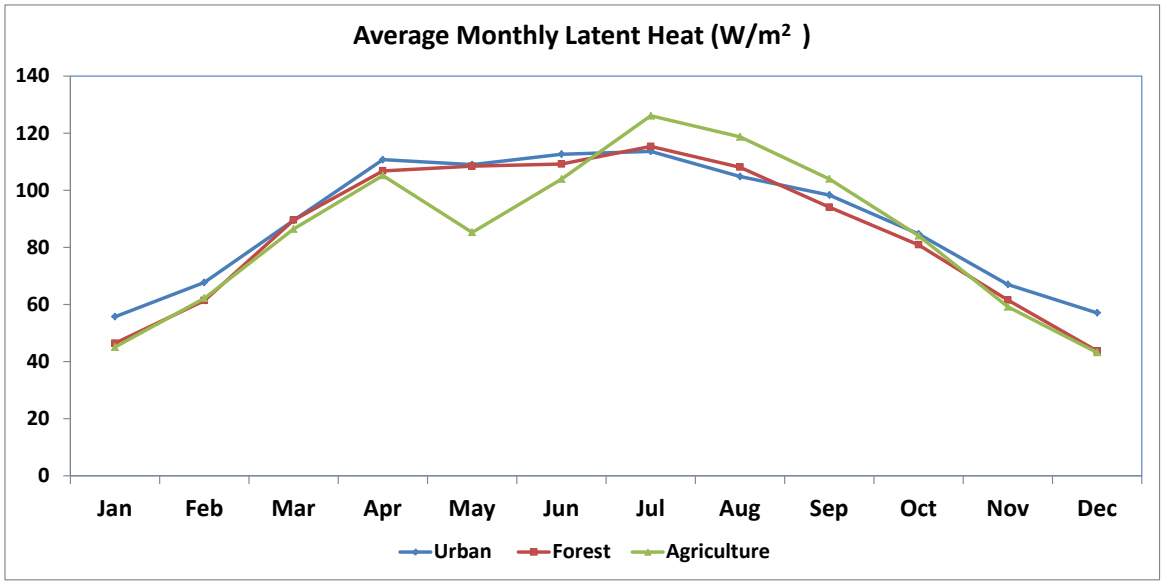

Figure 4.8:The average monthly latent heat in Northeast Florida

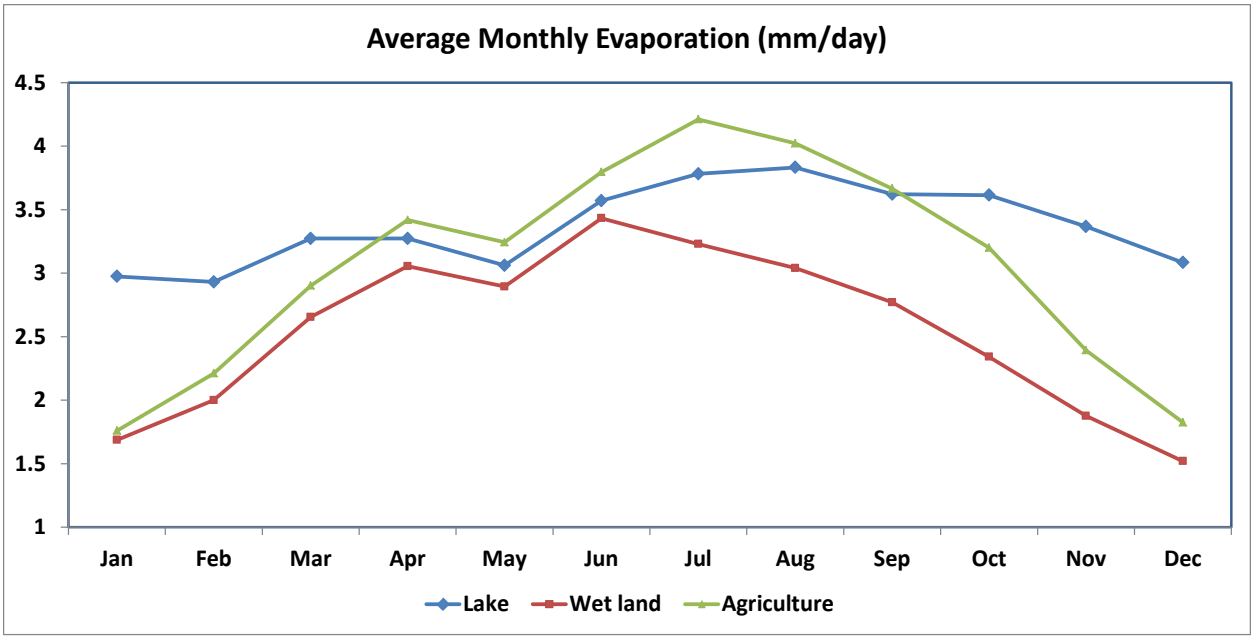

Figure 4.9: The average monthly actual evaporation in South Florida

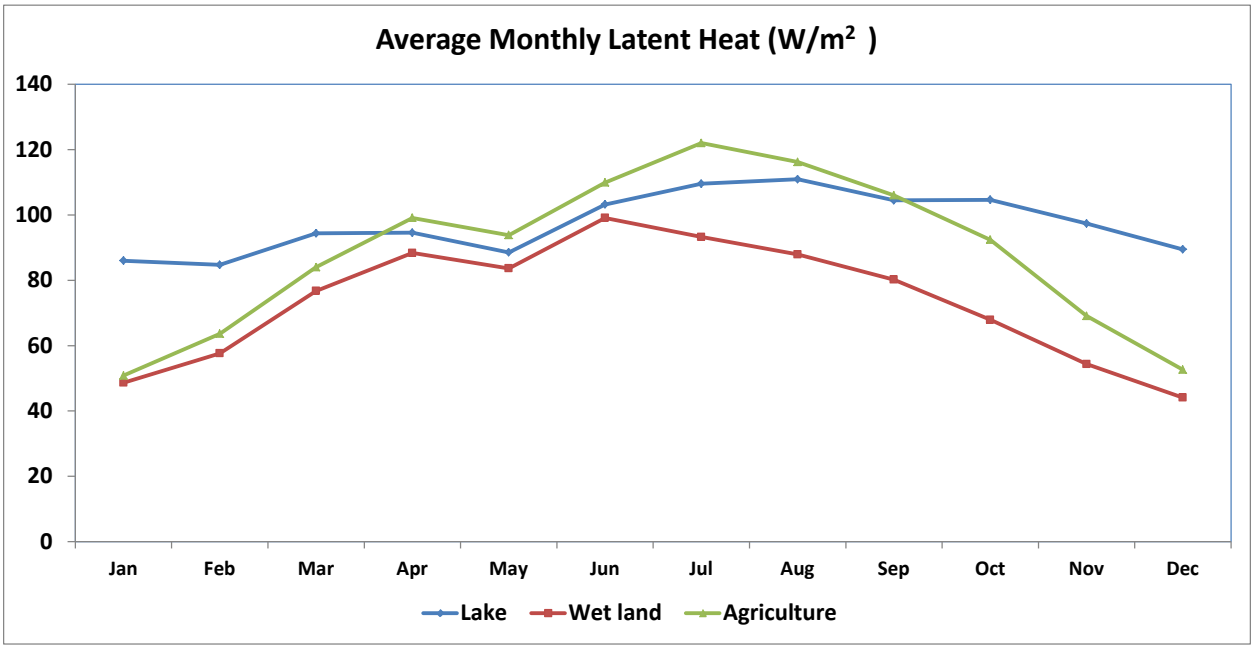

Figure 4.10: The average monthly latent heat in South Flori

Table 4.2: Seasonal Variation of Monthly Actual Evaporation and Latent Heat Flux in the selected Land use Areas

Land use	Actual Evaporation (mm/d)		Latent Heat Flux (W/m^2)		Months Reported	
	Max	Min	Max	Min	Max	Min
Northeast Florida Region						
Urban	3.93	1.90	113.63	55.72	July	January
Forest	4.00	1.52	115.36	43.72	July	December
Agriculture	4.35	1.49	126.00	43.18	July	December
South Florida Region						
Lake	3.83	2.93	110.90	84.72	August	February
Wetland	3.43	1.52	99.09	44.09	June	December
Agriculture	4.21	1.76	122	50.81	July	January

4.4.2 Monthly Actual Evaporation and Latent Heat Anomaly

To determine the anomaly patterns during the study period, the monthly averages of the climatology parameters, including actual evaporation, latent heat, sensible heat and surface

temperature were calculated. Individual monthly anomalies were then calculated as percent departure from the 11 years average of monthly averages using Equation 4.2:

$$P_a = \left(\frac{P_o - P_m}{P_m}\right) \times 100 \qquad (4.2)$$

where P_a is the respective monthly percent anomalies; P_o is the monthly climatology parameters; and P_m is the long-term average of the climatology parameters.

Figures 8a and b show the time series of monthly actual evaporation and latent heat anomaly patterns for Northeast Florida, respectively. These anomalies were positive from March to September for the three land uses, with values between 0.39 % and 57.37 % for actual evaporation, and 0.84% and 50.09% for latent heat.. However, during the drought years, March 2000 through 2001, these anomalies dropped to negative values in all three land uses as shown in Figures 4.11 and 4.12.

Figures 4.13 and 4.14 suggest that the anomalies in the monthly actual evaporation were positive in all land uses studied between March and October. The variation ranges from 2.16% to 46.69%, while the positive anomalies in the latent heat values range from 0.79% and 47.23% for all land uses for the same period. In May, however, the lake area had negative values for both actual evaporation and latent heat. Negative values were also observed during the drought years for all land use areas, except in April of both drought years for the wet land and agriculture areas.

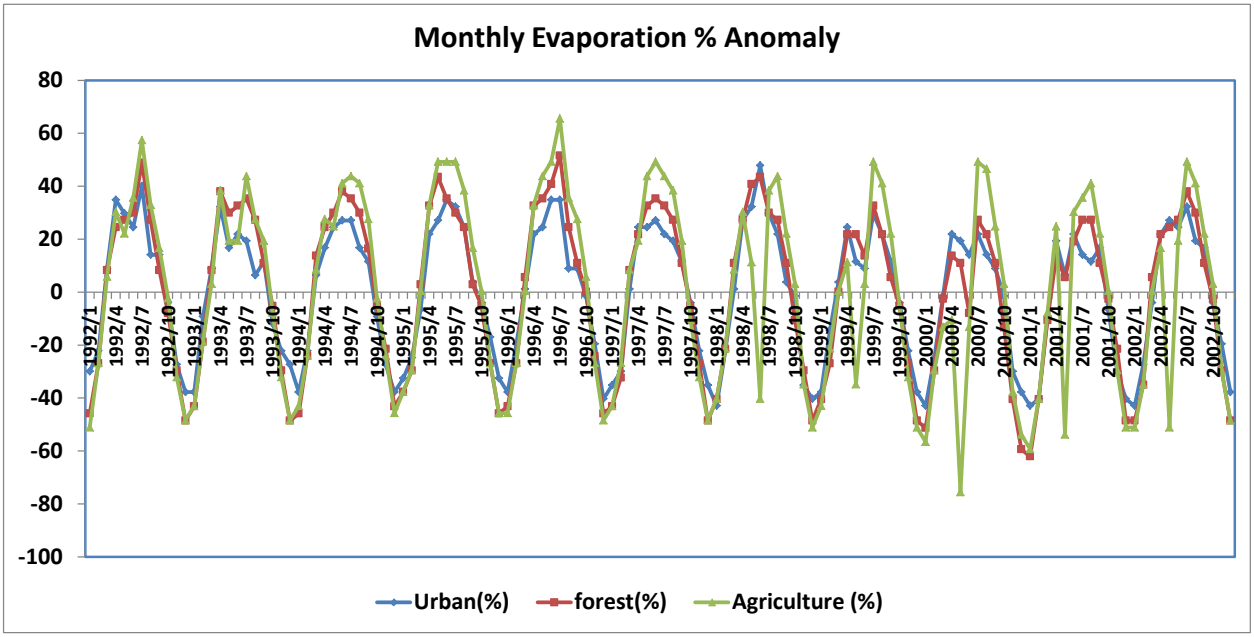

Figure 4.11: The time series monthly evaporation anomaly patterns for Northeast Florida

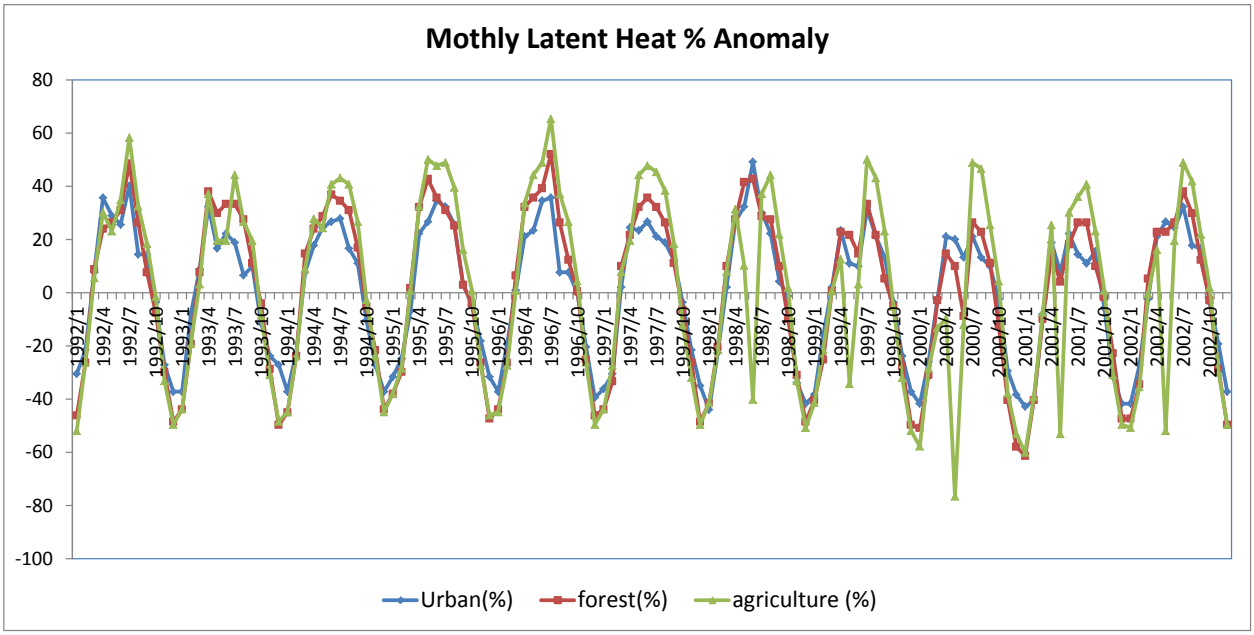

Figure 4.12: The time series monthly latent heat anomaly patterns for Northeast Florid

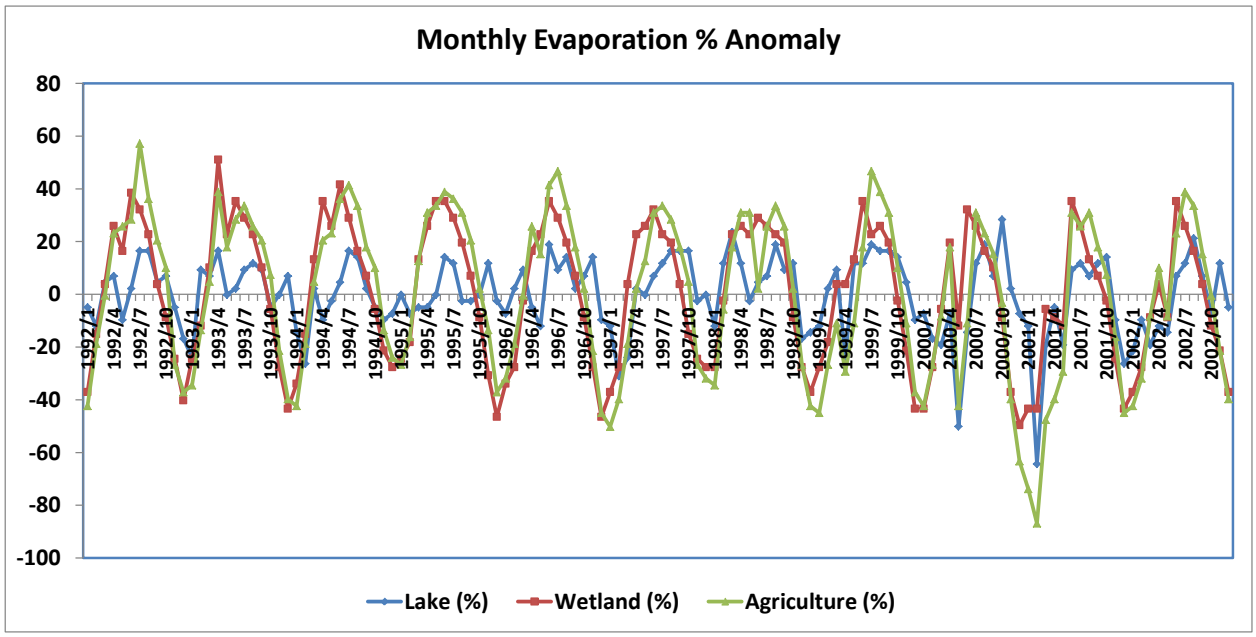

Figure4.13: The time series monthly evaporation anomaly patterns for South Florida

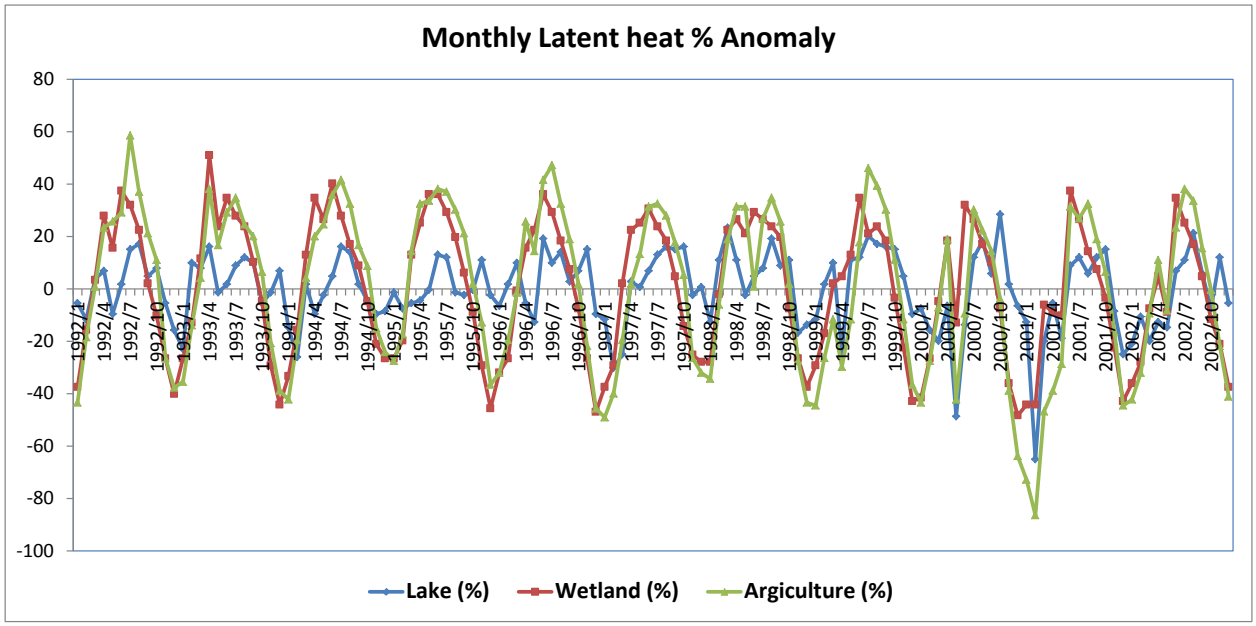

Figure 4.14: The time series monthly latent heat anomaly patterns for South Florid

4.4.3 Monthly Sensible and Heat Variations

Based on the energy budget (equation 4.1), the available land surface energy partitions into latent heat and sensible heat. As, more energy is partitioned into latent heat, less energy is converted to sensible heat. Figures 4.15 and 4.16 show the average annual and monthly sensible heat in Northeast Florida for all land uses. During drought years, most of the land surface energy would be partitioned into sensible heat, hence higher sensible heat were observed in the urban area, with values of 44.08 W/m^2, 51.5 W/m^2 in the forest area, and 51.8 W/m^2 in the agriculture area. Additionally, during the summer and fall seasons, most of the surface energy would convert to latent heat for evaporation, thus resulting in lower values of sensible heat from June to December in Northeast Florida. Hence, for all three land uses, lower average monthly sensible heat values were observed, at 23 W/m^2 and 57.63 W/m^2 in summer and fall respectively, while higher values were observed in winter and spring, as 25.09 W/m^2 and 84.09 W/m^2, respectively.

In the South, the average annual and monthly values of the sensible heat also varied with land uses as shown in Figures 4.17 and 4.18. These annual values are 41 W/m^2 in 2000, 55.41 W/m^2 in 2000, and 51.58 W/m^2 in 2001 for lake, wetland and agriculture, respectively. During summer and fall, when most of the land surface energy is converted to latent heat for evaporation, lower sensible heat values were observed for the three land uses, with values between 15.18 W/m^2 and 45.54 W/m^2. The higher values of average monthly sensible heat were in April for the wetland and agriculture areas, with values of 77 W/m^2 and 67.54 W/m^2, respectively, and in May for the lake, with a value of 44.54 W/m^2.

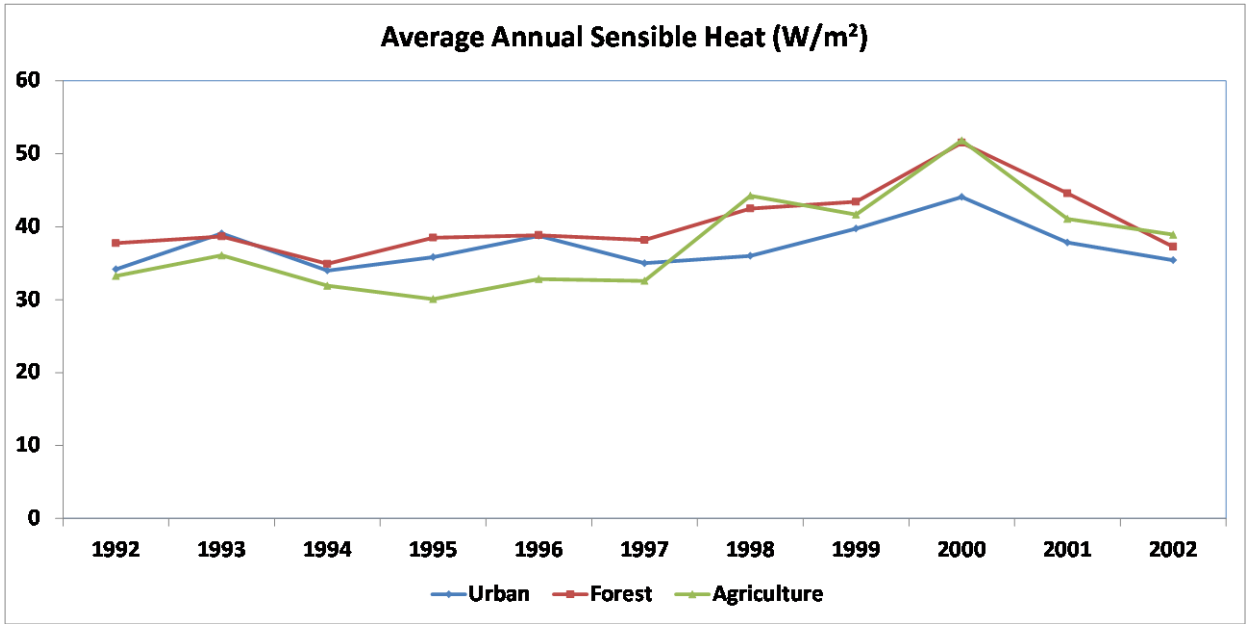

Figure 4.15: The average annual sensible heat in Northeast Florida

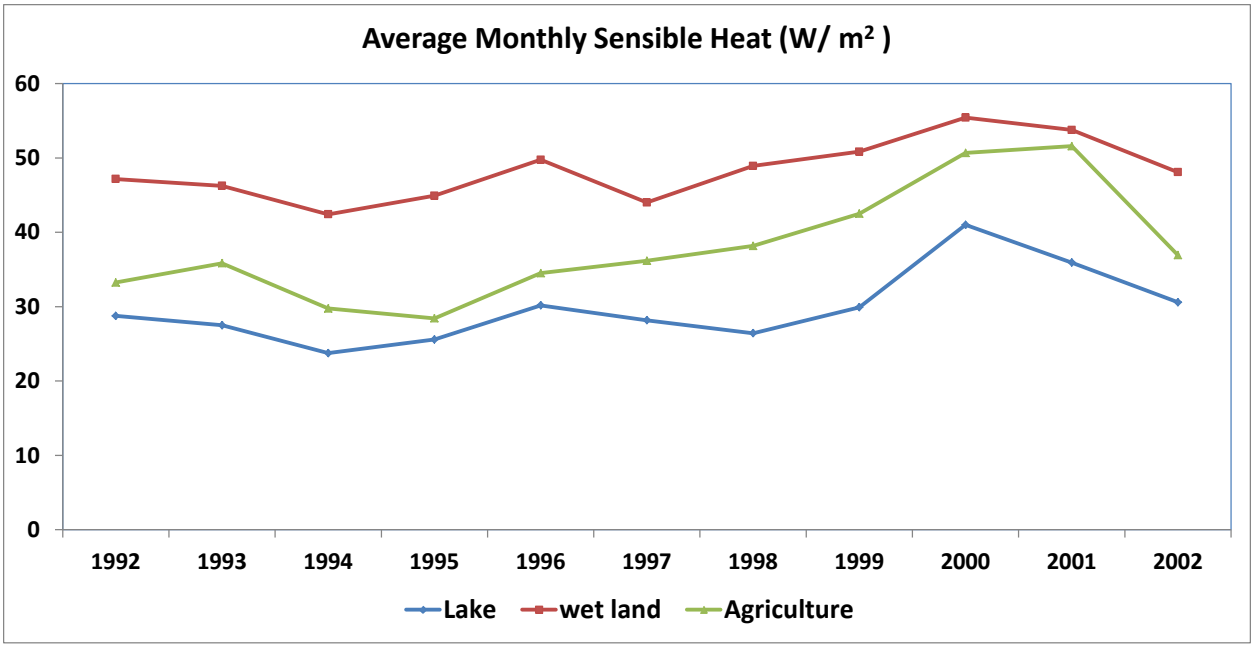

Figure 4.16: The average monthly sensible heat in Northeast Florida

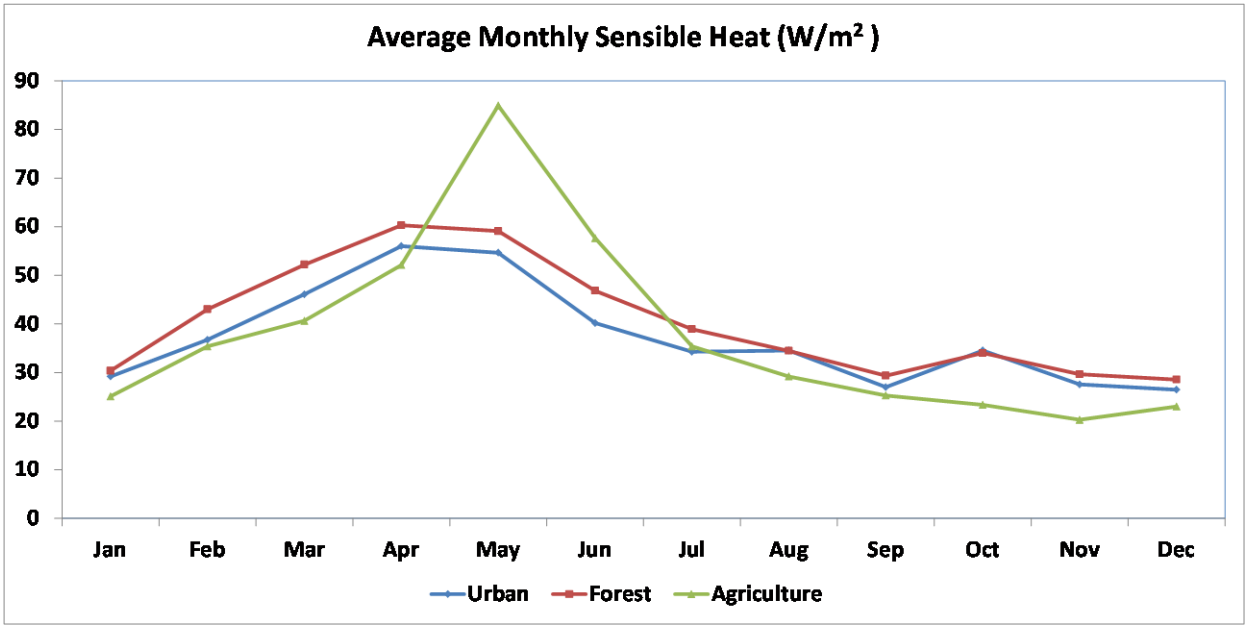

Figure 4.17: The average annual sensible heat in South Florida

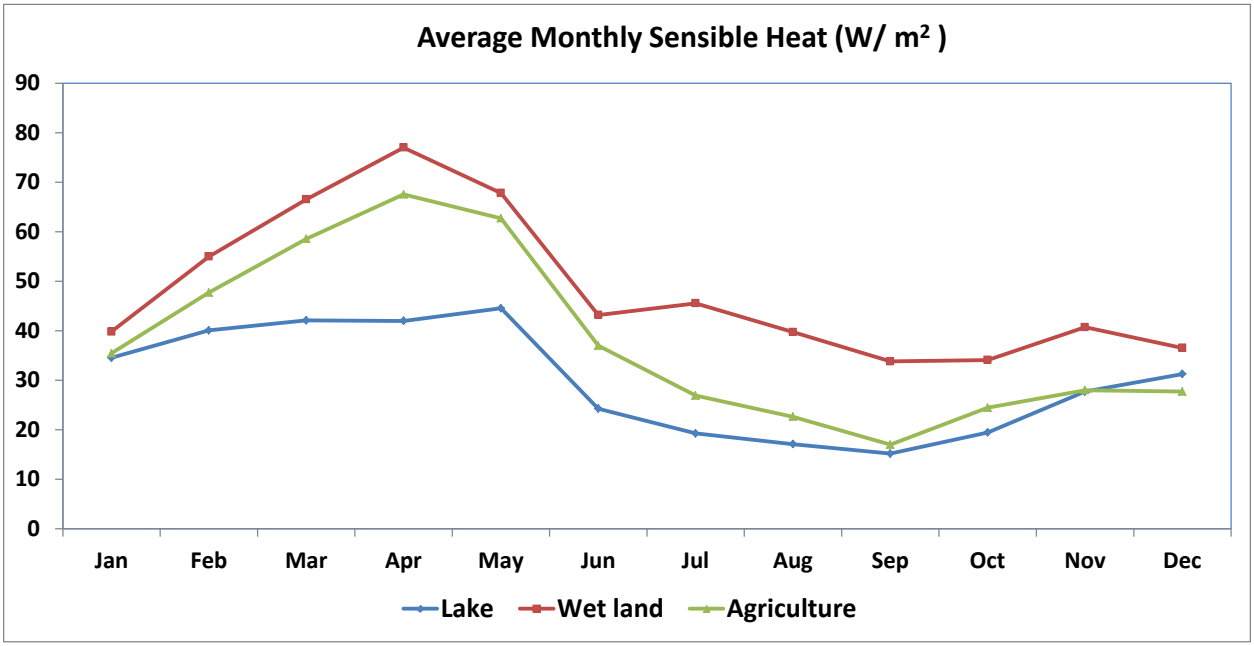

Figure 4.18: The average monthly sensible heat in South Florida

4.4.4 Monthly Sensible Latent Heat Anomaly

Inter-annual variations in monthly sensible heat in Northeast Florida are shown in Figure 4.19 In normal years, the monthly sensible heat anomalies were negative from June to January, with values between -0.71% and -54.88%, while positive values were found from February to May, with values between 0.88% and 58.32% for all three land uses. During the drought years, however, the positive sensible heat anomalies appeared in June 1998 and from June to August in 1999 and 2000, with values between 0.84% and 263.57% for all three land uses.

It has been suggested that soil moisture acts as a strong control on the partitioning between sensible heat flux and latent heat flux at the surface (the Bowen ratio), thus modulating precipitation over a given basin (Eltahir, 1998). Hence, different land use types had different responses to the drought events, and the agriculture area, which had lower soil moisture, had higher sensible heat anomalies in June of 1998, May of 1999 through 2002, and April of 2000, with values between 183.95% and 308.68%.

It has also been suggested that surface temperature is a factor in sensible heat variation and transfer. When the surface is warmer than the air above, heat will be transferred upward into the air as positive sensible heat. Figure 4.20 presents inter-annual variations in monthly surface temperatures in Northeast Florida. In normal years, the monthly surface temperature anomalies were negative from November to April, with values between -0.67% and -46.34%, while the positive values were from May to October, with values between 2.84% and 36.82%. During the drought years, however, higher surface temperatures transferred higher sensible heat, which

resulted in a higher surface temperature anomaly in June 1998, with a value of 53.95%, and a higher sensible heat over the agriculture area, with a value of 269.57%.

Figure 4.21 shows the inter-annual variations in monthly sensible heat in South Florida. In normal years, negative monthly sensible heat anomalies were observed from June to December, with values between -2.67% and -68.4%, while positive anomalies were observed from February to May, with values between 0.68% and 68.52%, for the three land uses. The sensible heat anomalies were from February to May during the drought years, especially for the lake and agriculture areas, with values between 30.89% and 188.63%, respectively.

Figure 4.22 presents the inter-annual variations in monthly surface temperature in South Florida. In normal years, high values occurred between April and May, with values between 1.05% and 23.07%. During the drought years, the lake and agriculture areas had higher surface temperature anomalies, with higher values in April to May of 1999 through 2002 between 6.54% and 29.57%.

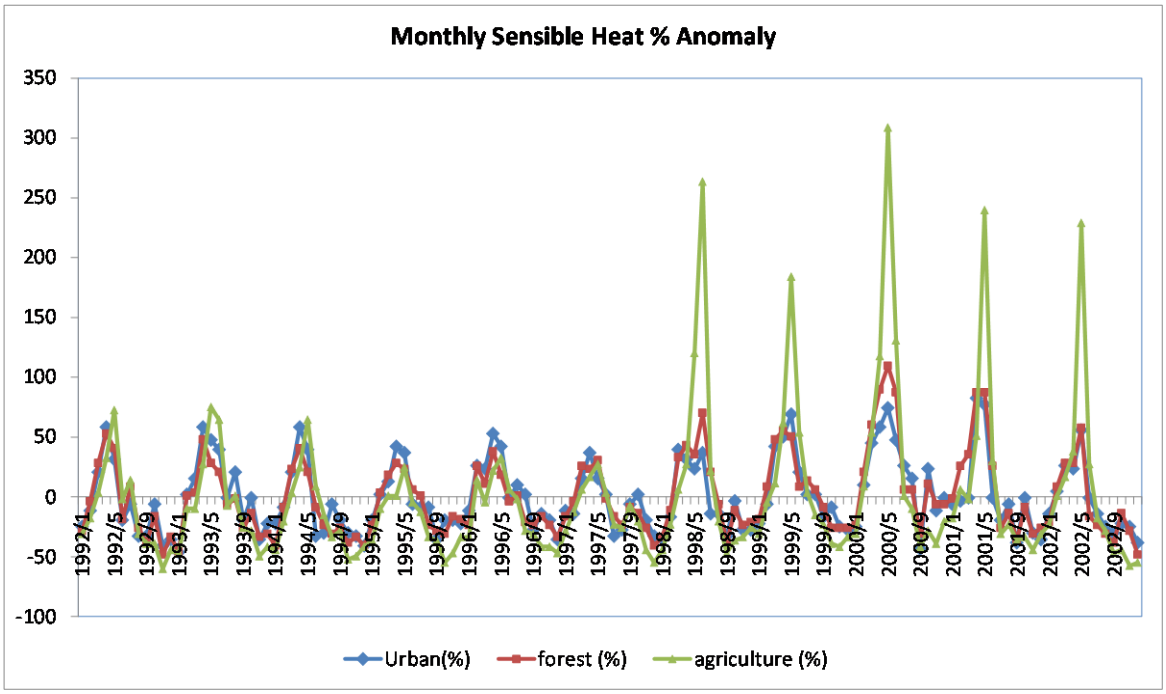

Figure 4.19: The time series monthly sensible heat anomaly patterns for Northeast Florida

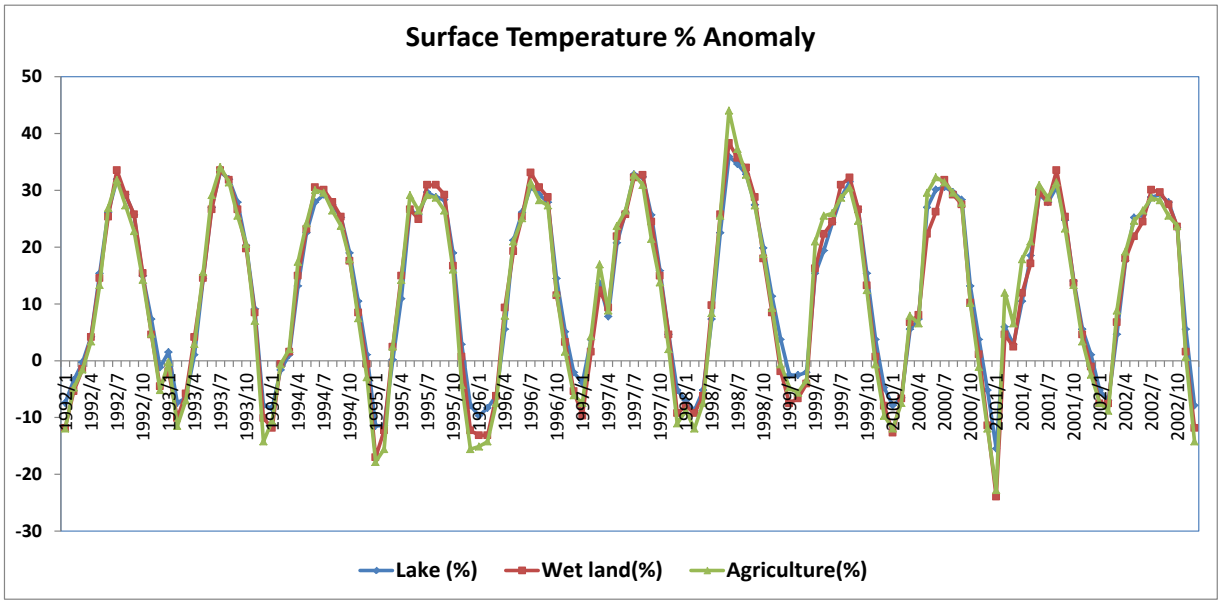

Figure 4.20: The time series monthly surface temperature anomaly patterns for Northeast Florida

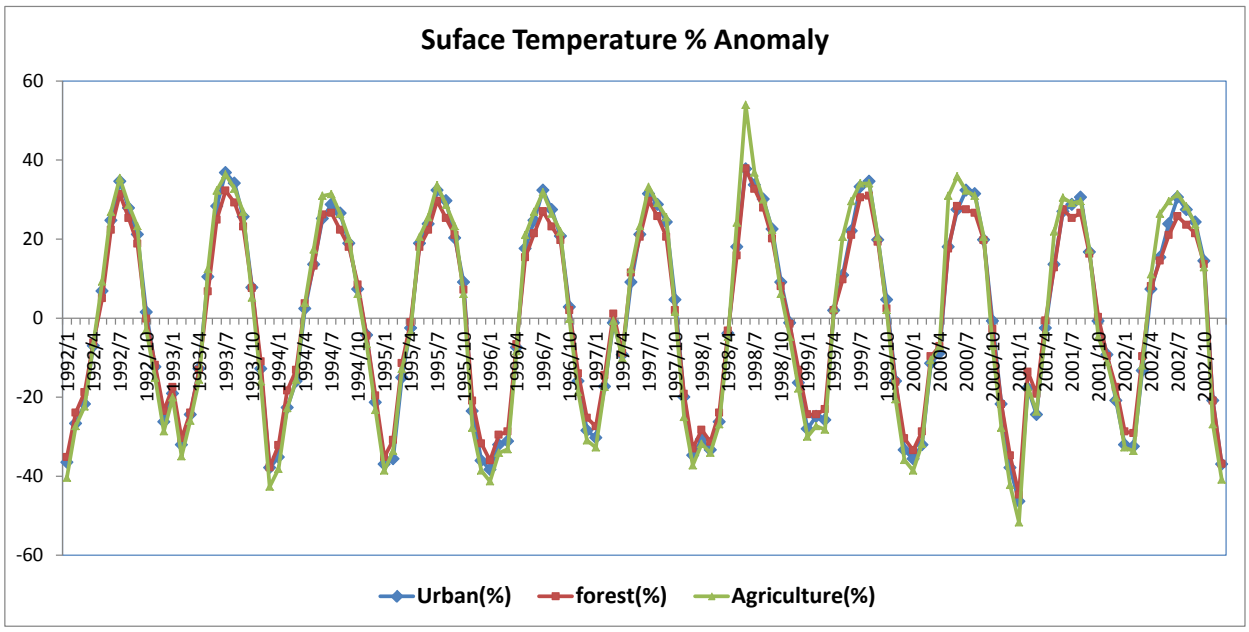

Figure 4.21: The time series monthly sensible heat anomaly patterns for South Florida

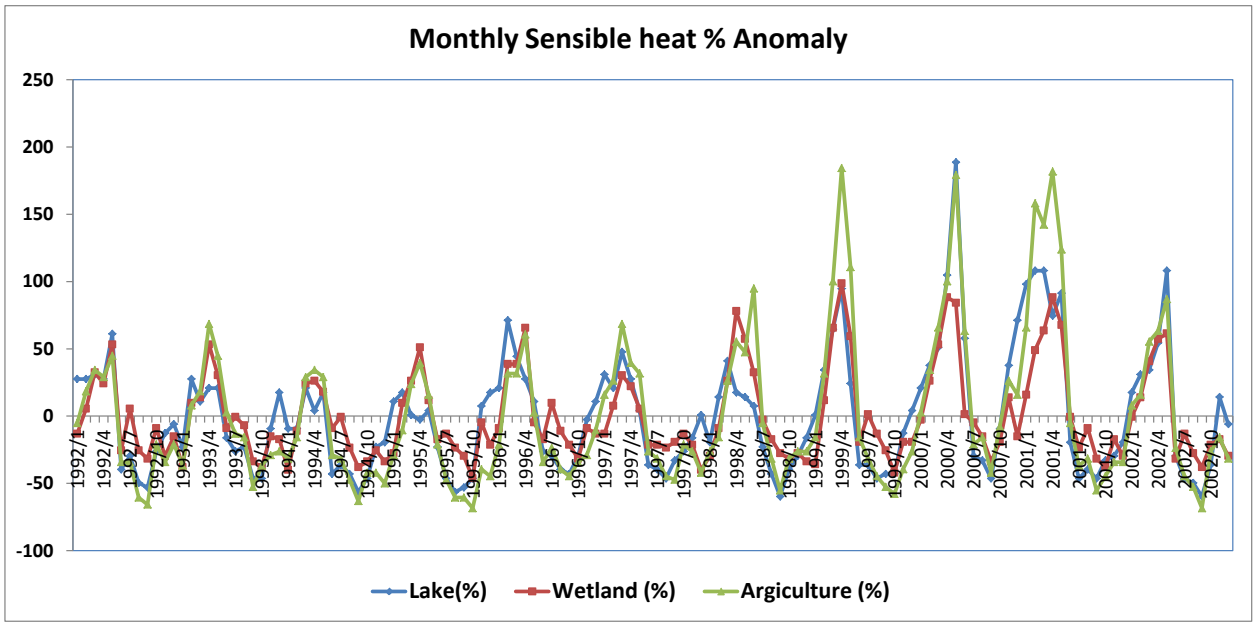

Figure 4.22: The time series monthly surface temperature anomaly patterns for South Florida

4.4.5 Monthly Bowen ratio

During drought, the Bowen ratio is higher suggesting that partitioning of net radiation is skewed, with more heat going into the sensible heat flux and less into the latent flux. The increased sensible heat flux acts to heat the canopy and boundary layer. Figure 4.23 and 4.24 show the average annual Bowen ratio in Northeast and South Florida, respectively. Hence, during the drought years, higher Bowen ratio were shown on the agriculture areas with values of 1.19 in 2000 in Northeast Florida and 1.5 in 2001 in South Florida. This shift indicates that increased sensible heat was lost compared to latent heat as water flux from the ecosystem abruptly decreased.

Figure 4.25 and 4.26 show the average monthly Bowen ratio in Northeast and South Florida, respectively. The seasonal variation was clearly concave sharped and the lower values occurred from June to September, with a range of 0.24 and 0.69 in Northeast Florida and 0.14 and 0.48 in South Florida. Higher values were observed in early spring, with values between 0.47 and 1.79 in Northeast Florida and 0.45 and 1.32 in South Florida.

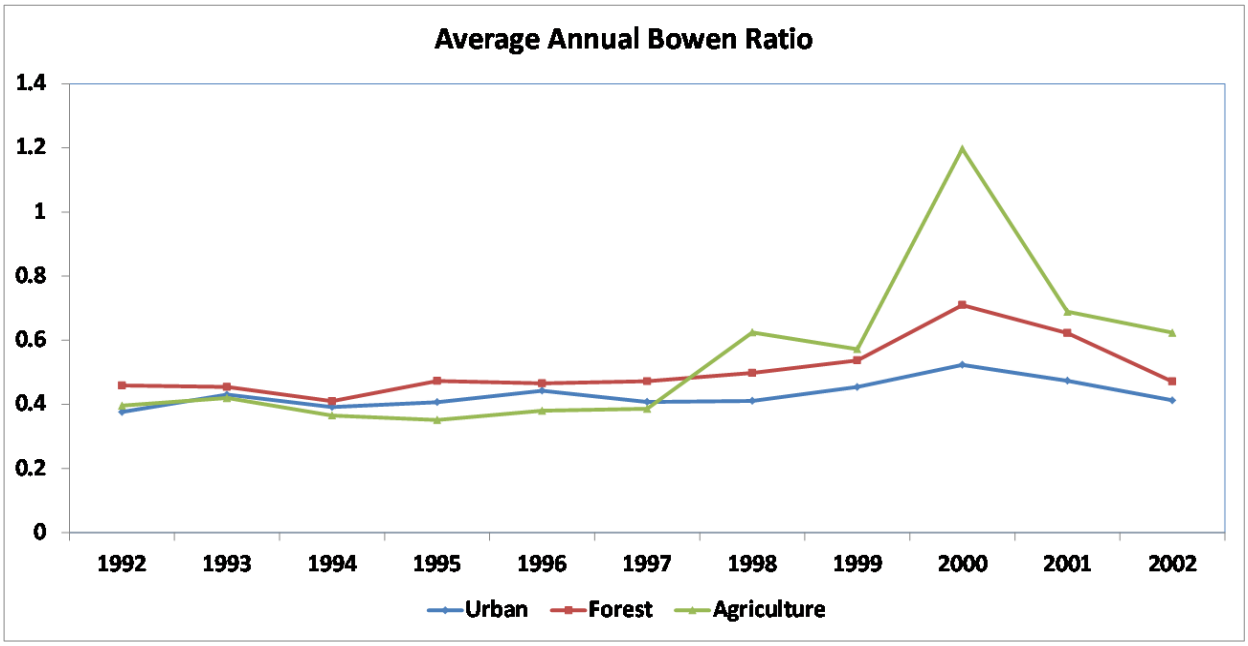

Figure 4.23: The average annual Bowen ratio in Northeast Florida

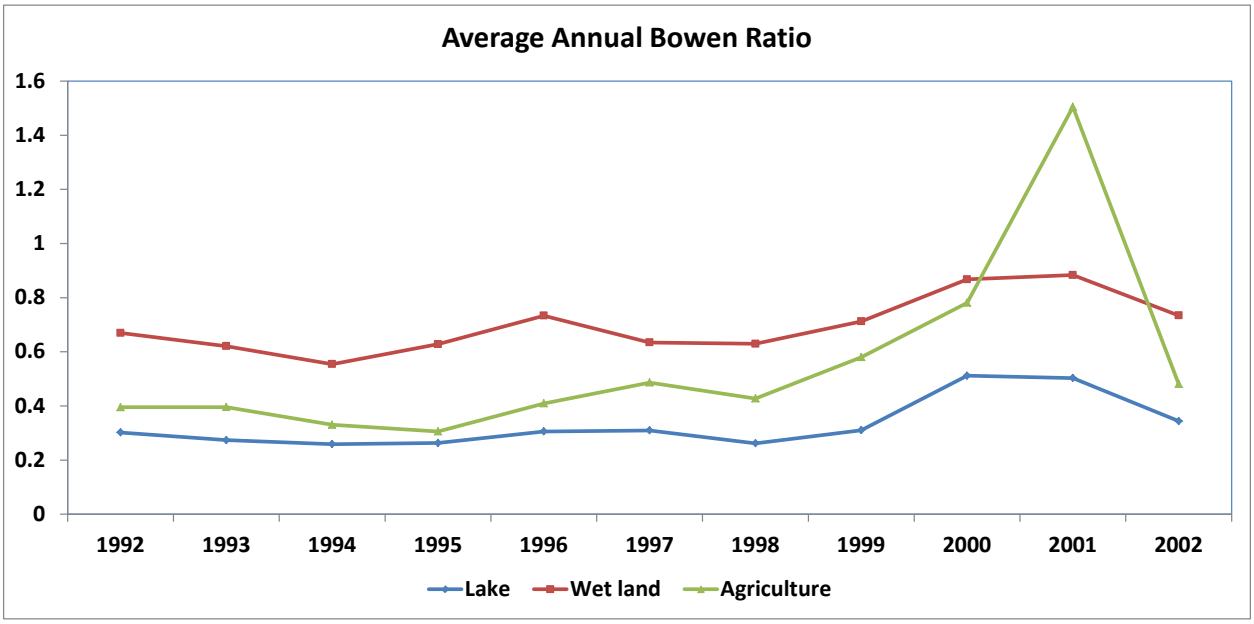

Figure 4.24: The average annual Bowen ratio in South Florida

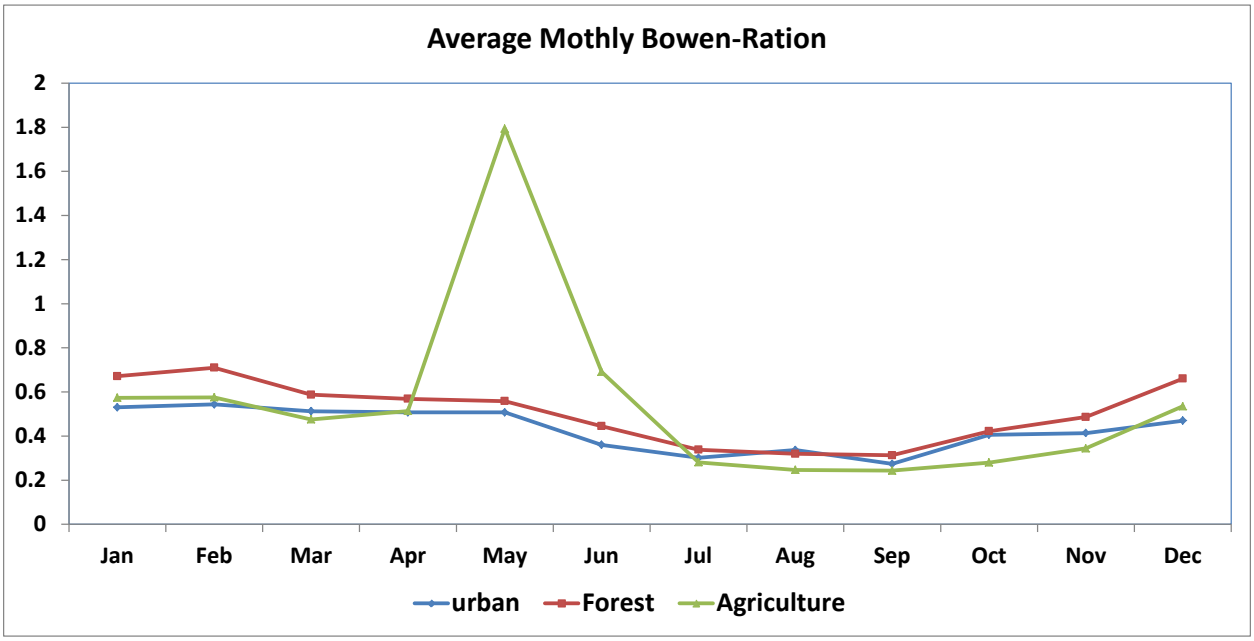

Figure 4.25: The average monthly Bowen ratio in Northeast Florida

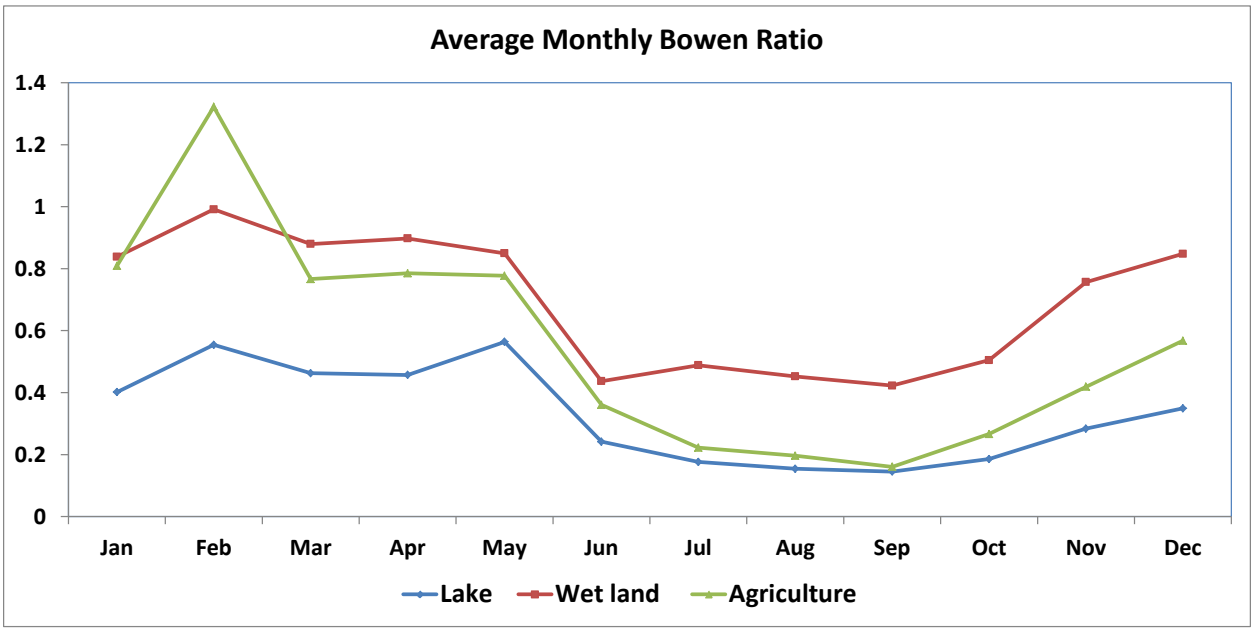

Figure 4.26: The average monthly Bowen ratio in South Florida

4.4.6 Monthly Bowen Ratio Anomaly

Figure 4.27 and 4.28 show the inter-annual variations in monthly Bowen ratio in Northeast and South Florida, respectively. In Northeast Florida, during the drought year, the values of Bowen ratio were high on three land uses with the agriculture area as the highest in May. This suggests that a decrease in evapotranspiration through the growing season due to the decrease of soil moisture and maintenance of the energy balance through changes in the sensible heat flux. In South Florida, the highest Bowen ratio occurred in February of 2001 when the surface temperature was above normal by 11.96 %, hence showing negative anomalies. It was also noted that under drier conditions, the availability of soil moisture becomes the primary source of moisture for ET, which strongly controls Bowen ratio, and therefore affects the surface temperature and evaporate rate.

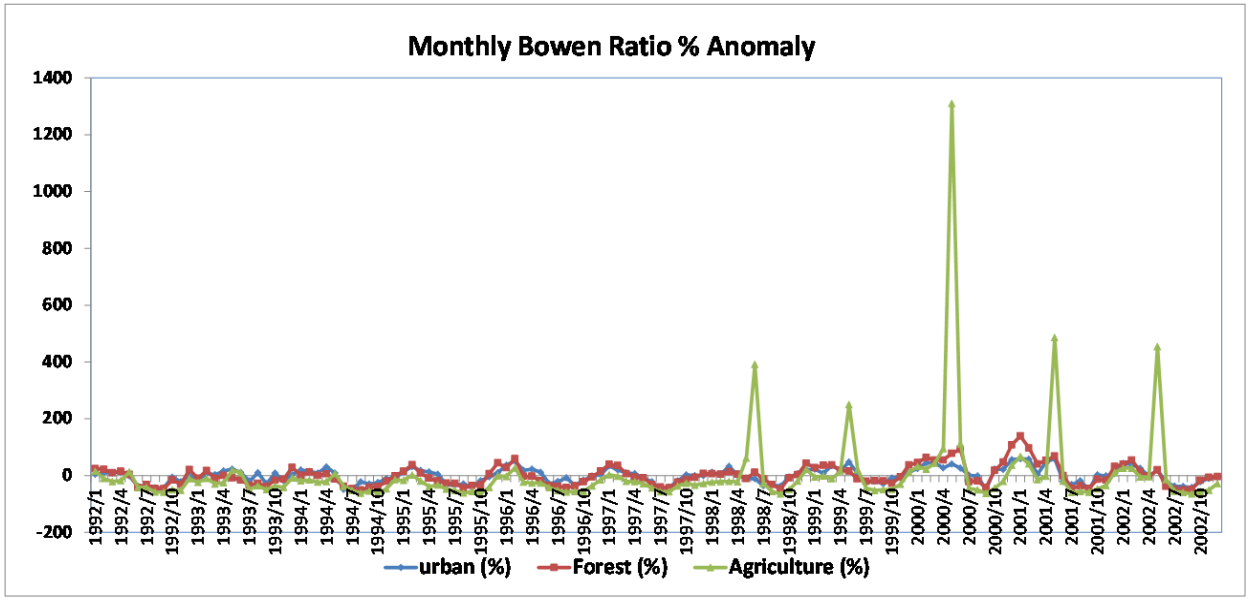

Figure 4.27: The time series monthly Bowen ratio anomaly patterns for Northeast Florida

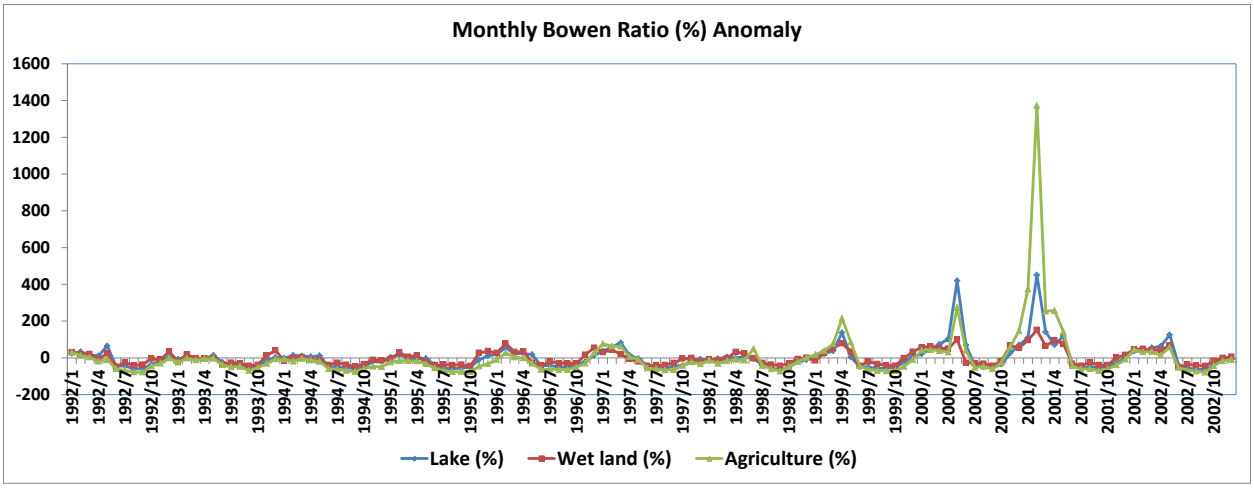

Figure 4.28: The time series monthly Bowen ratio anomaly patterns for South Florida

4.4.7 Energy Budget Balance

Tables 4.3 and 4.4 present the 11-year mean energy budget terms for the various land uses in Northeast and South Florida, respectively. In this study, the total net radiation is defined as the summation of latent and sensible heat, and the evaporation rate is defined as the ratio of latent heat/net radiation. In Northeast Florida, the urban area located at St. Johns River had the highest net radiation, latent heat, evaporation rate, actual evaporation and lower sensible latent heat, while the agriculture area had lower net radiation and latent heat. In South Florida, the lake area had the highest net radiation, latent heat, evaporation rate and lower sensible heat and Bowen ratio. However, because wetlands have hydric soil, the net radiation, latent heat, evaporation rate, and actual evaporation were lower, while the sensible heat and Bowen ratio were higher. In general, the agriculture area had a similar Bowen ratio, with a value of 0.55 in both study areas. The open area was observed to have the lowest Bowen ratio, and the wetland had the highest.

Table 4.3: Annual mean (1992-2001) Energy budget for various land uses in Northeast Florida

Energy budget	Urban	Forest	Agriculture
Net radiation(W/m^2)	126.424	126.015	122.962
Latent heat (W/m^2)	89.159	85.462	85.280
Sensible heat (W/m^2)	37.265	40.553	37.682
Evaporation rate	0.703	0.672	0.695
Actual evaporation (mm/day)	3.085	2.956	2.948
Bowen ratio	0.430	0.507	0.546

Table 4.4: Annual mean (1992-2001) Energy budget for various land uses in South Florida

Energy budget	Lake	Wet land	Agriculture
Net radiation(W/m^2)	127.11	121.80	126.27
Latent heat (W/m^2)	97.31	73.48	88.30
Sensible heat (W/m^2)	29.80	48.32	37.98

Evaporation rate	0.77	0.60	0.70
Actual evaporation (mm/day)	3.37	2.54	3.05
Bowen ratio	0.33	0.70	0.55

4.5 Summary and Conclusions

The energy budget is closely related to the hydrological cycle because evapotranspiration (ET) or latent heat is a key component in both energy and water budgets. Hence, quantifying the energy budget of various land uses is critical for understanding the water budget, and it provides useful support for decision making in land use planning, management, policies and feedback of land use changes to climate change at the regional scale. However, traditional methods, including in-situ measurements and model-only approaches, have deficiencies, as most studies were conducted in limited areas, such as grassland, forest and agriculture. Therefore, an NARR dataset from 1992 to 2002 was employed in this study to investigate the energy budget on various land uses (lake, wetland, agriculture, forest, and urban) at the regional scale in Florida.

In Northeast Florida, the urban area had highest net radiation, latent heat, evaporation rate and lower sensible heat and Bowen ratio, while the agriculture area had the lowest net radiation, latent heat, actual evaporation and the highest Bowen ratio. In South Florida, Lake Okeechobee (lake) had the highest net radiation, latent heat, evaporation rate, actual evaporation and the

lowest sensible heat and Bowen ratio, while the wetland area had the lowest net radiation, latent heat, evaporation rate and the highest sensible heat and Bowen ratio because of the lower evaporation. From the annual energy budgets, the agriculture in both study areas had similar Bowen ratios, therefore suggesting that the Bowen ratio may be used for identifying the characteristics of different land uses.

Evapotranspiration varies with vegetation as a result of the effects of water supply and demand on plants. Under wet conditions, ET is principally limited by the atmospheric demand of water vapor and driven by advection and radiation, which may explain why the lake and urban areas have higher actual evaporation, latent heat, and evaporation rate and lower Bowen ratio with a higher net radiation. However, during the drought year, most of the surface energy would partition into sensible heat, hence the lower average annual evaporation and latent heat as shown by the various land uses with higher average monthly sensible heat in the summer and fall seasons. Under drier conditions, the availability of soil moisture becomes the primary control of ET, and the differences in the response of plants to water access, which is often dictated by the rooting depth, can result in contrasting evaporative losses across vegetation types (Calder, 1998). In Northeast Florida, therefore, negative evaporation and latent heat were observed in June 1998, April 2000, and May 1999 through 2002 for the agriculture area, but the forest and urban areas had positive values in these months. In South Florida, the agriculture area had lower evaporation and latent heat within the drought period than the lake and wetland areas.

References

Aubinet M., A. Grelle, A. Ibrom, Ü. Rannik, J. Moncrieff, T. Foken, A.S. Kowalski, P. H. Martin, P. Berbigier, C. Bernhofer, R. Clement, J. Elbers, A. Granier, T. Grünwald, Morgenstern K, Pilegaard K, Rebmann C, Snijders W, Valentini R, Vesala T, 2000, Estimates of the annual net carbon and water exchange of forests: the EUROFLUX methodology. Adv Ecol Res., 30,113–175

Azevedo, P.V., Silva, B.B., da Silva, V.P.R., 2003, Water requirements of irrigated mango orchards in northeast Brazil. Agric. Water Manage., 58, 241–254

Barr, A.G., Morgenstern, K.., Black, T.A., McCaughey, J.H., Nesic, Z., 2006, Surface energy balance closure by the eddy-covariance method above three boreal forest stands and implications for the measurement of the CO2 flux. Agr Forest Meteorol, 140, 322–337

Black, R J., 1993, Florida Climate Data 1, no, July: 1-4

Blanken P. D., Neumann, T. A., den Hartog H.H., G., Yang, P.C., Nesic, Z., Staebler, R., Chen W, X. Lee, 1998, Turbulent flux measure- ments above and below the overstory of a boreal aspen forest, Bound-Lay Meteorol, 89, 109–140

Bonan, 1999, Frost followed the plow: Impacts of deforestation on the climate of the United States. Ecol. Appl., 9, 1305–1315.

Bonan, G. B., 1997, Effects of land use on the climate of the United States. Climatic Change, 37, 449–486.

Brenner, J., 1991, Southern Oscillation anomalies and their relation to wildfire activity in Florida, Int. J. Wildland Fire, 1, 73–78

Bruijnzeel, L.A., 1990, Hydrology of moist tropical forests and effects of conversion: a state of knowledge review. In: UNESCO International Hydrological Program, 224.

Calder I. R., Rosier, P.T.W., Prasanna, K.T., 1997, Eucalyptus water use greater than rainfall input – a possible explanation from southern India, Hydrology and Earth System Science, 1, 249–256.

Carter, D.R., Jokela, E. J., 2002, Florida's renewable forest resources, CIR1433: Gainesville: University of Florida, Institute of Food and Agricultural Sciences, Florida Cooperative Extension Service, 9.

Castellvi F, R., Snyder, L., Baldocchi D. D., 2008, Surface energy-balance closure over rangeland grass using the eddy covariance method and surface renewal analysis, Agr Forest Meteorol 148, 1147–1160

Chase, T. N., Pielke, R. A., Kittel, T. G. F., Nemani, R. R., Running, S. W., 1996, Sensitivity of a general circulation model to global changes in leaf area index. J. Geophys. Res., 101 (D3), 7393–7408

Copeland, J. H., Pielke, R. A., Kittel, T. G. F., 1996, Potential climatic impacts of vegetation change: A regional modeling study. J. Geophys. Res., 101 (D3), 7409–7418

Costa, M. H., Foley, J. A., 1997, Water balance of the Amazon basin: Dependence on vegetation cover and canopy conductance. J. Geophys. Res., 102 (D20), 23 973–23 989

Croke, B.F.W., Merritt, W.S., Jakeman A.J., 2004, A dynamic model for predicting hydrologic response to land cover changes in gauged and ungauged catchments. J. Hydrol, 291, 115–131.

Dickinson, R. E., Sellers, A. H., 1988, Modelling tropical deforestation: A study of GCM land-surface parametrizations. Quart. J. Roy. Meteor. Soc., 114, 439–462.

Douglas, E. M., Jacobs, M. J., Sumner, D. M., Ray, R. L. 2009, A comparison of models for estimating potential evapotranspiration for Florida land cover types, Journal of Hydrology, 373, no. 3-4 (7): 366-376.

Drummond, M. A., Loveland. T. R., 2010, Land-use Pressure and a Transition to Forest-cover Loss in the Eastern United States. BioScience 60, no. 4 (April): 286-298 Ecology and Evolution, 21,5, 254-260

Ek, M. B., Mitchell, K. E., Lin, Y., Rogers, E., Grunmann, P., Koran, V., Gayno, G., Tarpley, J. D., 2003, Implementation of Noah land surface model advances in the National Cen- ters for Environmental Prediction operational Mesoscale Eta Model. J. Geophys. Res., 108, 8851

Eltahir, E. A. B., 1998, A soil moisture–rainfall feedback mechanism. 1. Theory and observations. Water Resour. Res., 34, 765–776.

Florida Division of Forestry, undated(a), Wildfire statistics for Florida: 1981-present: Accessed August 31, 2005, at http://www.fl-dof.com/wildfire/stats_fires_since1981.html.

Folks, J. C., 2005, Lake Okeechobee TMDL: Technologies and Research. North Carolina State University College of Agriculture and Life Sciences, 1-12.

Hernandez R. G., Hatfield, J. L., Prueger J. H., Sauer T. J., 2009, Energy balance and turbulent flux partitioning in a corn–soybean rotation in the Midwestern US.” Theoretical and Applied Climatology

Jarosz N, Y., Brunet E., Lamaud, M., Irvine J.M., Loustau D., 2008, Carbon dioxide and energy flux partitioning between the understorey and the overstorey of a maritime pine forest during a year with reduced soil water availability. Agr Forest Meteorol, 148, 1508–1523

Knowles, 1996, Estimation of Evapotranspiration in the Rainbow Springs and Silver Springs Basins in North-Central Florida, Water Management

Leuning, R., Cleugh, H., Zegelin, S., Hughes, D. 2005, Carbon and water fluxes over a temperate Eucalyptus forest and tropical wet/dry savanna in Australia. Agric. Forest Meteorol, 129, 151–173.

Li, K., Coe, M., Ramankutty, N., Jong, R., 2007, Modeling the hydrological impact of land-use change in West Africa, J. of Hydrology 337:258-268

Luo, Y., Ernesto H. B., Kenneth, E. M., 2005, The Operational Eta Model Precipitation and Surface Hydrologic Cycle of the Columbia and Colorado Basins. J. Hydrometeor, 6, 341–370.

Massman W. J., Lee, X.., 2002, Eddy covariance flux corrections and uncertainties in long-term studies of carbon and energy exchanges. Agr Forest Meteorol 113, 121–144

Matheussen, B., Kirschbaum, R. L., Goodman, I. A., O'Donnell, G. M., Lettenmaier, D. P., 2000, Effects of land cover change on streamflow in the interior Columbia River basin (USA and Can- ada). Hydrol. Processes, 14, 867–885.

McPherson, R. A., 2007, Review of vegetation, atmosphere interactions and their influences on Mesoscale phenomena, Progress in Physical Geography, 31, 3.

Meir, P., 2006, The influence of terrestrial ecosystems on climate, Trends in

Mesinger, F., 2005, North American Regional Re- analysis, Bull. Amer. Meteor. Soc., 87, 343–360

Mitchell, K., 2004, NCEP completes 25-year North American Reanalysis: Precipitation assimilation and land surface are two hallmarks. GEWEX News, Vol. 14, No. 2, International GEWEX Project Office, Sliver Spring, MD, 9–12.

Paco, T., Ferreira, M., Conceicao, N., 2006, Peach orchard evapotranspiration in a sandy soil: Comparison between eddy covariance measurements and estimates by the FAO 56 approach, Agricultural Water Management, 85, 305-313.

Pereira, H.C., 1992, Keynote paper. In: 10th World Forestry Congress, Proc. 3, Paris, 1991, 139–150.

Pielke, R. A., Walko, R. L., Steyaert, L. T., Vidale, P. L., Liston, G. E., Lyons, W. A., Chase, T. N., 1999, The influence of anthropogenic landscape changes on weather in south Florida. Mon. Wea. Rev., 127, 1663–1673.

Pielke, R. Avissar, A., R., Raupach, M., Dolman, A. J., Zeng,, X., Denning, A. S., 1998, Interaction between the atmosphere and terrestrial ecosystems: influence on weather and climate. Global Change Biol. 4, 461–475.

Rana, G., N., Lorenza, K. F., 2005, Measuring and modelling of evapotranspiration of irrigated citrus orchard under Mediterranean conditions. Agric. For. Meteorol. 128, 199–209.

Richard, B., J., Verdi, Tomlinson, S. A., Marella, R. L., and U S Geological Survey, 2002, The Drought of 1998-2002: Impacts on Florida ’ s Hydrology and Landscape Circular 1295 System.

Ritter, E., 2006, The Physical Environment: an Introduction to Physical Geography. Date visited.

Sammis, T.W., Mexal, J.G., Miller, D., 2004, Evapotranspiration of flood-irrigated pecans, Agric. Water Manage. 69, 179–190.

Savenije, H.H.G., 1995, New definitions for moisture recycling and the relation with land-use changes in the Sahel, H. Hydrol. 167, 57–78.

Snyder, G.H., 1987, Agricultural flooding of organic soils. Bulletin No. 570, Institute of Food and Agricultural Sciences, University of Florida, Gainesville.

Teixeira, A.H., de, C., Bastiaanssen, W.G.M., Bassoi, L.H., 2007, Crop water parameters of irrigated wine and table grapes to support water productivity analysis in Sao Francisco river basin Brazil. Agric. Water Manage. 94, 31–42.

Testi, L., Orgaz, F., Villalobos, F. J., 2006, Variations in bulk canopy conductance of an irrigated olive (Olea europaea L.) orchard. Environ. Exp. Bot. 55, 15–28.

The South Florida Everglades Restoration Project, http://www.ce.utexas.edu/prof/maidment/grad/dugger/GLADES/glades.html

Twine T. E., Kustas., W.P., Norman, J. M., Cook, D.R, Houser, P.R., Meyers, T.P., Prueger, J. H., Starks, P. J., Wesely, M.L., 2000, Correcting eddy- covariance flux underestimates over a grassland. Agr Forest Meteorol 103, 279–300

Twine, T. E., Kucharik, C. J., Foley, J. A., 2004, Effects of Land Cover Change on the Energy and Water Balance of the Mississippi River Basin, J. of Hydrometeorology, 5, 640

Verma S. B, Kim, J., Clement, R. J., 1992, Momentum, water vapour, and carbon dioxide exchange at a centrally located prairie site during FIFE, J Geophys Res, 97, 8629–18639

Vilalolobos, F .J., Testi, L., Rizzalli, R., Orgaz,, F., 2004, Evapotranspiration and crop coefficients of irrigated garlic (Allium sativum L) in a semi-arid climate. Agric. Water Manage. 64, 233–249.

Wayne R. Rouse, J., Binyamin, P., Blanken, N., Bussières, C. R., Duguay, C. J., Oswald, W. M., Schertzer and C., Spence, 2006, The Influence of Lakes on the Regional Energy and Water Balance of the Central Mackenzie River Basin. In: DiCenzo P, Proc. 11 the Sci-Workshop Mackenzie GEWEX Study, Ottawa ON Canada,

Wever L.A., Flanagan, L.B., Carlson, P. J., 2002, Seasonal and inter-annual variation in evapotranspiration, energy balance, and surface conductance in northern temperate grassland, Agr ForestMeteorol, 112,31–49

Yan, L., 2006, Regional aspects of the North American land surface-atmosphere interactions and their contributions to the variability and predictability of the regional hydrologic cycle, Ph. D dissertation

Yunusa, I. A. M., Walker, R. R., Lu, P. 2004, Evapotranspiration components from energy balance, sapflow and microlysimetry techniques for an irrigated vineyard in inland Australia. Agric. For. Meteorol. 127, 93–107.

CHAPTER 5:

DEVELOPING A REGIONAL LAND USE DROUGHT INDEX IN FLORIDA

This chapter has been submitted for publication with the following citation: C. H., Cheng and F., Nnadi. "Developing a Regional Land Use Drought Index in Florida," Purdue's e-Pubs Repository (Accepted, May, 2011)

5.1 Introduction

When a large area over a period of time loses significant amount of water and with no availability of replenishment, the area is said to be under drought condition (Tsakiris, 2009). Hence, during droughts, water supplies are inadequate to meet the water demand of water-related systems, and lack of rainfall can produce serious agriculture, hydrologic, and socio-economic damages. According to a report by the U.S. Federal Management Agency (FEMA), droughts occur almost every year across a portion of the nation (e.g., the widespread events of 1995–96 in the southwest and southern Great Plains; 1998 in the south; 1999 in the northeast; 2000 in the south, mid-west, and Great Plains; 1998– 2002 in the southeast; and 2002 in the east). The report also suggested that the United State loses $6 - 8 billion annually on average due to drought (FEMA, 1995). Therefore, there is great interest in better defining, monitoring, and predicting droughts.

Drought indices could integrate various hydrological and meteorological parameters and quantify climate anomalies in term of intensity, duration, and spatial extent, thus making it easier to communicate information to diverse users (Wilhite, 2000). In the United States, great efforts have been made to develop a variety of drought indices used for water resources management, agricultural drought monitoring and forecasting. These include, the Palmer Drought Severity Index (PDSI) (Palmer, 1965), Crop Moisture Index (CMI) (Paler, 1968), Standardized Precipitation Index (SPI) (McKeeet et al., 1993), and Surface Water Supply Index (SWSI) (Shafer and Dezman, 1982). However, drought is a complex phenomenon and is difficult to detect and monitor based on: (1) it develops slowly, and the onset and end are indistinct (2) it is not universally defined, and (3) its impact is nonstructural and often spreads over very larger areas (Wilhite, 2000). Therefore, until recently, there was no single accepted definition of a drought; there was no single and universal drought index, either.

Current drought indices have limitations and drawbacks as they are calculated using climate data from meteorological stations, which are point measurements. In addition, weather stations are scarce in remote areas and are not uniformly distributed. However, the identification and intensity of drought must be considered as factors that should affect regional or national economic planning. Hence, for monitoring purpose, it is necessary to track drought from point measurements to drought developments on a regional scale. Secondly, evapotranspiration can consume up to 80% of rainfall according to a general circulation model (GCM) experiment and have a marked influence on drought condition but it lacks validity as little data has been observed (Abramopoulos et al., 1988, and Kim, Byun, and Choi, 2009). Hence, in PDSI,

potential evapotranspiration (PET) is calculated using Thornthwaite's method, which estimates ET based on an empirical relationship between evapotranspiration and temperature (Thornthwaite, 1948). But, the Thornthwaite equation does not perform well in estimating ET under various climatic conditions (Jensen et al., 1990) Thirdly, the consideration of spatial variability of hydrological parameters related to soil properties and land use and meteorological parameters such as rainfall and temperature is a better approximation of the hydrologic system and will improve the ability to monitor drought at a much better spatial resolution (Narasimhan and Srinivasan, 2005).

However, in reality, parameters like land use/cover and soil properties vary widely and are sparsely measured by ground-based measurements. As human activities affect land use characteristics, which impact the distribution of ecosystem, energy (latent and sensible heat), and mass fluxes (e.g. water vapor, trace gases and particulates), contrasting land use patterns induce convection and circulation that affect cloud formation and precipitation. Hence, traditionally, developing a drought index from water balance is not enough to reflect the level of severity in drought events resulting from land use effects. So, the simplistic approaches based on measures of rainfall deficiency, such as, SPI, RI, RAI, and BMDI, would underestimate the severity of drought (Tsakiris and Vangelis, 2005).The more complex drought indices, which are based on water balance model, PDSI and CMI, assumed that parameters such as land use/land cover, and soil properties are uniform over the entire climatic zone (7000–100,000 km^2) (Narasimhan and Srinivasan, 2005). Moreover, the SWSI does not directly consider other elements of the

hydrological cycles that are critical for drought monitoring, such as evaporation, soil moisture and land use characteristic (Keyantash, 2004).

Data assimilation techniques, integration of virtues of observations, and modeling by fusing them together, have been studied and used for decades in meteorological and oceanic applications (Pan and Wood, 2006). North American Regional Reanalysis (NARR) data, which include model-based four-dimensional data assimilation procedures, may provide a great possibility for more accurate evaluation of interactions of the land surface-atmosphere and could be used for improving the limitations of current drought indices. Hence, the objective of this study is to develop a regional land use adapted drought index in Florida based on the North American Regional Reanalysis (NARR) data set. Improvements in current drought monitoring and forecasting techniques will allow for better preparation, lead to better management practices, and mitigate the vulnerability of society to drought and its subsequent impacts.

5.2 Data Set

This study employs the NARR data set developed at the Environmental Modeling center (EMC) of the National Centers for Environmental Prediction (NCEP). This dataset is based on the April 2003 frozen version of the operational Eta Model and its associated Eta Data Assimilation System (EDAS), and uses many observed quantities in its data assimilation scheme, including gridded analysis of rain gauges precipitation over the continental United States (CONUS), Mexico, and Canada (Luo, et al., 2005). Hence, this regional reanalysis is produced at

high spatial and temporal resolutions (32-km, 45-layer, 3-hourly) and spans a period of 25 years from October 1978 to December 2003. Full details on the NARR products can be found online at http://www.emc.ncep.noaa.gov/mmb/rreanl/.

The EDAS is successful with downstream effects, including two-way interaction between precipitation and improved land-surface model (Ek et al., 2003). Mitchell et al., (2004) demonstrated significant regional improvements in a number of variables when using precipitation assimilation over the CONUS. Therefore, it is expected that this dataset will be useful not only for energy and water budget studies, but also for analysis of atmosphere-land relationships. The 24-yr monthly averages of soil moisture, runoff, actual surface evaporation and precipitation, latent heat, sensible heat and surface temperature from 1979 through 2002 of the NARR data were utilized in this study.

5.3 Study Area

Florida climate is humid and subtropical with rainy wet season extending from May through October. Most areas in Florida receive at least 1270 mm of rainfall annually. The long-term annual mean temperature is 22.4°C based on historical records of a weather station located in Kissimmee, Florida (Southeast Regional Climate Center, http://www.sercc.com/climate). Florida has varied annual precipitation as floods in one year may be followed by drought the next

5.3.1 ENSO in Florida

El Niño Southern Oscillation (ENSO), a global climate fluctuation, originates in the equatorial Pacific Ocean through larger-scale interaction between the ocean and atmosphere and operates on a timescale of 2-7 year (Pade and Nin, 2003). ENSO has three phases: warm tropical Pacific Sea Surface Temperature (SST) (El Niño), cold tropical Pacific SSTs (La Niña), and near-neutral conditions. This study used the NOAA's operational definitions of El Niño and La Niña conditions based upon the Oceanic Niño Index [ONI]. ONI is defined as the 3-running means of SST anomalies in the Niño 3.4 region [5N-5S, 120-170W], derived from the 1971-2000 SST climatology and thought as representing the average equatorial SST anomalies across the Pacific from about the dateline to South American (NOAA/ National Weather Service). To be classified as a full-fledged El Niño and La Niña episode the ONI must exceed +0.5 [El Niño] or -0.5 [La Niña] for at least five consecutive months. Hence, the period from 1979 to 2002 includes 7 El Niño (1982, 1886, 1987, 1991, 1994. 1997, and 2002) and 6 La Niña events (1984, 1988, 1995, 1998, 1999, and 2000).

ENSO influences the climate of the southeastern U.S. coastal plain, including Florida: El Niño years tend to be cooler and wetter, and La Niña years tend to be warmer and drier than normal in the Fall through the Spring, with the strongest effect in the Winter (Ropelewski and Halpert ,1986; Kiladis and Diaz, 1989; Hanson and Maul, 1991; Sittel, 1994a). During El Niño the additional rain could lead to greater net precipitation and ground water recharge because it occurs during Winter at a time when evaporation is low (Twine et al., 2005). In contrast, La Niña events keep the polar jet stream and extra-tropical systems north of Florida and keep Florida dry (Douglas and Englehart, 1981). The low monthly precipitation increases the severity and

frequency of drought and wildfires during La Niña events. Hence, major statewide or regional droughts in recent decades occurred, in early 1970s, early 1980s, 1985, 1988-1990 and 1999-2001 periods.

Agriculture is one of the most important economic resources in Florida. Florida in 1995-96 crop year produced 63 % of the Winter vegetables in the U.S. with a revenue of $1.48 billion (FASS, 1996). Studies have shown that Florida vegetable yields are correlated with ENSO-related Pacific sea surface temperatures (SST) for the Winter, Summer, and Fall quarters (FASS, 1997; Mills, 2009) Drought-induced wildfire is also a serious problem in Florida. For example, the rapid emergence of drought in 1998 following the strong El Niño event resulted in drought-induced wildfires in Florida and statistics show that 25,137 fires burned 1.5 million acres between 1998 and 2002 (Florida Division of Forestry, undated (a)). Hence, understanding local ENSO patterns on the regional scale and developing a new land use drought index in Florida are critical and necessary in agriculture and water resources managements.

5.3.2 The Selected Areas

In this study, data from 1992 National Land Cover Dataset on five different land uses in six 32×32 km regional study areas were selected based on Florida's different climatic zones as shown in Figure 5.1. These land uses include urban, forest and agriculture in northeast Florida, and lake, wetland and agriculture in South Florida (Figure 5.2). The climate of northeast Florida

is somewhat cooler and receives abundant precipitation between 1000 and 1500 mm annually. The combination of long frost-free periods of more than 240 days and plentiful water has historically enabled the production of specialized crops, hence a regional agriculture land use was selected (Drummond and Loveland, 2010). Extensive pine plantations are relatively common in north Florida such as Ocala National Forest (Carter and Jokela, 2002). Furthermore, substantial population growth has occurred, causing an expansion of urban and developed land. Within 30 years, the population increased by more than 140 percent, suggesting larger urban areas as in Orlando, St. Petersburg, Tampa and Jacksonville. Hence, Jacksonville, which is the largest city in the State of Florida, was selected for regional urban analysis.

South Florida, exposed to onshore breezes, enjoys comfortable temperatures most of the year. The climate is generally frost-free and subtropical and annual rainfall is about 1400 mm. The main regional characteristics are wetland, lake, agriculture and urban areas (Figure 5.1). The Everglades region is a subtropical wetland that covered much of South Florida, and comprises of over 4000 square miles stretching from Lake Okeechobee in the north to the Florida Bay at the southern end of the peninsula (Munson et al., 2005). Hence, it was selected to represent the regional 32×32 km grid of wetlands in the south Florida. Lake Okeechobee (Figure 5.1), the second largest freshwater lake in the U.S and covers a surface area of 1800 square km, with an average depth of 2.7 m is a large, shallow, eutrophic lake located in south central Florida, and is frequently hit by hurricanes. As the central part of a larger interconnected aquatic ecosystem and as the major surface water body, Lake Okeechobee provides a number of societal and environmental service functions including water supply for agriculture and urban areas (Folks,

2005). Therefore, investigating impacts of drought events on the Lake is very critical and necessary. Finally, the Everglades Agriculture area (EAA), a small portion of the Everglades region consisting of artificially rich organic soil supporting a thriving agriculture industry with annual benefits around $500 million was also considered for the study (Snyder, 1987).

Comparing National Land cover Dataset of two different periods of 10 years interval, Figures 5.1 and 5.3, the land use changes could be monitored and detected. The regional agriculture land use, which is located in west Alachua, changed the land use from row crop in 1992 to pasture hay in 2001, but other land use areas didn't change appreciably within the 10-year period. Hence, in this study, we assumed land use types of the selected areas did not changed from 1979 to 2002.

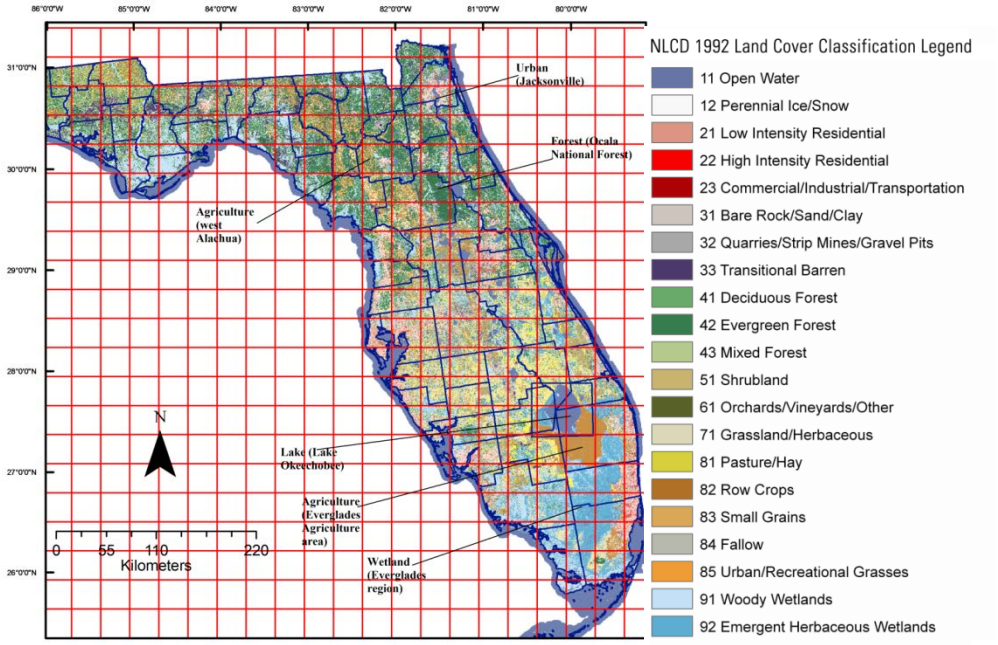

Figure 5.1: Six selected 32×32 km^2 regional study areas along with land-use/ land cover from the 1992 National Land Cover Dataset

Figure 5.2: Map of Florida depicting the four regions of the State (Richard et al., 2002).

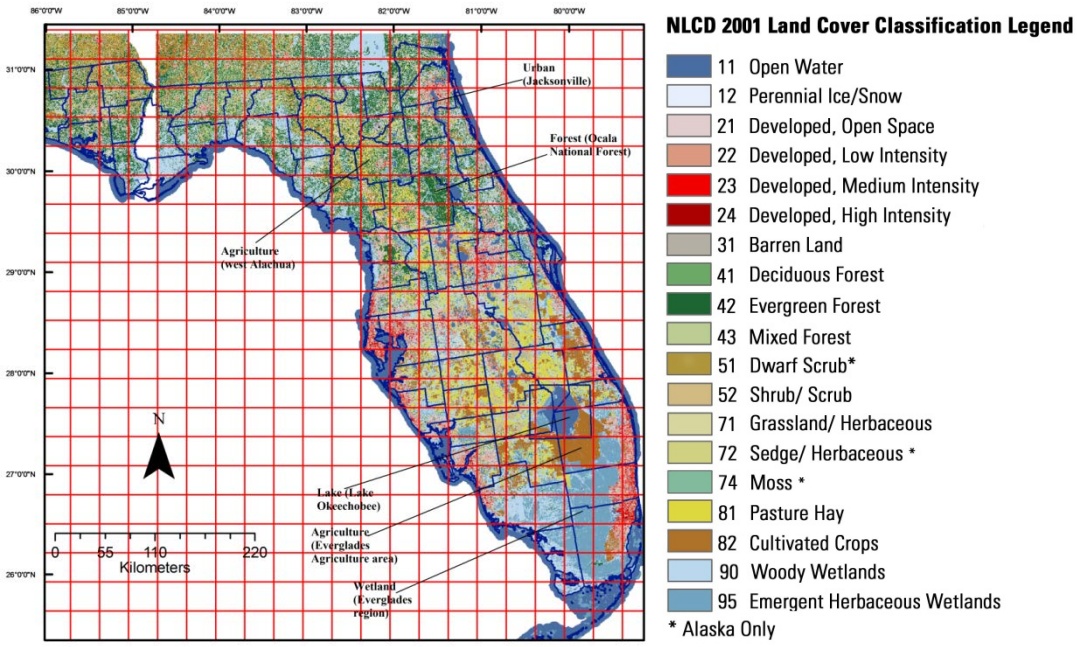

Figure 5.3: Six selected 32×32 km^2 regional study areas along with land-use/ land cover from the 2001 National Land Cover Dataset

5.4. Methods

Within the hydrologic cycle, evapotranspiration (ET) or latent heat (LE) is driven primarily by the evaporative power of the net radiation and establishes a fundamental linkage between energy and water balances. The partitioning of net radiation between sensible and latent heat flux is markedly dependent on the amount of available water on the surface. During the wet conditions, ET is principally limited by the atmospheric demand of water vapor, and driven by solar energy. Hence, because of the importance of solar energy, ET varies with latitude, season of year, time of day, and cloud clover. In contrast, during dry conditions, changes in evaporation and transpiration depend on the availability of moisture at the onset of drought and the severity and duration of a drought. Hence, the availability of soil moisture becomes the primary control of ET and differences in capacity of plants to access water, often dictated by the rooting depth, can result in contrasting evaporative losses across vegetation types. For example, Trees tend to have deeper roots than herbaceous plants (Canadell et al., 1996; Schenk and Jackson, 2002), and hence can maintain higher ET than grasslands when the supply declines (Calder et al., 1997; Sapanov, 2000). Decrease in ET during droughts is generally greater in agriculture areas because crop die or their foliage (and, therefore, their ability to transpire water) is severely stunted during prolonged droughts. Hence, the drought's duration and intensity would be different on various land use types and a new drought index should be able to reflect the level of severity in drought events in relation to land use effects.

In this study, Bowen ratio, which is the ratio of sensible to latent heat fluxes, was used as an indicator to monitor drought events based on the following: (a) the Bowen ratio is higher during drought events. During drought events, the partitioning of net radiation is skewed, with more heat going into the sensible heat flux and less into the latent flux. The increased sensible heat flux acts to heat the canopy and boundary layer. (b) Bowen ratio reflects the characteristics of land use. Under drier conditions, the availability of soil moisture becomes the primary source of ET, which strongly controls the partition between sensible heat flux and latent heat flux and affects the surface temperature and evaporation rate. For example, trees contain more moisture than grass, and therefore can maintain higher ET during drought event as more net energy would convert into latent heat for evaporation, hence the Bowen ratio is lower in trees than the grassland area.

A Regional Land use Drought Index (RLDI) was computed as the normalized monthly Bowen ratio on the different land use areas.

$$\text{RLDI} = \frac{B_m - B_{mv}}{3\,\sigma_y} \tag{5.1}$$

where B_m is the monthly Bowen ratio; B_{mv} is the long term average of monthly Bowen ratio; σy is the standard deviation of monthly Bowen ratio.

5.5. Results and discussions

5.5.1. Monthly Rainfall Variations and Standardized Precipitation Index (SPI)

The temporal and spatial rainfall distribution varies in annually. Figures 5.4 and 5.6 present the time series plots of monthly rainfall on the various land use areas in both northeast and south of

Florida, respectively. In the northeast the monthly rainfall ranged from 0.16 mm/day to 12.64 mm/day, and from 0 mm/day to 15.28 mm/day in the south during the study period. The drought index, standardized precipitation index (SPI), designed by [7] to quantify the precipitation deficit for multiple time scales was calculated on 1-month time scale and used to identify drought events. This reflects short time soil moisture condition. Figure 5.5 and 5.7 presented time series plots of 1-month SPI in northeast and south respectively. The figures suggest drier conditions during 1980 to 1982, 1984-1985, 1988-1990, and 1999-2001 periods due to extreme short rainfall events in winter and early spring.

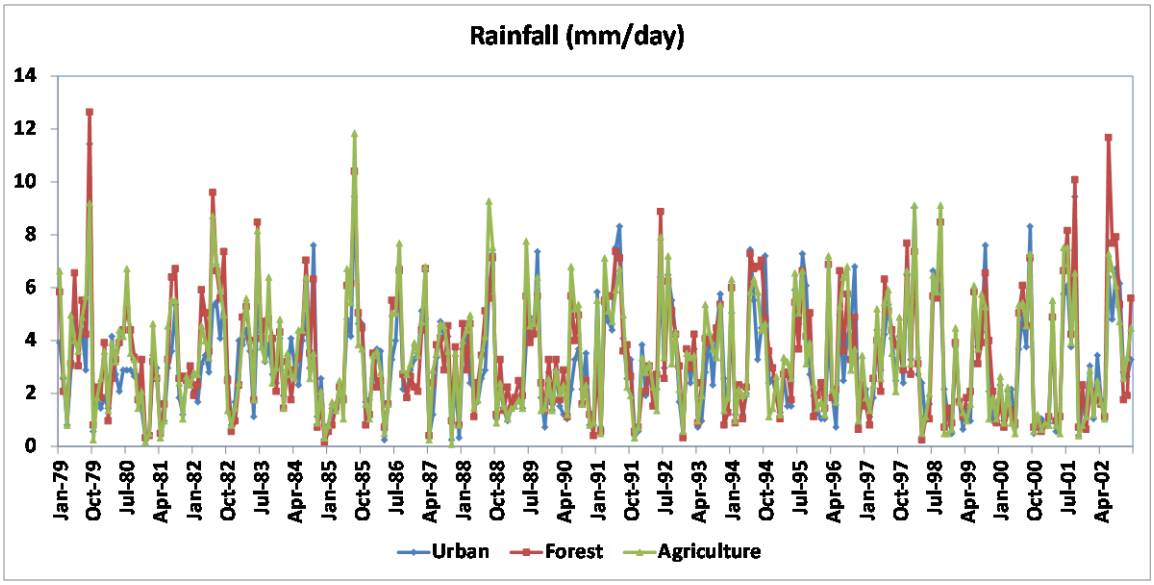

Figure 5.4: The Time Series for Monthly Rainfall Patterns for Northeast Florid

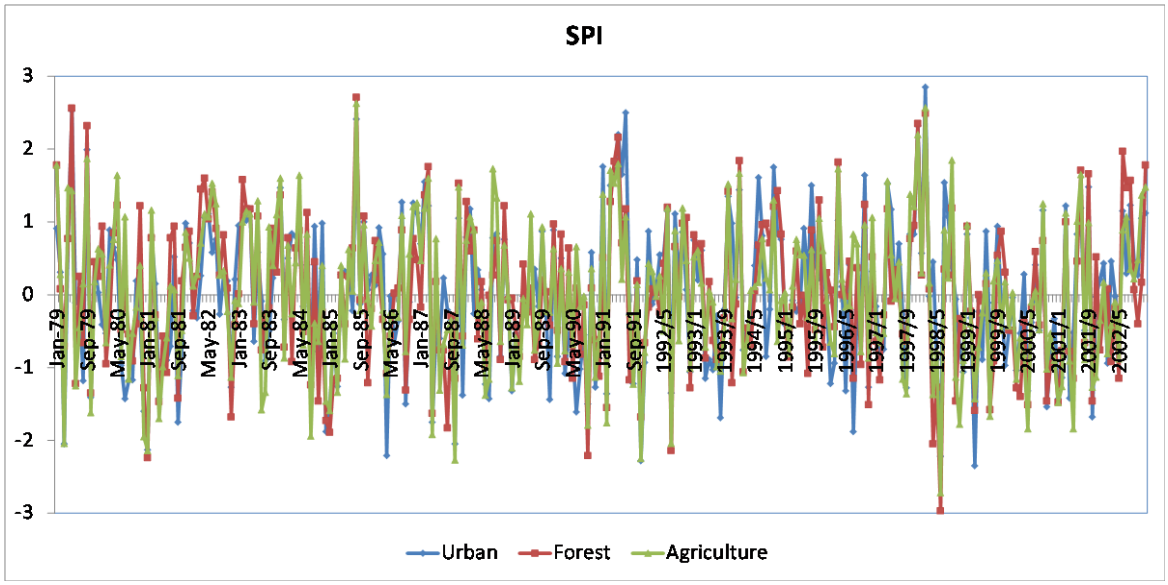

Figure 5.5: The Time Series of SPI for Northeast Florida

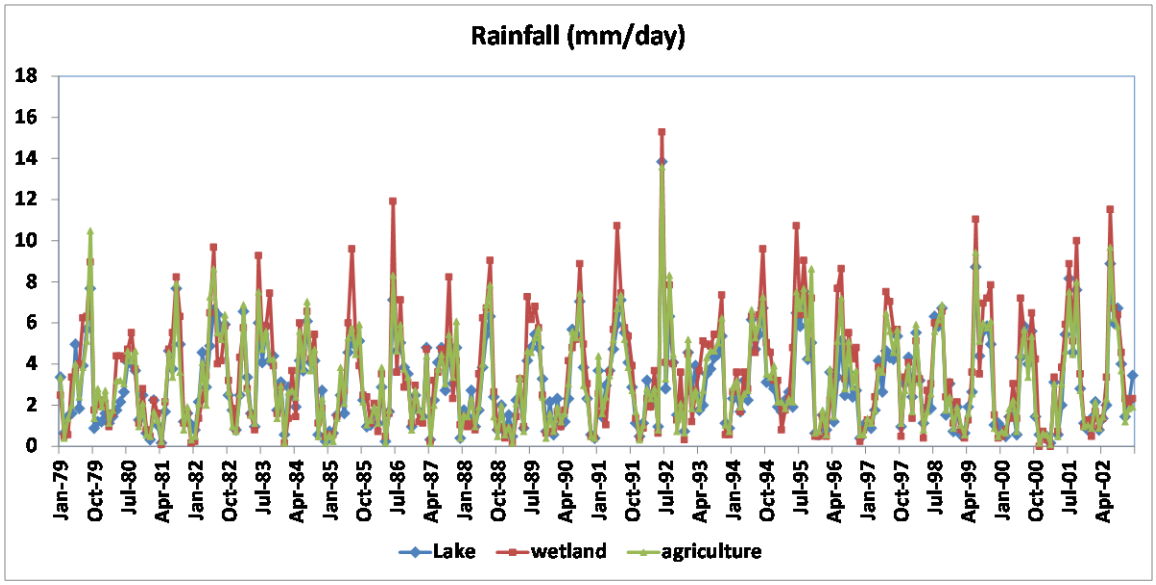

Figure 5.6: The Time Series for Monthly Rainfall Patterns for South Florida

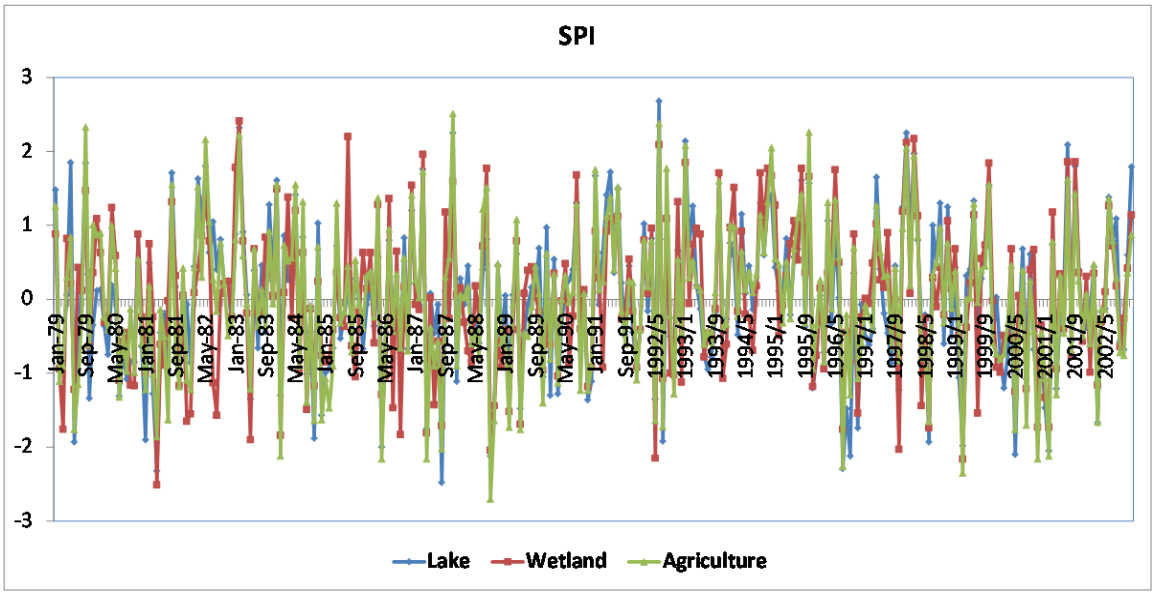

Figure 5.7: The Time Series of SPI for South Florida

5.5.2. Monthly Evaporation and Soil Moisture Variations

In the hydrologic budget of Florida, ET is the second most important component after precipitation (Knowles, 1996). It is influenced by seasonal changes in climate and can vary considerably within basins with different types of vegetation or different proportions of water surface areas. Figures 5.8 and 5.9 show the inter-annual variations of evaporation from 1979 to 2002 for various land use areas in northeast and south Florida, respectively. In the northeast, the monthly evaporation ranged from 1.6 mm/day to 4.56 mm/day in the urban area, 1.12 mm/day to 4.48 mm/day in the forest area, and 0.72 mm/day to 4.88 mm/day in the agriculture area. While in the south, monthly evaporation ranged from 1.2 mm/day to 4.4 mm/day in the lake area, 1.28 mm/day to 3.84 mm/day in the wetland area, and 0.4 mm/day to 4.8 mm/day in the agriculture area. During spring drought events in the northeast, the agriculture area had lower evaporation

rate in Spring, with values between 0.72 mm/day and 2.24 mm/day, while the urban and forest areas had higher values between 3.12 mm/day and 4.16 mm/day. In the south, the agriculture area also had the lower values between 0.56 mm/day and 2.8 mm/day, while the lake and wetland areas had the higher values, between 1.68 mm/day 2.88 mm/day.

Soil moisture can reflect past precipitation, evaporation, infiltration and runoff. In turn, the soil moisture acts as a strong control on the partitioning between sensible heat and latent heat flux at the surface, thus modulating precipitation over a given basin. Figures 5.10 and 5.11 show a range of 0 - 200 mm monthly soil moisture for agriculture, forest and wetland areas in northeast and south Florida, respectively. The urban and lake areas were not evaluated because monthly soil moisture reanalysis data were not available. The soil moisture ranged from 122 mm to 561 mm on the forest and agriculture areas in northeast, while in the south, it ranged from 261 mm to 706 mm on the wetland and agriculture areas respectively. Table 5.1 presents the mean rainfall and evaporation from 1979 to 2002 on the study area, thus suggesting that the wetland areas had the lowest average value of evaporation. In the northeast, the urban area located around St. John's River had higher evaporation as most of rainfall was returned to the atmosphere locally by evaporation; hence the ratio of evaporation/rainfall (E/P) was almost unity. The forest area had higher rainfall and evaporation than the agriculture area, because forests could maintain more soil moisture for evaporation, which results in higher rainfall and lower runoff. In the south, evaporation loss in the lake area exceeded the amount of water gained from rainfall, thus the evaporation/rainfall ratio (E/P) is higher than unity. These results are comparable to previous

studies that showed annual evaporation rate for Lake Okeechobee area as between 3.45 to 3.54 mm/day (Viessman et al., 1977).

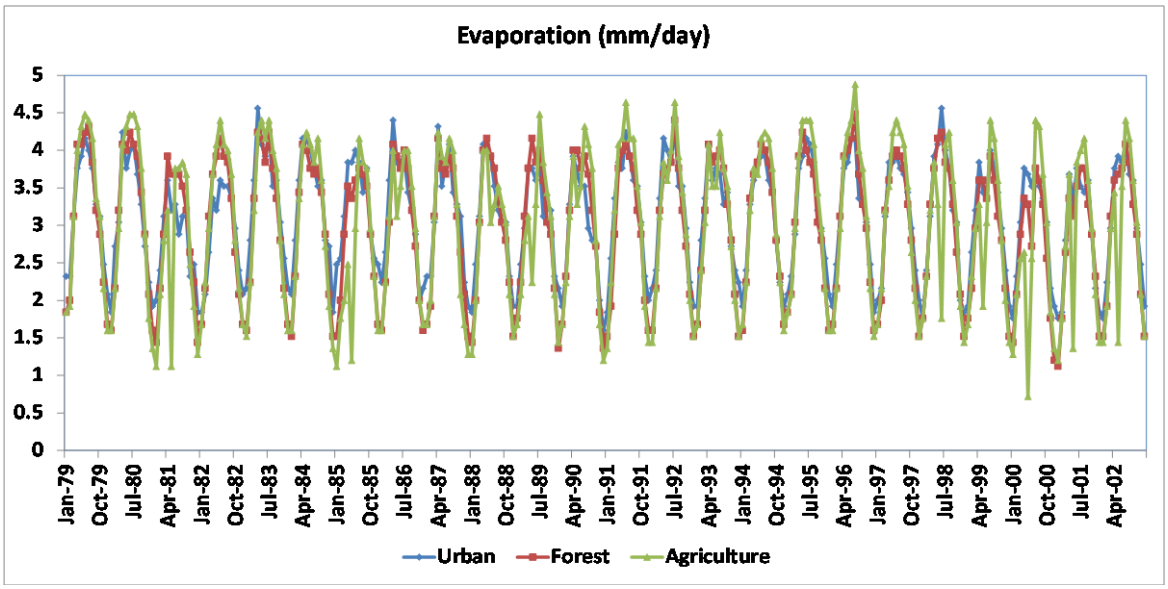

Figure 5.8: The Time Series for Monthly Evaporation Patterns for Northeast Florida

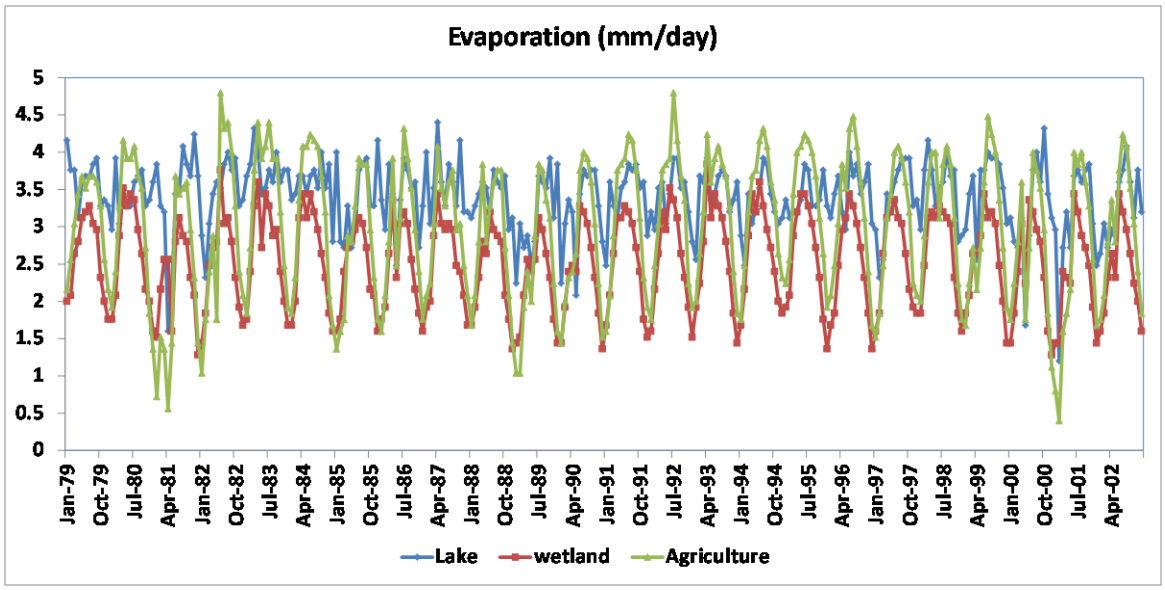

Figure 5.9: The Time Series for Monthly Evaporation Patterns for South Florida

5.5.3 Monthly Bowen Ratio Variations

Figures 5.12 and 5.13 showed the inter-annual variations of monthly Bowen ratio in both study areas. In the northeast, the monthly Bowen ratio ranged from 0.18 to 0.8 on the urban areas, 0.22 to 1.21 on the forest areas, and 0.17 to 7.7 on the agriculture areas. In south, the values ranged from 0.11 to 1.82 on the lake areas, 0.33 to 2.33 on the wetland areas, and 0.11 to 9.41 on the agriculture areas. While Table 2 shows the mean Bowen ratio for the study periods. The lake and urban areas had lower Bowen ratio because more surface energy would partition into latent heat for evaporation, while the wetland areas had the higher value because of the lower evaporation value. The Bowen ratio on the forest and agriculture areas ranged from 0.49 to 0.6. Figures 5.14 and 5.15 showed the Bowen ratio map over Florida during April and May 1996 respectively, suggesting that at no drought events, Bowen ratio was lower over Florida. However, during drought events (April 2000 and May 2001), agriculture and urban land uses (Figure 5.1 and 5.3) had the higher Bowen ratio as shown in Figures5.16 and 5.17. Hence, Bowen ratio could be used as an indicator to monitor drought events and land use response.

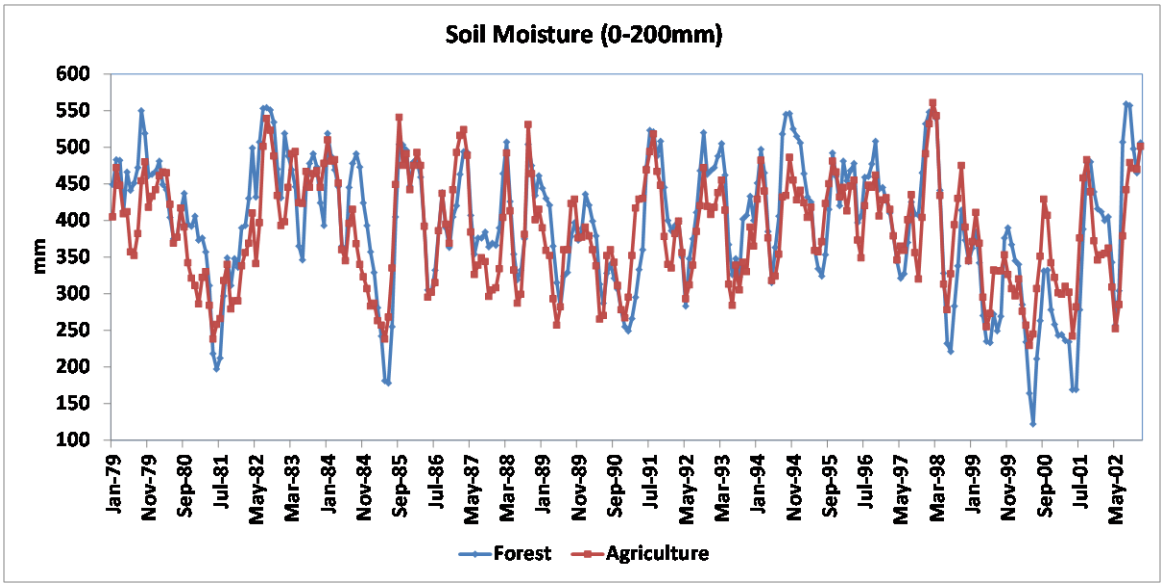

Figure 5.10: The Time Series for Monthly Soil Moisture Patterns for Northeast Florida

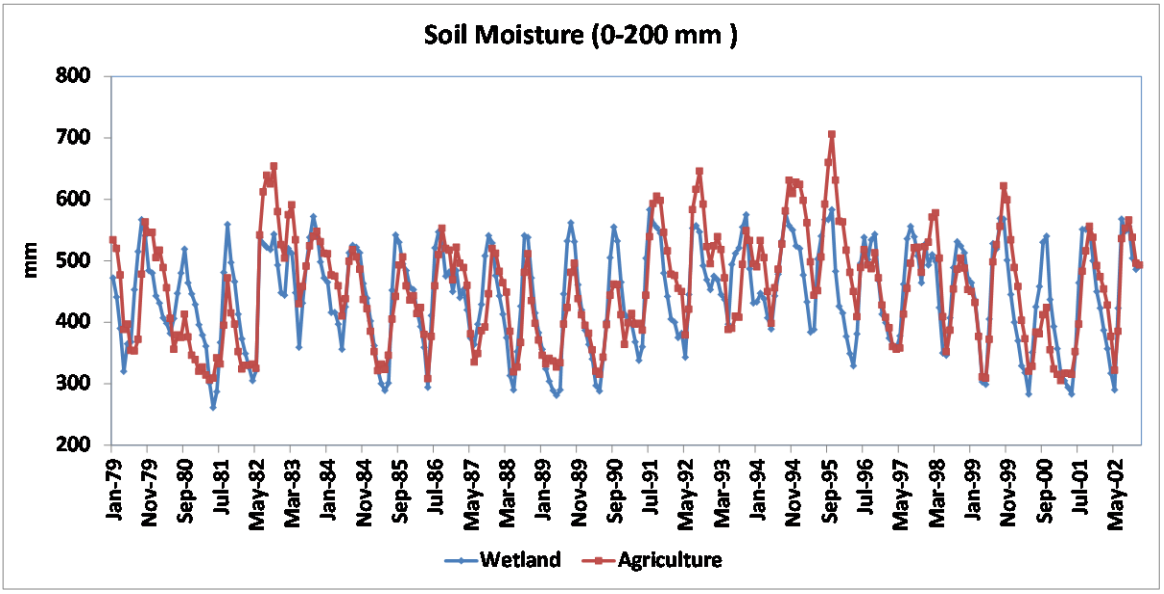

Figure 5.11: The time series monthly soil moisture (0-200 mm) patterns for South Florida

Table 5.1: Annual Mean (1979-2002) Rainfall and Evaporation for the Various Land Uses in Florida

1979-2002 Monthly Average	**Rainfall (P) (mm/day)**	**Evaporation (E)(mm/day)**	**E/P**
Urban	3.10	3.09	1.00
Forest	3.43	2.98	0.87
Northeast Agriculture	3.39	2.96	0.87
Lake	3.02	3.40	1.13
Wetland	3.54	2.51	0.71
South Agriculture	3.18	2.97	0.93

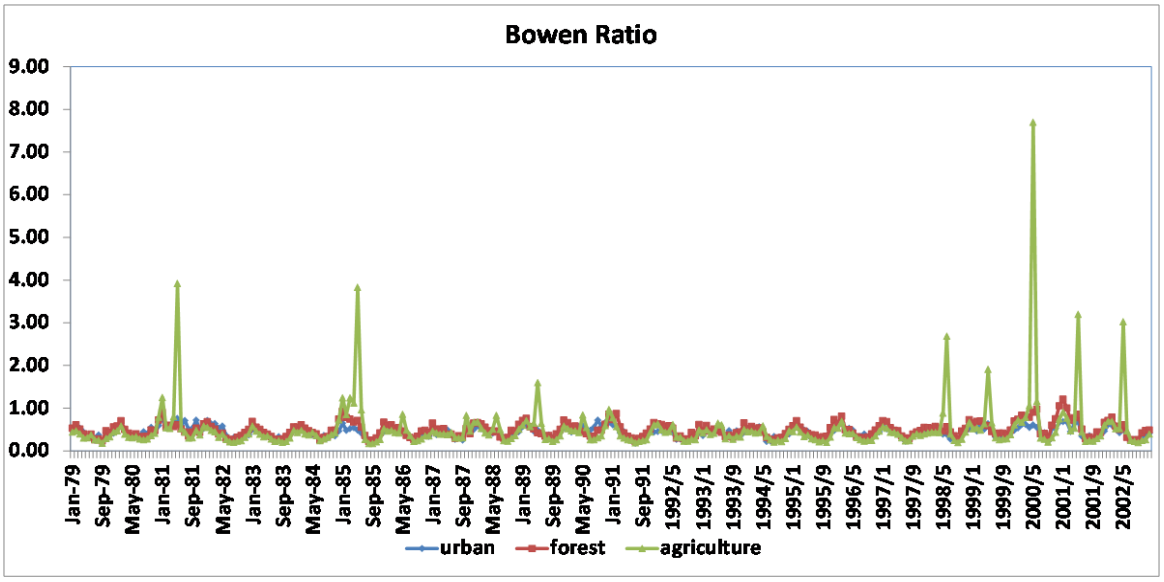

Figure 5.12: The Time Series for Monthly Bowen Ratio Patterns for Northeast Florida

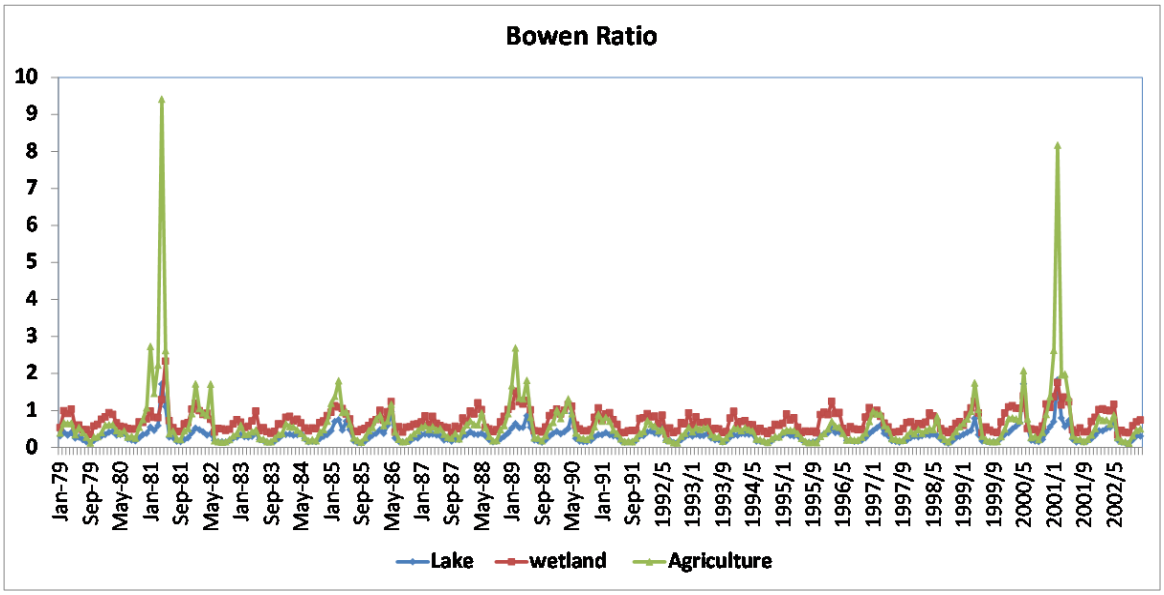

Figure 5.13: The Time Series for Monthly Bowen Ratio Patterns for South Florida

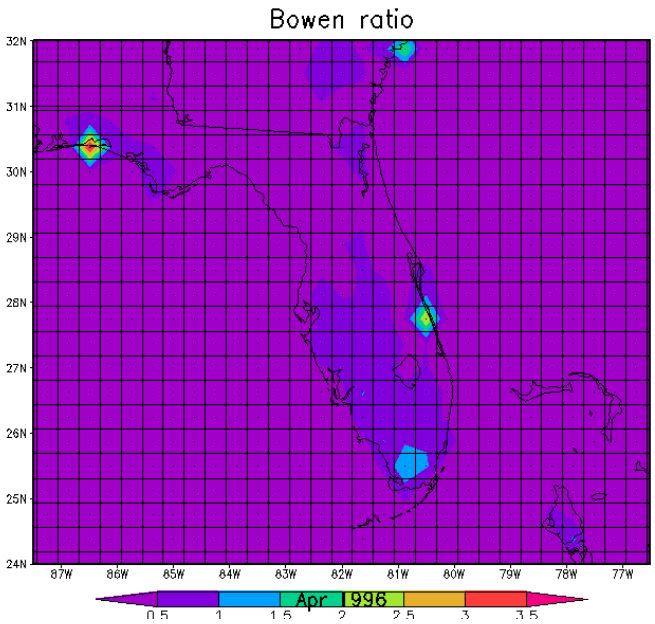

Figure 5.14: The Maps of Bowen Ratio in April 1996 over Florida

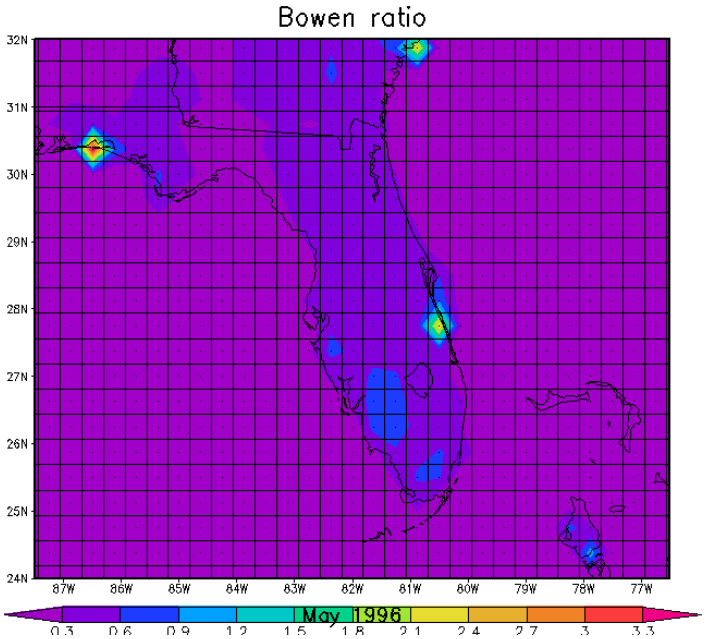

Figure 5.15: The Maps of Bowen Ratio in May 1996 over Florida

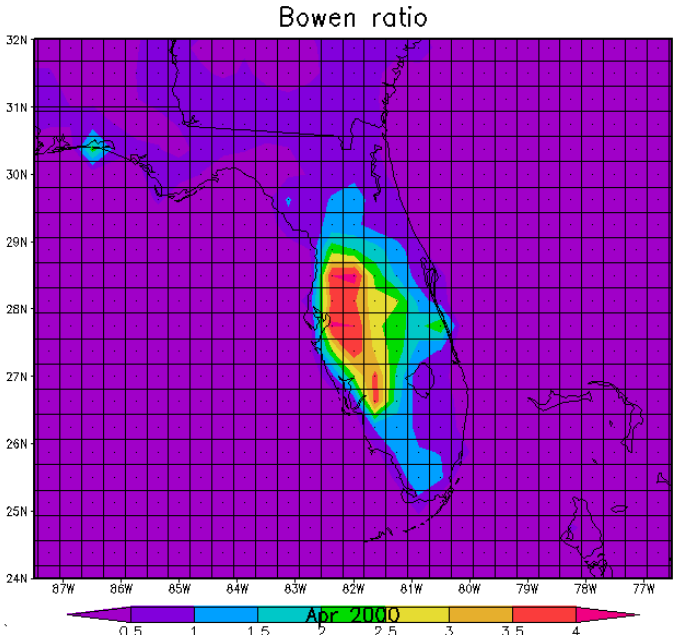

Figure 5.16: The Maps of Bowen Ratio in April 2000 over Florida

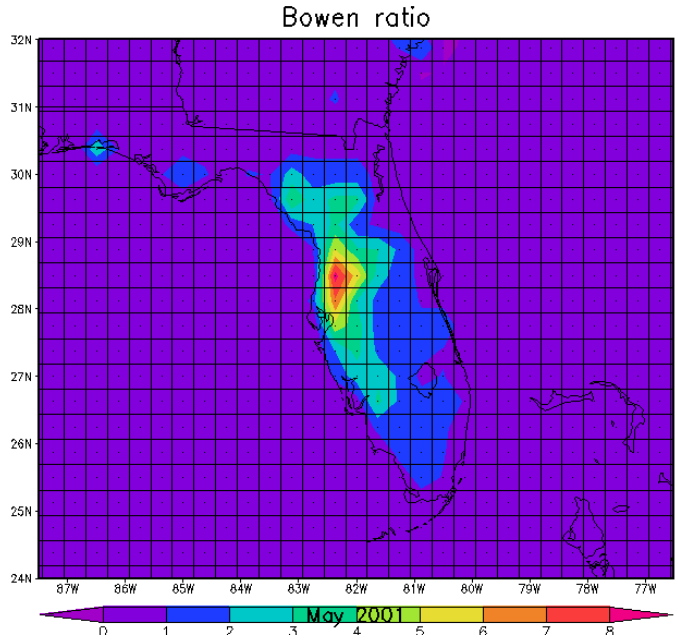

Figure 5.17: The Maps of Bowen Ratio in May 2001 over Florida

Table 5.2: Annual Mean (1979-2002) Bowen Ratio for the Various Land Uses in Florida

1979-2002 Monthly Average	Bowen ratio
Urban	0.44
Forest	0.49
Northeast Agriculture	0.51
Lake	0.33
Wetland	0.71
South Agriculture	0.60

5.5.4 Regional Land use adapted Drought Index (RLDI)

A Regional Land use Drought Index (RLDI) was calculated as the normalized monthly Bowen ratio on various land use areas. Normalized distribution allows for estimating both dry and wet periods. Figure 5.18 shows the time series plot of RLDI on the study areas, therefore suggesting higher values happened during drought periods, and also reflect the land use response to drought. To classify drought severity, the monthly RLDI values and monthly evaporation and rainfall were sorted and compared. Figures 5.19 and 5.20 show the relationships between the sorted RLDI and evaporation and rainfall, respectively, thus suggesting higher RLDI with lower

evaporation and rainfall and vice versa.. When the value is greater than unity, evaporation and rainfall were extreme low, while for values small than -0.5, the evaporation and rainfall were extremely high. Hence, an extreme drought condition would have a RLDI value of 1 or greater, whereas an extreme wet condition would be -0.5 or less (Table 5.3). Figure 5.21 and 5.22 show extreme events on the study areas and period with the RLDI drought classification, thus validating RLDI scale.

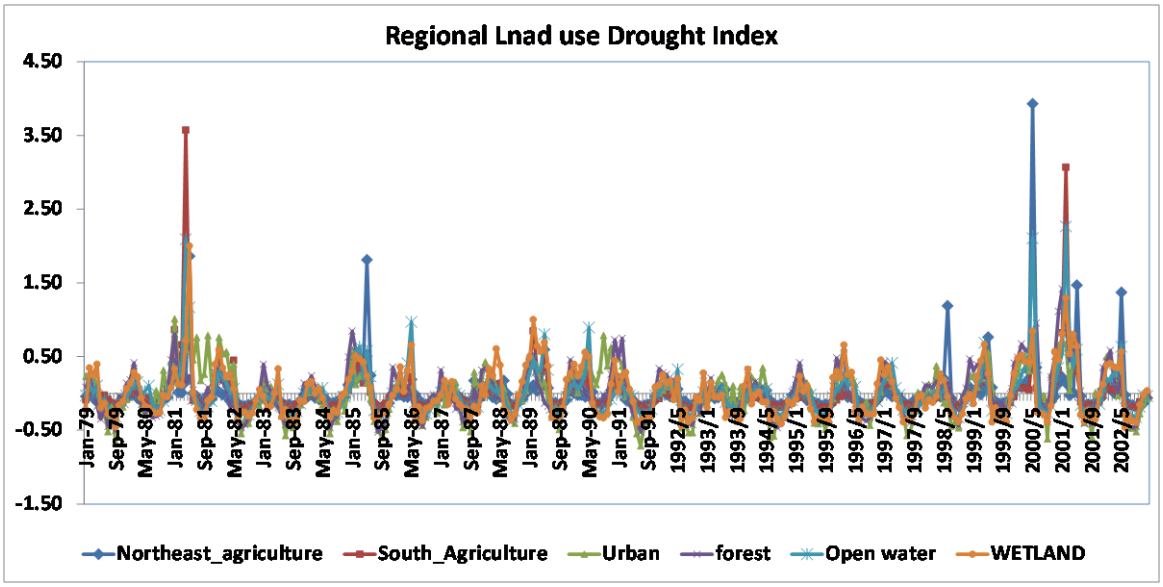

Figure 5.18: The Time Series for Monthly RLDI in the Study Areas

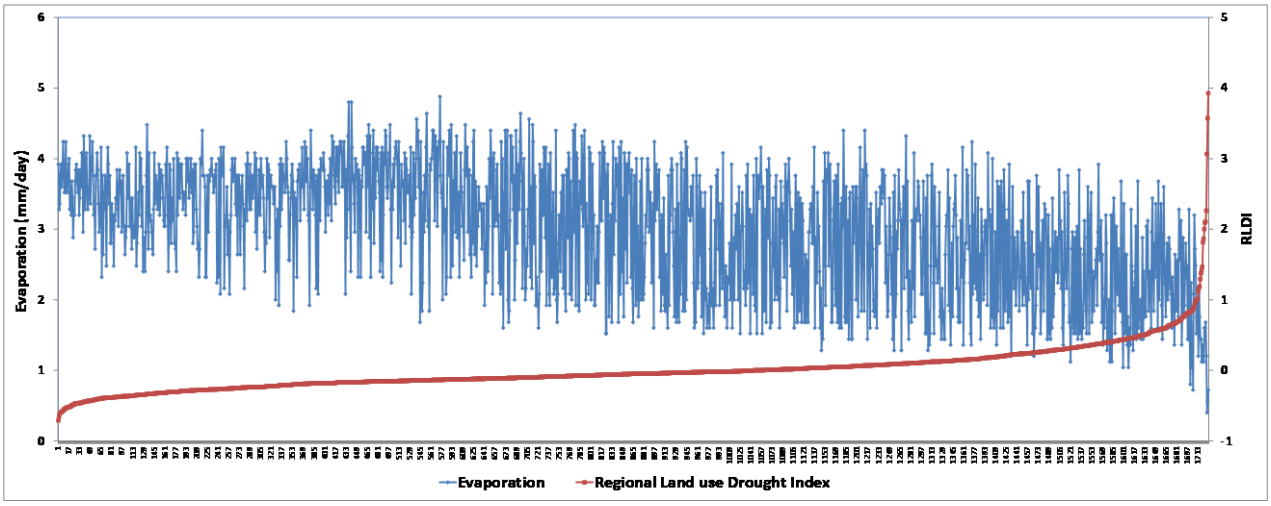

Figure 5.19: Relationship between Sorted RLDI and Evaporation

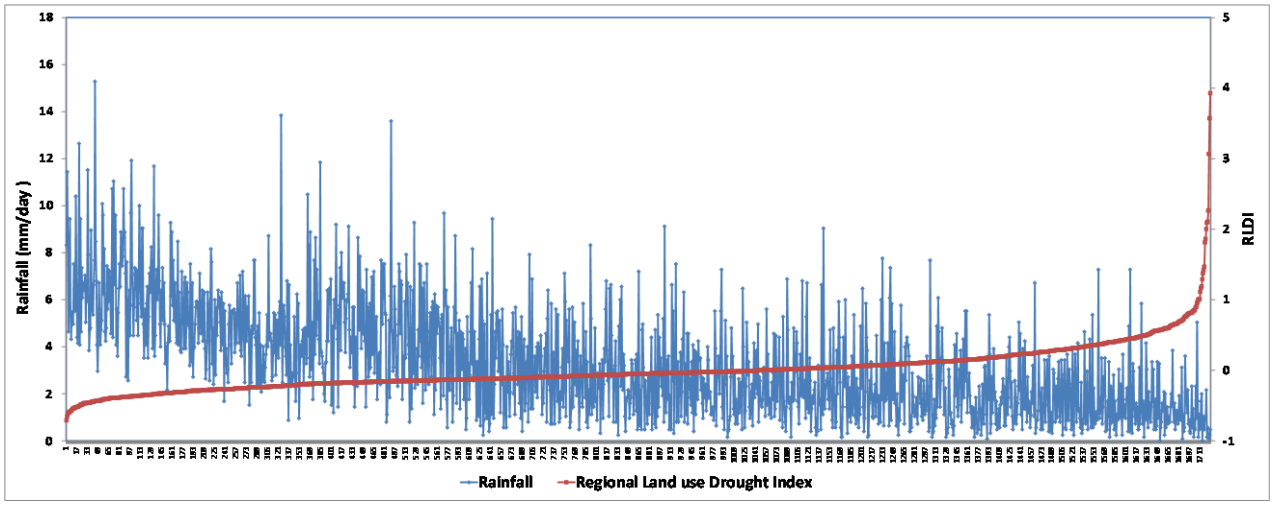

Figure 5.20: Relationship between Ordered RLDI and Rainfall

Table 5.3. The Classification of RLDI

RLDI	Drought Classes
>= 1	Extreme Drought
<=-0.5	Extreme Wet

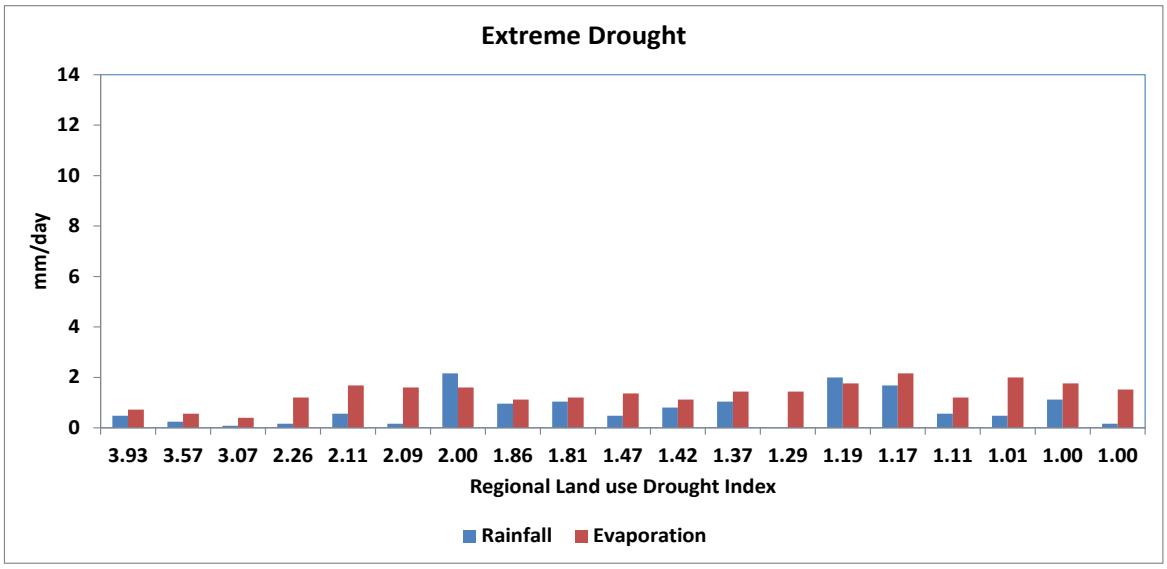

Figure 5.21: Extreme drought and the RLDI Drought Classification

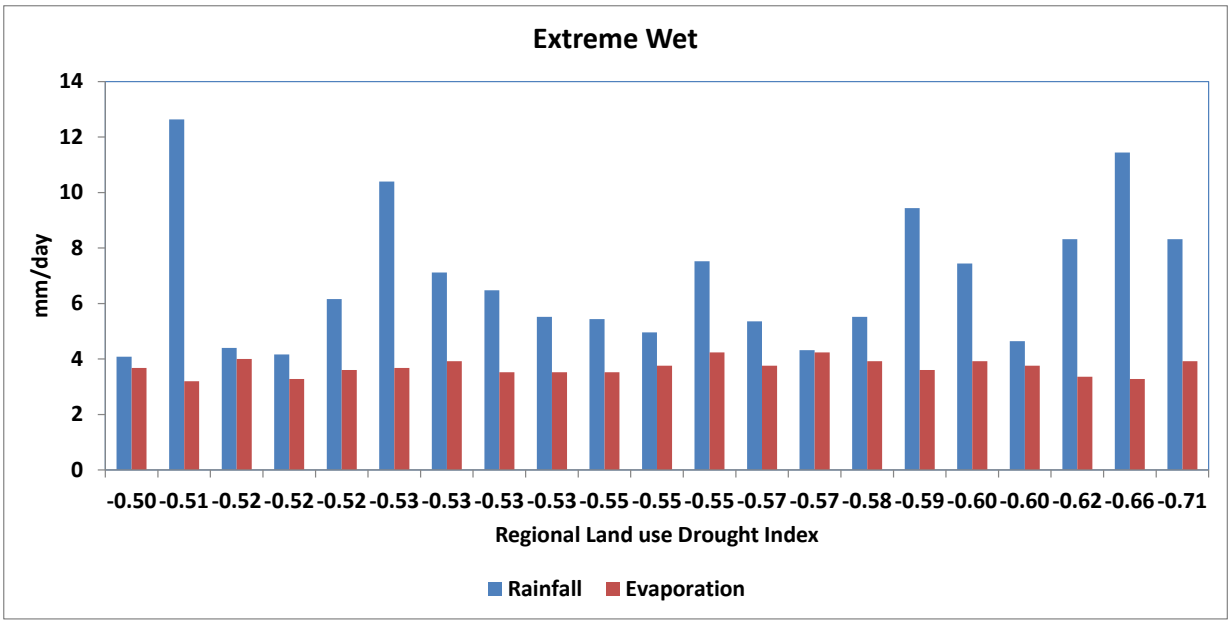

Figure 5.22 Extreme wet and the RLDI Drought Classification

5.6 Oceanic Niño Index (ONI) and RLDI

The Oceanic Niño Index (ONI), used for definitions of El Niño and La Niña conditions was compared to the RLDI in Figures 5.23 through 5.25 for the study period. In the ONI, low negative values indicated cold sea surface temperature, and the ONI must exceed -0.5 for at least five consecutive months to be classified as La Niña episode. During the La Niña episodes of 1984-85, 1988-89, 1995-96 and 1998-2000 in the study area, the RLDI values were higher, and during the drought events of 1981-1982 the ONI values were negative, which also resulted in higher RLDI values too. Hence, the RLDI can be a useful tool in ENSO forecast, agricultural planning and water resource managements and can play a key role in mitigating the impacts of flood and drought.

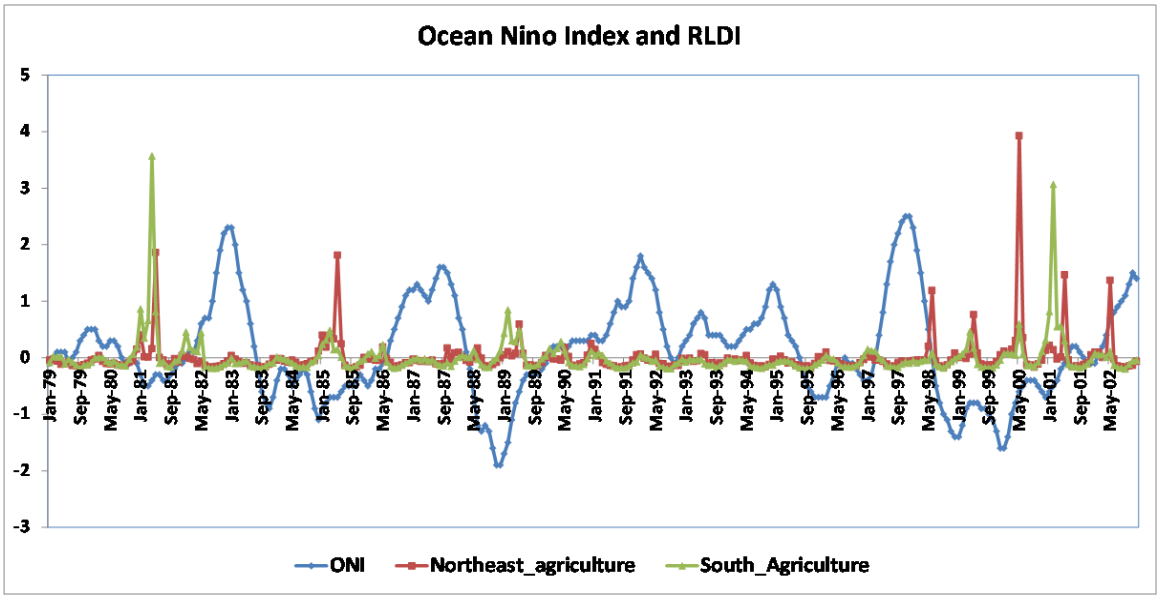

Figure 5.23: The Time Series Plots of ONI and RLDI in the Northeast and South agriculture areas

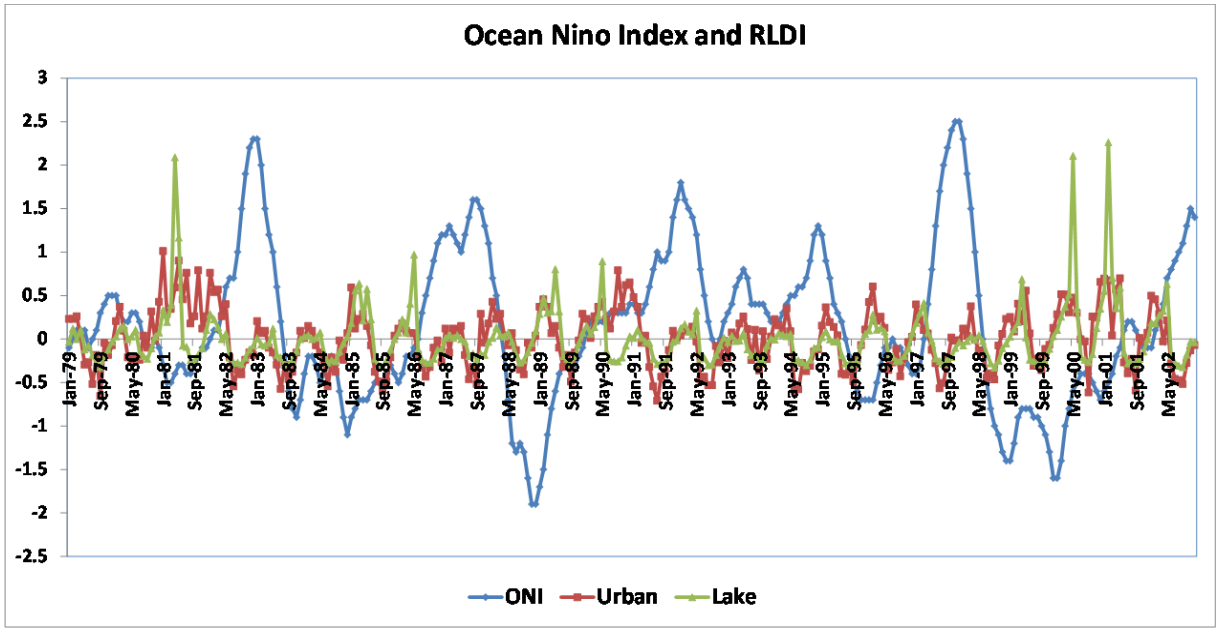

Figure 5.24: The Time Series Plots of ONI and RLDI in the urban and lake areas

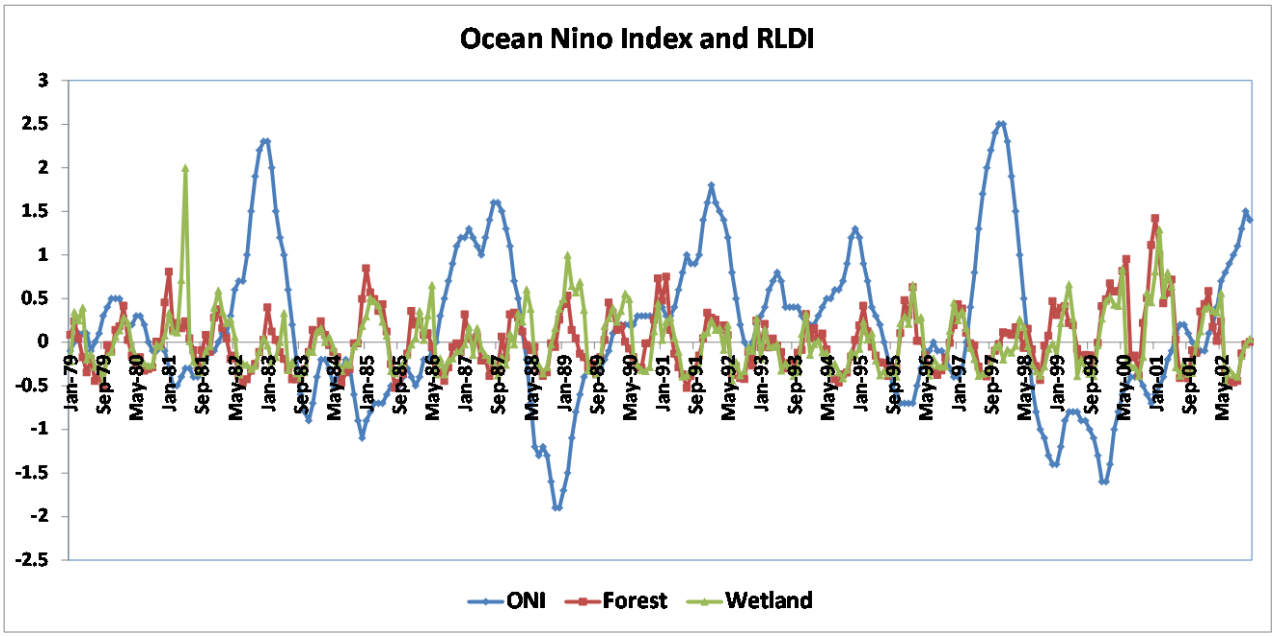

Figure 5. 25: The Time Series Plots of ONI and RLDI in the forest and wetland areas

5.7 Summary and Conclusions

A Regional Land use Drought Index (RLDI) was developed in the State of Florida based on North American Regional Reanalysis (NARR) data set from 1979 to 2002. The 24-year monthly data for precipitation, evaporation, and soil moisture were analyzed within five different land uses (lake, urban, forest, wetland, and agriculture) in both northeast and south areas in Florida. The standardized precipitation index (SPI), was calculated to identify and validate reported drought events. The results showed that the study areas experienced drier conditions during 1980 to 1982, 1984-1985, 1988-1990, and 1999-2001 periods. The intensive, short-term drought events occurred due to extreme deficits in rainfall in winter and early spring.

The analyses suggested that different land use types are strongly affected by evaporation and therefore had different responses to the drought events. The agriculture area had lower evaporation rates in the spring, while, the forest, urban, wetland, and open water areas, had higher values. Previous studies suggested that evaporation rate measurement at Lake Okeechobee was difficult, but the NARR data set provided valuable resource for estimating evaporation rate over water bodies.

The Bowen ratio was used as an indicator to monitor drought events. The results showed that the lake and urban areas had the lower Bowen ratio while the wetland areas had the higher values because of the lowest value of evaporation. The land use response to Bowen ratio was due to the soil moisture acting as a strong control on the partitioning between sensible heat and latent heat flux at the surface that in turn affects the surface temperature and evaporation rate.

A Regional Land use adapted Drought Index (RLDI) was calculated based on normalized monthly Bowen ratio on the various land use areas. Drought severity was evaluated and the results showed that when the values of RLDI were larger than unity, the evaporation and rainfall were extremely low, while for values smaller than -0.5, the evaporation and rainfall were extremely high. The RLDI approach gave a unique opportunity to predict and correlate drought events with rainfall, evaporation and soil moisture, and also evaluate land use response to drought conditions. RLDI can also be used to help us to understand local ENSO patterns on the regional scale and reflects the level of severity in drought events resulting from land use effects.

References

Abramopoulos, F., Rosenzweig, C. Choudhury B., 1988, Improved ground hydrology calculations for global climate models (GCMs): Soil water movement and evapotranspiration. Journal of Climate, 1, 921–941.

Brolley, J. M., James, J. O., Brien, J. S., David, Z., 2007, Experimental drought threat forecast for Florida, Agricultural and Forest Meteorology 145: 84-96, doi:10.1016/j.agrformet.2007.04.003

Calder, I. R., Rosier, P. T., W., Prasanna, K. T., 1997, Eucalyptus water use greater than rainfall input – a possible explanation from southern India, Hydrology and Earth System Science, 1, 249–256.

Canadell J., Jackson R. B., Ehleringer J. R., 1996, Maximum rooting depth of vegetation types at the global scale, Oecologia, 108, 583–595.

Carter, D. R., Jokela, E., J., 2002, Florida's renewable forest resources, CIR1433: Gainesville: University of Florida, Institute of Food and Agricultural Sciences, Florida Cooperative Extension Service, 9.

Douglas, A., Englehart, P., 1981, On a statistical relationship between autumn rainfall in the central equatorial Pacific and subsequent winter precipitation in Florida. Mon. Wea. Rev. 109, 2377–2382

Drummond, M., A., Thomas R. L., 2010, Land-use Pressure and a Transition to Forest-cover Loss in the Eastern United States, BioScience, 60, no. 4 (April): 286-298.

Ek, M. B., Mitchell, K. E., Lin, Y., Grunmann, P., Rogers, E., Gayno, G., Koren, V., Tarpley J. D., 2003. Implementation of Noah land surface model advances in the National Centers for Environmental Prediction operational mesoscale Eta model. J. Geophys. Res., 108(D22), 8851, doi:10.1029/2002JD003296.

FASS, 1996, Florida agriculture: Vegetables winter acreage, Florida Agricultural Statistics Service, Florida Department of Agriculture and Consumer Services, January 19, 2

FASS, 1997, Florida agricultural statistics: Vegetable summary (1995– 96). Florida Agricultural Statistics Service, Florida Department of Agriculture and Consumer Services, 70

FEMA, 1995, The 1993 and 1995 midwest floods: flood hazard mitigation through property hazard acquisition and relocation program. FEMA Mitigation Directorate, Washington, DC

Florida Division of Forestry, undated (a), Wildfire statistics for Florida: 1981-present: Accessed August 31, 2005, at http://www.fl-dof.com/wildfire/stats_fires_since1981.html.

Folks, J. C., 2005, Lake Okeechobee TMDL: Technologies and Research. North Carolina State University College of Agriculture and Life Sciences: 1-12.

Hanson, K., Maul, G. A., 1991, Florida precipitation and the Pacific El Niño, 1895–1989, Florida Sci., 54, 160–68.

Heim Jr., R. R., 2000, Drought indices: A review. In D. A. Wilhite (Ed.), Drought. A Global Assessment, 1, 159–167. London: Routledge.

Jensen, M., E., Burman, R., D., Allen, R.G., 1990, Evapotranspiration and irrigation water requirements, ASCE Manuals and Reports on Engineering Practice, 70. American Society of Civil Engineers, New York, NY

Keyantash, J. A., Dracup, J. A., 2004, An aggregate drought index: Assessing drought severity based on fluctuations in the hydrologic cycle and surface water storage. Water Resources, 40, 1-14. doi: 10.1029/2003WR002610.

Kiladis, G. N., Diaz, H. F., 1989, Global climatic anomalies associated with extremes in the Southern Oscillation. J. Climate, 2, 1069–1090.

Kim, D., Hi-ryong B., Ki-seon C., 2009, Evaluation, modification, and application of the Effective Drought Index to 200-Year drought climatology of Seoul, Korea. Journal of Hydrology, 378, 1-2, 1-12. doi:10.1016/j.jhydrol.2009.08.021. http://dx.doi.org/10.1016/j.jhydrol.2009.08.021.

Luo, Y., Ernesto H. B., Kenneth E. M., 2005, The Operational Eta Model Precipitation and Surface Hydrologic Cycle of the Columbia and Colorado Basins. J. Hydrometeor, 6, 341–370.

McKee, T. B., Doesken, N. J., Kleist, J., 1993, The relationship of drought frequency and duration to time scales. Proceedings of the Eighth Conference on Applied Climatology, 179 – 184. Boston, MA: American Meteorological Society.

Mills, D. M., 2009, Climate change, extreme weather events, and us health impacts: what can we say? Journal of occupational and environmental medicine / American College of Occupational and Environmental Medicine, 51, no. 1 (1): 26-32.

Munson, A., B., Joseph J. D., Douglas A., L., 2005, Determining Minimum Flows and Levels: the Florida Experience. Journal of the American Water Resources Association, 41, 1 (2): 1-10.

Narasimhan, B., Srinivasan, R., 2005, Development and evaluation of Soil Moisture Deficit Index (SMDI) and Evapotranspiration Deficit Index (ETDI) for agricultural drought monitoring, Agricultural and Forest Meteorology, 133(1-4), 69-88, doi: 10.1016/j.agrformet.2005.07.012.

NOAA/ National Weather Service, http://ggweather.com/enso/oni.htm

Pade, E. L. Nin, E. R. S., 2003, Notes and correspondence a quantitative evaluation of ENSO indices, Society, 1249-1258

Palmer, W. C., 1965, Meteorological Drought. US Department of Commerce, Weather Bureau Research Paper, 45, Washington DC.

Palmer, W. C., 1968, Keeping track of crop moisture conditions, nationwide: The new crop moisture index. Weatherwise, 21, 156– 161

Pan, M., Wood, E. F., 2006, Data Assimilation for Estimating the Terrestrial Water Budget Using a Constrained Ensemble Kalman Filter, Journal of Hydrometeorology, 7(3), 534, doi: 10.1175/JHM495.1.

Richard, B., Verdi, J., Tomlinson, S. A., Marella, R. L., Survey, U. S. G. 2002, The Drought of 1998-2002: Impacts on Florida' s Hydrology and Landscape Circular 1295. System

Ropelewski, C., F., Halpert, M., S., 1986, North American precipitation and temperature patterns associated with the El Nino Southern Oscillation (ENSO). Mon. Wea. Rev., 114, 2352–2362.

Sapanov, M. K., 2000, Water uptake by trees on differen soils in the Northern Caspian region. Eurasian soil science, 33, 1157–1165

Schenk, H. J., Jackson, R. B., 2002, The global biogeography of roots. Ecologial Monographs, 72, 311–328

Shafer, B. A., Dezman, L. E., 1982, Development of a Surface Water Supply Index (SWSI) to assess the severity of drought conditions in snowpack runoff areas. Proceedings of the 50th Annual Western Snow Conference, 164–175. Fort Collins, CO: Colorado State University.

Sittel, M. C., 1994a, Marginal probabilities of the extremes of ENSO events for temperature and precipitation in the southeastern United States. Tech. Rep. 94-1, Center for Ocean–Atmospheric Studies, The Florida State University, Tallahassee, FL, 155

Snyder, G., H., 1987, Agricultural flooding of organic soils, Bulletin No. 570, Institute of Food and Agricultural Sciences, University of Florida, Gainesville

Thornthwaite, C.W., 1948, An approach toward a rational classification of climate, Geograph. Rev. 38, 55–94

Tsakiris, G., Vangelis, H., 2005, Establishing a drought index incorporating evapotranspiration, Eur Water, 9–10, 1–9.

Tsakiris, I. N. G., 2009, Assessment of Hydrological Drought Revisited. Media, (April 2007), 881-897. doi: 10.1007/s11269-008-9305-1

Twine, T., E., Christopher, J. K., and Jonathan A., F., 2005, Effects of El Niño–Southern Oscillation on the Climate, Water Balance, and Streamflow of the Mississippi River Basin. J. of Climate, 18, 22 (11)

Viessman, W., Klapp, J. W., Lewis, G. L., Harbaugh, T. E. 1977, Introduction to hydrology, Harper and Row, New York.

Wilhite, D. A., 2000, Drought as a natural hazard: Concepts and definitions, in Drought: A Global Assessment, Hazards Disasters Ser., vol. I, edited by D. A. Wilhite, 3–18, Routledge, New York.

Wilhite, D. A., Hayes, M. J., Svoboda, M. D., 2000, Drought monitoring and assessment: Status and trends in the United States. In J. V. Vogt, and F. Somma (Eds.), Drought and drought mitigation in Europe, 149–160, Dordrecht: Kluwer Academic Publishers.

CHAPTER 6:

SUMMARY OF RESEARCH AND FUTURE IMPLICATIONS

6.1 Summary of Work

Accurate estimate of the surface longwave fluxes is important for the calculation of surface radiation budget, which in turn controls all components of the surface energy budget, such as evaporation and sensible heat fluxes. Regional scale of land use change can impact local weather conditions; for example, air temperature and water vapor pressure, which are more commonly used as inputs in existing models for estimating downward longwave radiation flux density (LW_d), would be affected by heterogeneous land use patterns and temporal changes in atmospheric circulation patterns.

In Chapter 2, we analyzed the effect of cloud cover and various of land use types on LW_d using yearly observed LW_d radiation data in northeast Florida, and a modified land use adapted model for LW_d radiation estimation under all sky conditions. The results show that factors, such as, seasonal effects, cloud cover, and land use are of importance in the estimation of LW_d and they cannot be ignored when developing a model for LW_d prediction.

The all-sky land use adapted model with all factors taken into account performs better than other existing models statistically. The results of the statistical analyses indicated that the Bias (BIAS), Root Mean Square Error (RMSE), Mean Absolute Error (MAE), Percent Mean Relative

Error (PMRE) are -0.18, 10.81, 8.00, 2.30; -2.61, 14.45, 10.64, 3.19; -0.07, 10.53, 8.03, 2.27; -0.62, 13.97, 9.76, 2.87 for urban, rangeland, agricultural and wetland areas respectively.

In *Chapter 3*, 1992 to 2002 data from North American Regional Reanalysis (NARR) were used to investigate water budget on five land-use areas; urban, forest, agriculture, lake and wetland in the State of Florida, USA. The data were evaluated based on the anomalies of rainfall, evaporation and soil moisture from the average condition. The anomalies were used to investigate the effect of extreme conditions on water budget parameters for various land uses in both northeast and south of Florida.

The results showed that annual mean water budget of Lake Okeechobee in the south and urban area located at St. Johns River basin in the northeast suggested higher evaporation, lower values of difference between potential evaporation and evaporation, and the precipitation-evaporation ratios closed to unity. The results also show that during drought years, the lower average annual precipitation and evaporation were observed in both study areas, hence drought strong effect on the water budget. Extreme events such as La Niña strongly affected the water budget on land-use areas in both regions as the negative monthly rainfall anomalies were observed during the 1999/2000 event, while EI Niño and thunderstorms in summer caused positive rainfall anomalies with more than 70% in all study areas.

Higher rainfall led to higher soil moisture anomalies for the agriculture, forest and wetland from 1992 to May 1998 in both study regions. However, soil moisture becomes primary source for evaporation in drier conditions, and differences in capacity of plants access water, often

dictated by the rooting depth, can result in contrasting evaporative losses across vegetation types. Hence, the forest, which had the deeper roots, had the lower soil moisture anomalies, but higher evaporation anomalies than agriculture area during the drought event. Moreover, the wetland area had the higher anomalies for soil moisture and evaporation during the drought event.

In Chapter 4, 1992 to 2002 data from North American Regional Reanalysis (NARR) were also used to investigate energy budget on five land-use areas; urban, forest, agriculture, lake and wetland in the State of Florida, USA. The data were evaluated based on the anomalies of actual evaporation, latent heat, sensible, and surface temperature from the average condition. The anomalies were used to investigate the effect of extreme conditions on energy budget parameters for various land uses in both northeast and south of Florida.

The results showed that based on annual mean values, the energy budget of Lake Okeechobee and urban area located at St. Johns River, had higher net radiation, latent heat, actual evaporation, and lower sensible heat and Bowen ratio, while the wetland area had the lower net radiation, latent heat, actual evaporation and higher sensible heat and Bowen rate. A comparison of forest and agriculture areas suggests that the agriculture areas had lower net radiation, latent heat, actual evaporation and higher Bowen ratio because of the shallow roots, which contained less soil moisture.

During the drought years, in Northeast Florida, the agriculture area had negative values of evaporation and latent heat in April 2000, May of 1999 through 2002, and June 1998, with values between -10.46% and -75%,, and -9.7% and -76.54% respectively, while the forest and

urban areas had positive values in these months. In South Florida, the agriculture area also had lower evaporation and latent heat within the drought period, than those of the lake and wetland areas.

Drought is a natural phenomenon that occurs when a significant decrease of water availability is observed during a significant period of time and over a larger area. Drought indices can be a useful tool to assess and respond to drought. However, current drought indices could not fully show the land use effects and they have limitations in data sources. ENSO influences the climate of Florida; where El Niño years tend to be cooler and wetter, and La Niña years tend to be warmer and drier than normal in the fall through the spring, with the strongest effect in the winter. Both prolonged heavy rainfall and drought potentially have impacts on land uses and many aspects of Florida's economy and quality of life. Hence, understanding local ENSO patterns on regional scales and developing a new land use drought index in Florida are critical and necessary in agriculture and water resources planning and managements. In Chapter 5, we presented a 32 km high resolution land use adapted drought index on five different land uses (lake, urban, forest, wetland, and agriculture) in Florida based on the National Centers for Environmental Prediction (NCEP) North American Regional Reanalysis (NARR) data from 1979 to 2002. The new regional land use drought indices were developed from normalized Bowen ratio and the results show that they could reflect not only the level of severity in drought events resulting from land use effects, but also La Niña driven drought impacts.

6.2 Future Implications

The future research plans are (1) combining a General Circulation Model (GCM) to simulate future year emission and climate scenarios to study the impacts on the water and energy budget on various land use areas (2) investigating drought event impacts on water quality by collecting water quality data (3) combing ecosystem models to study how altering land cover types and their associated physical changes impacts ecosystem functions such as decomposition, nitrogen cycling and soil carbon.